NASA/TM—2001-211099

Zr-Containing 4,4′-ODA/PMDA Polyimide Composites

Parts I and II

M.L. Illingsworth, J.A. Betancourt, L. He, Y. Chen, and J.A. Terschak
Rochester Institute of Technology, Rochester, New York

B.A. Banks and S.K. Rutledge
Glenn Research Center, Cleveland, Ohio

M. Cales
Cleveland State University, Cleveland, Ohio

August 2001

The NASA STI Program Office . . . in Profile

Since its founding, NASA has been dedicated to the advancement of aeronautics and space science. The NASA Scientific and Technical Information (STI) Program Office plays a key part in helping NASA maintain this important role.

The NASA STI Program Office is operated by Langley Research Center, the Lead Center for NASA's scientific and technical information. The NASA STI Program Office provides access to the NASA STI Database, the largest collection of aeronautical and space science STI in the world. The Program Office is also NASA's institutional mechanism for disseminating the results of its research and development activities. These results are published by NASA in the NASA STI Report Series, which includes the following report types:

- TECHNICAL PUBLICATION. Reports of completed research or a major significant phase of research that present the results of NASA programs and include extensive data or theoretical analysis. Includes compilations of significant scientific and technical data and information deemed to be of continuing reference value. NASA's counterpart of peer-reviewed formal professional papers but has less stringent limitations on manuscript length and extent of graphic presentations.

- TECHNICAL MEMORANDUM. Scientific and technical findings that are preliminary or of specialized interest, e.g., quick release reports, working papers, and bibliographies that contain minimal annotation. Does not contain extensive analysis.

- CONTRACTOR REPORT. Scientific and technical findings by NASA-sponsored contractors and grantees.

- CONFERENCE PUBLICATION. Collected papers from scientific and technical conferences, symposia, seminars, or other meetings sponsored or cosponsored by NASA.

- SPECIAL PUBLICATION. Scientific, technical, or historical information from NASA programs, projects, and missions, often concerned with subjects having substantial public interest.

- TECHNICAL TRANSLATION. English-language translations of foreign scientific and technical material pertinent to NASA's mission.

Specialized services that complement the STI Program Office's diverse offerings include creating custom thesauri, building customized data bases, organizing and publishing research results . . . even providing videos.

For more information about the NASA STI Program Office, see the following:

- Access the NASA STI Program Home Page at ***http://www.sti.nasa.gov***

- E-mail your question via the Internet to help@sti.nasa.gov

- Fax your question to the NASA Access Help Desk at 301–621–0134

- Telephone the NASA Access Help Desk at 301–621–0390

- Write to:
  NASA Access Help Desk
  NASA Center for AeroSpace Information
  7121 Standard Drive
  Hanover, MD 21076

NASA/TM—2001-211099

Zr-Containing 4,4′-ODA/PMDA Polyimide Composites

Parts I and II

M.L. Illingsworth, J.A. Betancourt, L. He, Y. Chen, and J.A. Terschak
Rochester Institute of Technology, Rochester, New York

B.A. Banks and S.K. Rutledge
Glenn Research Center, Cleveland, Ohio

M. Cales
Cleveland State University, Cleveland, Ohio

National Aeronautics and
Space Administration

Glenn Research Center

August 2001

Acknowledgments

This project was funded by NASA/University Joint Venture (JOVE) program. The work is under direct advisory of Dr. Marvin L. Illingsworth. His guidance, knowledge and help are greatly appreciated. I also owe my thanks to my committee members and chemistry department for their great support. Thanks to Dr. Bruce A. Banks and his co-workers at NASA for providing plasma ashing tests and taking photos on the 24 layer 10% $Zr(acac)_4$/PI (mol/mol) composite sample. Part of the calculations were done by them and is also appreciated. The elemental analysis and ^{1}H-NMIR results provided by Andrew Jensen of Astra Pharmaceuticals are greatly appreciated. Part of the work of Chapter IV is the reproduction of Shawn Wagner's research for verification purpose. Thanks to Shawn Wagner for his help. GPC analysis was done at Lucent Technologies. Thanks to RIT Microelectronic Engineering Department for letting me use their SEM. Thanks to everyone who helped me fulfill this thesis.

Available from

NASA Center for Aerospace Information
7121 Standard Drive
Hanover, MD 21076

National Technical Information Service
5285 Port Royal Road
Springfield, VA 22100

Available electronically at http://gltrs.grc.nasa.gov/GLTRS

TABLE OF CONTENTS

PAGE

Table of Contents …….. iii

Symbols ……. vi

PART I. Zirconium-Component Screening, Sample Fabrication, and Atomic Oxygen Testing of Multilayer Zr(acac)4/PMDA-ODA Polyimide Films

Chapter 1. Introduction: Atomic oxygen resistant polyimides …… . 1

Chapter 2. Multilayer Zr(acac)4 polyimide composites: Improved atomic oxygen resistance …… 7

Introduction …….. 7

Experimental ……. 7

Results …….. 12

Discussion ……. 18

PART II. Materials Science and Engineering Analysis of 10% (mol) Zr(acac)4/PMDA-ODA Polyimide Films

Chapter 1. Experimental …….. 22

Sample Preparation …….. 22

Mechanical Testing …….. 29

Plasma Ashing ……. 30

Scanning Electron Microscopy and Energy Dispersive Microscopy 30

Optical Microscopy …….. 31

Atomic Force Microscopy …… 32

Chapter 2. Results

Film Thickness ……. 32

Infrared Analysis …….. 32

Gravimetric method …….. 35

Profilometry …….. 35

Scanning Electron Microscopy …….. 36

Optical Microscopy …… 54

Atomic Force Microscopy …….. 63

Oxygen Plasma Resistance…….. 69

Mechanical Testing ……. 71

Chapter 3. Discussion

Sample Preparation …… 74

Mechanical Testing …… 74

Plasma Ashing …….. 75

Scanning Electron Microscopy and Energy Dispersive Microscopy 76

Optical Microscopy …… 78

Atomic Force Microscopy ……. 78

CONCLUSION …… 79

REFERENCES …… 81

APPENDICIES

Appendix A. Yang Chen, MS Project, "Zirconium-Containing Polymeric Materials" 83

Appendix B. X-ray Diffraction Data for the 24-layer 10% (mol) Zr(acac)4/PI Sample After Complete AO Ashing …….101

Appendix C. Juan A. Betancourt, MS Thesis, "Characterization of Kapton Polymer Containing an Inorganic Additive" ……..... 105

Symbols

η	Index of refraction
σ	Wavenumbers
μm	Micrometers
A^{o}	Angstroms
A	Appendix
AFM	Atomic force microscopy
AO	Atomic erosion
EDX	Energy dispersive x-ray
ISS	International Space Station
LN2	Liquid nitrogen
M	Number of fringes
N	Newtons
NMP	N-Methylpyrolidinone
ODA	Oxydi(4-aminophenyl)
PAA	Polyamic acid
PI	Polyimide acid
PMDA	Pyrometillic anhydride
SEM	Scanning Electron Microcopy
SPM	Scanning Probe Microscope

PART I. Zirconium-Component Screening, Sample Fabrication, and Atomic Oxygen Testing of Multilayer Zr(acac)4/PMDA-ODA Polyimide Films

Chapter 1. Introduction: Atomic Oxygen Resistance Polyimides (LH, YC)

The solar array for International Space Station (ISS) is being designed to provide the primary power for the first phase of the station.[1] A polyimide (PI) made from pyromellitic acid dianhydride (PMDA) and 4,4'-oxydianiline (ODA), trade name Kapton (Dupont), was the material originally selected for structural support of the solar cells for the flexible array. Its low density, flexibility, strength and thermo-stability make it a promising material for this application. However, it is readily oxidized by atomic oxygen in the Low Earth Orbit (LEO) environment.[2 - 4]

The existence of Atomic Oxygen (AO) in the LEO environment has been known for many years. However, it was not until the retrieval of the orbital hardware flown on the space shuttle in the early 1980s that an awareness of AO reaction with polymers in LEO became apparent.[5] Single, neutral oxygen atoms in the ground state are the most predominant species in LEO between altitudes of 180 and 650 km.[6] As spacecraft pass through the atmosphere at these altitudes, they collide with the oxygen atoms with an equivalent energy ranging from 3.3 to 5.5 eV.[6] These collisions are energetic enough to break many chemical bonds and allow the highly reactive AO to oxidize many organic and some metallic materials.[3] The volume of organic materials oxidized per incident AO atom, called the erosion yield, was found to be 3.0×10^{-24} cm^3/atom for Kapton.[7] When AO reacts with polymers it forms gaseous oxidation products (primarily CO) which results in material losses that can hinder system performance.[8] The ISS solar array is designed for a 15 years operating life in LEO. However, the oxidation rate of Kapton is great enough that structural failure of the blanket would occur in much less than 15 years. If a ISS photovoltaic array blanket was made of Kapton alone, it would be oxidized in six months, in spite of its 15-year durability requirement.[9]

Although efforts have been made to identify alternative materials which might be more durable to AO attack than Kapton, no satisfactory substitute has been found.[9]

Protective films containing a high fraction of metal oxides, such as SiO_2, fluoropolymer filled SiO_2, and Al_2O_3, have been demonstrated in both ground and space tests to be effective in protecting polyimide (Kapton) from oxidation by LEO AO.[9 - 11]

However, although such coating are themselves AO durable, defects in these coatings, which typically result from surface irregularities, contaminant particles, abrasion during processing and/or debris impacts in space, do allow AO attack of the underlying Kapton. Because unreacted AO can penetrate through defect areas on protective oxide coating, gradual undercutting occurs. Undercutting oxidation at defect sites ultimately leads to complete oxidation of the underlying Kapton if sufficiently high AO exposure occurs.[9]

To avoid the shortcoming of metal oxide coated Kapton, a modified Kapton designated as AOR (Atomic Oxygen Resistant) Kapton has been proposed as a back up material for the ISS solar array design.[6] It is a homogeneous dimethylpolysiloxane-polyimide film cast from a solution mixture and is manufactured by DuPont in an experimental batch process. The dimethylpolysiloxane is combined with the polyimide in an attempt to make the material resistant to attack by AO since polysiloxane forms silicon oxide upon AO exposure. Nonvolatile metal oxides, where the oxidation state of the metal matches the valence of its family in the periodic table, scatter AO upon collision and thus are highly resistant to AO attack. The ground-based plasma ashing tests performed at NASA showed that AOR Kapton represents a significant improvement in AO resistance over pure Kapton. The weight loss was between 10 to 17% that of unprotected Kapton in the plasma asher.[6] While this is a significant improvement, the material does degrade and eventually structurally fails upon arrival of between 7 and $10x10^{21}$ atoms/cm^2 of random atomic oxygen.[6] In addition, AO interactions with potential synergistic UV effects on silicon materials on LDEF have been shown to result in the formation of volatile vacuum condensable silicon intermediates. The deposition of a dark contaminant film on adjoining surface has potential for causing reduced solar illumination of the solar cells, which would greatly reduce the operating life of affected spacecraft.[12,13]

In 1993, Dr. M. L. Illingsworth found that a zirconium complex produced no volatile intermediates upon ground-based plasma AO exposure.[14] A sapphire disk located adjacent to a glassy film of the zirconium material bis(N,N'-disalicylidene-1,2-phenylenediaminato)zirconium(IV), $Zr(dsp)_2$, did not show any zirconium upon examination by x-ray photoelectron spectrometry (XPS).[14] This discovery set the stage for this project.

In addition, zirconium complexes were thought to have all other properties required for AOR materials:

a) ZrO_2 has standard formation free energy ΔG_f^o = -263 kcal/mol, and therefore is one of the most stable metal oxides;

b) Organically wrapped Zr complexes should blend well and thus distribute well in the polyamic acid of Kapton;

c) A ZrO_2 protective layer should form upon AO attack. If it cracks, more ZrO_2 will be formed by the exposed AOR polymer;

d) Zr is relatively abundant and is not expensive: Zr ranks 18th in terms of abundance in the earth's crust.[15, 16] 99.9% purity Zr is about $150/lb.[17]

Based on these judgments, John Terschak and Yang Chen tried to mix $Zr(dsp)_2$ with the polyamic acid (PAA) of Kapton in N-methylpyrolidinone (NMP) solution. However, very brittle films were obtained when the amount of $Zr(dsp)_2$ was increased to 4% (mol) Zr, a concentration which did not provide enough aerial density to form a protective layer when plasma etched.[18] It was readily recognized that phase separation and film quality were the main obstacles to achieving good AO resistance for the zirconium-containing polyimide materials.

In the 1996 MS thesis written by Liling He,[19] the solid state compatibility of other zirconium complexes with PI(PMDA/4,4'-ODA), and the AO resistance of these composite films, were investigated first (Chapter II). The Zr-containing candidates were dissolved in NMP and mixed with PAA(PMDA/4,4'-ODA)-NMP solution (DuPont), the structural precursor of Kapton. The highest concentration limit of any Zr complex tested was determined to be 10% (mol) $Zr(acac)_4$. Films of the 10% (mol) $Zr(acac)_4$/polyimide composite showed good uniformity, flexibility and tensile strength.[20] Upon forming a white zirconium dioxide protective layer on the surface, it demonstrated good AO resistance. Plasma ashing tests conducted at RIT showed promising results. Thus, a 24-layer 10% (mol) $Zr(acac)_4$ /polyimide sample was tested at the NASA Lewis Research Center, and demonstrated improved AO resistance by at least 20 fold. See Figure 1.1.

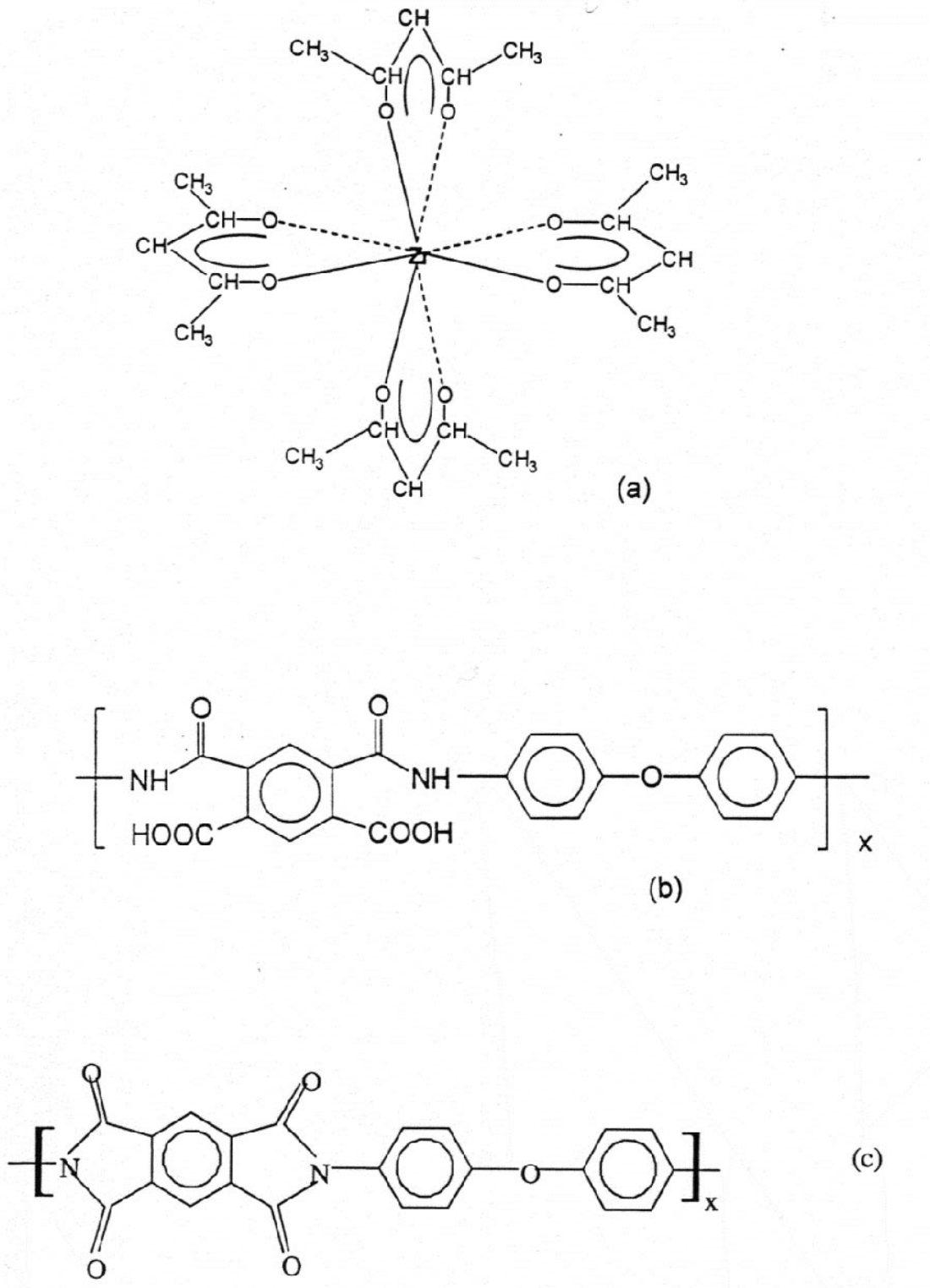

Figure 1.1 Structures of $Zr(acac)_4$ (a), polyamic acid of Kapton (b), and Kapton (c)

In order to increase the Zr concentration in commercial PAA (PMDA/4,4'-ODA) still further, the MS project written in 1996 by Yang Chen[18] describes additional screenings, to include two functionalized Zr complexes and two polymeric Zr-containing additives.

The zirconium complexes, bis(4-benzoyl-N,N'-disalicylidene-1,2-phenylenediamino)zirconium(IV), $Zr(bdsp)_2$, and bis(N,N'-disalicylidene-3,4-diaminopyridino)zirconium(IV), $Zr(dsdp)_2$, were prepared (see Appendix A), mixed, respectively, with commercial polyamic acid of Kapton, cast into films, and heated at 100°C, 200°C, and 300°C for one hour each to obtain Zr complex/polyimide Kapton composite films (see Figure 1.2).

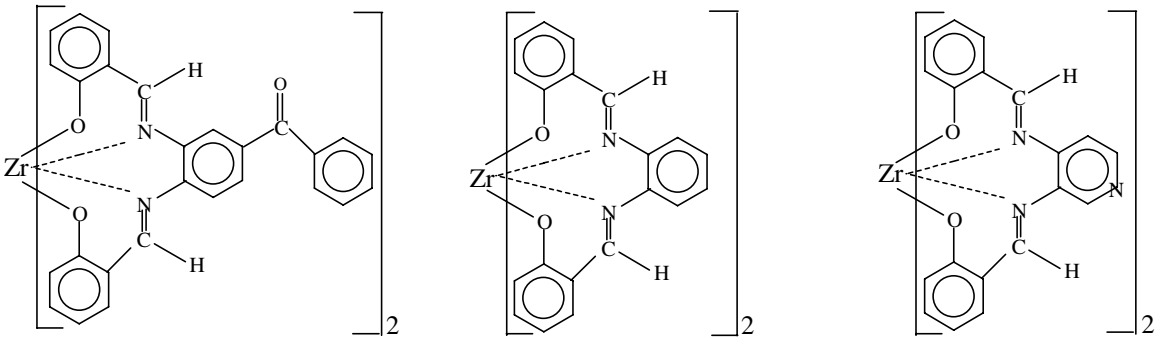

Figure 1.2. Structure of $Zr(bdsp)_2$ (a), $Zr(dsp)_2$ (b), and $Zr(dsdp)_2$ (c)

The coordination polymer, [bis(4-amino-N,N'-disalicylidene-1,2-phenylene-diamino)zirconium(IV) - pyromellitic dianhydride], $[Zr(adsp)_2\text{-PMDA}]_n$ [21] and the terpolymer $[Zr(adsp)_2\text{-PMDA-ODA-PMDA}]_n$ where ODA is 4,4'-oxydianiline, were synthesized, blended with the PAA, respectively, and treated as above (see Figures 1.3-1.5). As a starting point, the Zr concentration was set at 10% (mol) for the blends in each case.

The next chapter relates the details of the above work as performed by L. He, Y. Chen, and their collaborators.

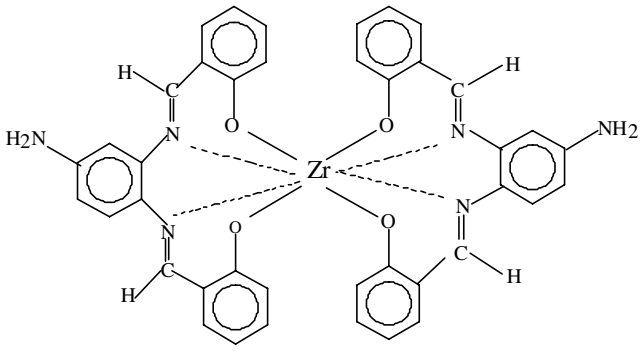

Figure 1.3. Structure of $Zr(adsp)_2$

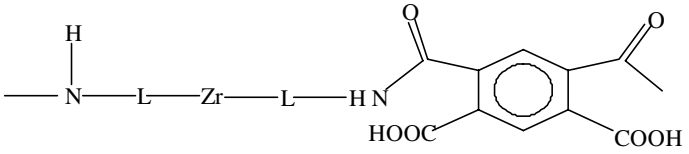

Figure 1.4. Structure of $[Zr(adsp)_2\text{-}PMDA]_n$ polyamic acid coordination polymer

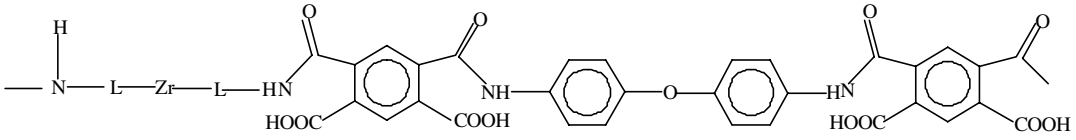

Figure 1.5. Structure of $[Zr(adsp)_2\text{-}PMDA\text{-}ODA\text{-}PMDA]_n$ polyamic acid terpolymer

Chapter 2. (LH, YC, MC)

Multi-layer $Zr(acac)_4$/Polyimide Composites: Improved Atomic Oxygen Resistance

INTRODUCTION

Of the eight zirconium complex candidates initially investigated by L. He, tetra(acetylacetonato)zirconium(IV), $Zr(acac)_4$, was identified as the best zirconium-containing component for enhancing polyimide atomic oxygen resistance. A simple method of film sample preparation was developed. Film samples were exposed to atomic oxygen in a RF plasma asher at RIT, and then at NASA Lewis Research Center, to simulate the survivability of the materials in the LEO (Low Earth Orbit) environment. Phase separation is proposed as the most likely reason why an upper limit of 10% (mol) $Zr(acac)_4$ can be incorporated into PMDA-ODA polyimide (Kapton structure) while maintaining good film quality.

EXPERIMENTAL

Inorganic Component Screening

Initially, eight inorganic components, $(Cp)_2Zr(Cl)(OAc)$, $(Cp)_2Zr(Cl)(H)$, $Zr(OBu)_4$, $Zr(ox)_2$, $ZrOCl_2.8H_2O$, ZrH_2, $Zr(dsp)_2$, and $Zr(acac)_4$ were mixed with commercially-obtained polyamic acid of Kapton solution (Pyralin, Pyre-ML RC5019, DuPont), respectively. See Figure 2.1. Films of these eight mixtures were cast onto glass slides using strips of adhesive tape on each side and clean glass slides to spread out the viscous liquid to a uniform thickness. The films were then imidized by baking at 100, 200, and 300 °C for one hour each.[22] Film quality was examined visually.

Starting Materials

Tetra(acetylacetonato)zirconium(IV) (Aldrich) was purified by recrystallization before use. Typically, 2.0 g $Zr(acac)_4$ (0.0041 mol) was dissolved in 3.0 mL of benzene. The solution was filtered to remove zirconium dioxide which had formed from the hydrolysis/decomposition of $Zr(acac)_4$. Then 2 mL of hexane was added into the filtrate. The solution was put in a refrigerator at 0°C for 30 minutes. White needle like crystals were formed, suction filtered and air dried. Melting point of the recrystallized $Zr(acac)_4$ was 192-194°C (literature, 195°C).[23]

The polyamic acid of Kapton (Dupont), 15.5% by weight solution in N-methyl-2-pyrrolidinone (NMP), was stored in cold room and used as received. NMP (Aldrich, anhydrous, sure seal) was used without further purification and was stored under slight positive pressure of nitrogen.

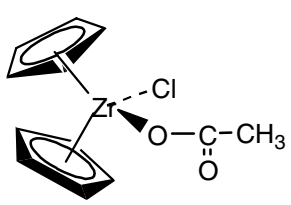

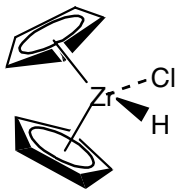

$Zr(OCH_2CH_2CH_2CH_3)_4$

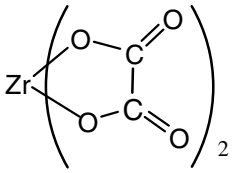

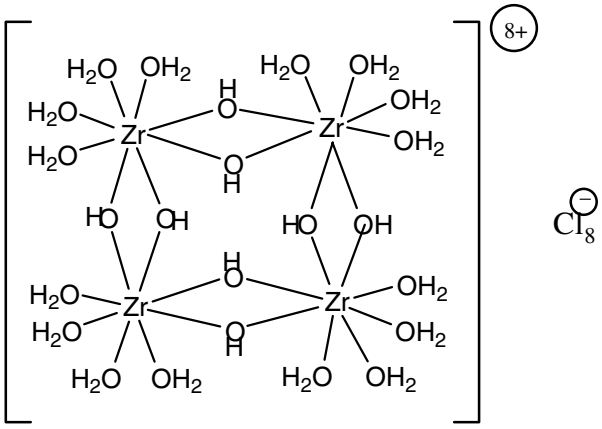

Cl_8^{-}

Figure 2.1. Structures of $(Cp)_2Zr(Cl)(OAc)$, $(Cp)_2Zr(Cl)(H)$, $Zr(OBu)_4$, $Zr(ox)_2$, and $ZrOCl_2.8H_2O$

$Zr(acac)_4$/Polyimide Composite Films

The $Zr(acac)_4$ /polyimide composite was made by dissolving recrystallized $Zr(acac)_4$ in NMP, mixed with commercial polyamic acid of Kapton as calculated and stirred for about 30 minutes.

10% mol Zr = moles of $Zr(acac)_4$ / [moles of $Zr(acac)_4$ + moles of mer unit PAA]

= (0.095/487) / [0.095/487 + (0.155)(x)/418]

where, x = 5.0000 g, the weight of commercial PAA solution used.

For typical 10% (mol) $Zr(acac)_4$ composite, 95.0 mg of $Zr(acac)_4$ was dissolved in 5.0 mL of NMP (12 h, with stirring) and mixed with 5.0000 g of commercial polyamic acid of Kapton. After standing for 1 h, the viscous solution was cast on a clean glass substrate to form a thin film. (The solution will completely gel if allowed to stand for 24 h.) Films were formed by uniformly spreading the above polymer solutions on glass plates using strips of adhesive tape on either side of the polymer solution and dragging a clean glass edge over the solution surface two or three times in the same direction.

The film was baked at 100°C, 200°C and 300°C for one hour each. Following the exact same procedure, the second layer film was cast on the top of the first layer, and so forth, using additional layers of adhesive tape. In one experiment this process produced a film having 24 layers.

Plasma Ashing Tests

The preliminary plasma ashing tests of 13-layer 10% (mol) $Zr(acac)_4$ /PI sample and pure polyimide Kapton were conducted at Rochester Institute of Technology in a SPI plasma asher. The pressure used is 80 mTorr. Two free standing films for each type of sample were ashed for taking average purpose. The dimensions of each sample were measured for calculating plasma exposure area. All four samples were weighed before ashing, and after 0.5, 1.5, 2.5, 3.5, 5.0, 7.0, 9.0, and 11.0 hours of ashing.

The atomic oxygen durability of the 24 layer composite was further evaluated in a plasma asher (SPI Plasma Prep II) at NASA Lewis Research Center. The asher used a 13.56 MHz RF discharge to create an air plasma of oxygen and nitrogen ions and atoms in various energy states in a glass sample chamber kept at 80-100 mTorr. A graphite witness coupon placed on a glass substrate was ashed alone before the actual sample was

ashed to determine the flux and examine the contamination of the asher. The evaluation of the composite was performed with a Kapton witness coupon in the asher during testing. Both the sample and the witness coupon were placed in a vacuum desiccator to remove moisture (to constant mass) before ashing. The dimensions of the witness coupon were measured for calculating fluence of atomic oxygen and the thickness of the 24-layer composite sample was also measured by Sloan Dek Tac II profilometer. The exposure of the sample was continued until only little amount of brown color remained on the glass substrate. Photos were taken of the sample before, during and after plasma ashing.

Solar Absorptance and Emittance

Solar absorptance between 250 and 2500 nm and emittance at 9 μm were determined for unexposed PMDA/4,4'-ODA polyimide, unexposed 10% (mol) $Zr(acac)_4$ in PMDA/4,4'-ODA polyimide, and atomic oxygen exposed 10% (mol) $Zr(acac)_4$ in PMDA/4,4'-ODA polyimide film samples using a Lambda 9 spectrophotometer.

Scanning Electronic Microscopy (SEM) Study

The surfaces of the single layer 10% (mol) $Zr(acac)_4$/PI sample before and after two hours of plasma ashing were examined by SEM. Spot size used was 500, KV setting was 30kv and the magnifications were 320 and 2,500.

Additional Screening

Zirconium complexes, bis(4-benzoyl-N,N'-disalicylidene-1,2-phenylenediamino)zirconium(IV), $Zr(bdsp)_2$, and bis(N,N'-disalicylidene-3,4-diaminopyridino)zirconium(IV), $Zr(dsdp)_2$ were prepared as described in Appendix A, and mixed, respectively, with commercial PAA to form composites having functionalized Zr complex components.

The Zr complexes $Zr(bdsp)_2$ and $Zr(dsdp)_2$ were separately dissolved in a small amount of solvent (NMP) and mixed with commercial polyamic acid (PAA) of Kapton in NMP (DuPont). For example, 0.0556 g of $Zr(bdsp)_2$ in 2.00 mL NMP was mixed with 4.000 g of PAA (15.5% solids) in NMP to make 4% (mol) Zr solution. Films were prepared from these solutions on glass substrates, and then imidized by baking at 100°C,

200°C and 300°C for one hour each[21] to produce the Zr-PI composites. The concentration of each complex could be increased to 4% (mol) Zr before the films cracked upon imidization.

The $[Zr(adsp)_2\text{-}PMDA]_n$ coordination polymer was prepared as reported previously.[20] The terpolymer was prepared as described in Appendix A. The two polymers were dissolved in NMP, respectively, to make 15 wt.% solutions and mixed with commercial PAA in NMP also 15 wt%. The Zr mole percentage of the two polymer blends was 10% (mol) Zr for each solution. The preparations of the solutions are described below.

One gram of coordination polymer (mer unit molecular weight MW = 968) was dissolved in 5.7 mL NMP, yielding a 15 wt.% solution. The solution was then mixed with 26 gram 15 wt.% commercial polyamic acid of Kapton to obtain a 10% mol Zr blend polymer solution to be used in film formation.

10% mol Zr = moles of mer unit coord.polymer / [moles of mer unit coord. polymer + moles of mer unit PAA]

= (1/968) / [1/968 + (0.15)(x)/418]

where, x = 26 g, the weight of commercial PAA solution used.

In the same way, for one gram terpolymer (repeat unit MW = 1386), 5.7 mL NMP and 18 gram PAA were used to make 10 % mole Zr blend polymer solution to be used in film formation.

The two types of polymer blend films were cast on glass plates using the technique described above. Using a standard imidization procedure,[22] the films were heat-treated at 100°C, 200°C, and 300°C for one hour each. This film preparation procedure was repeated to make multilayer film samples until crack formation was observed.

The thickness of the films was measured using a profilometer (Dektak M-611, see lab notebook YC-II-30). The surface of the single layer coordination polymer blend and terpolymer blend which contain 10% (mol) Zr were examined by SEM (Philips 501 scanning electron microscope) before and after two hours of plasma ashing.

Samples were coated with approximately 100 angstroms of gold. KV setting was 30kv and the magnification was 10,000.

RESULTS

Inorganic Component Screening

From the total of ten zirconium compounds and two coordination polymers examined, $Zr(acac)_4$ is found to be the best additive for the commercial PAA(PMDA-ODA) of those used in this study. $(Cp)_2Zr(Cl)(H)$ reacts with the polyamic acid and forms gel. Small amount of ZrH_2 decreases the viscosity of the polyamic acid solution dramatically making it very difficult to cast a good film. At a concentration of only 4% (mol) Zr, films of $Zr(dsp)_2$, $Zr(bdsp)_2$, and $Zr(dsdp)_2$ (see Figure 1.2) each show significant cracking upon imidization. Addition of $Zr(OBu)_4$, $Zr(ox)_2$, and $ZrOCl_2.8H_2O$ to the polyamic acid either caused films to become brittle or scorched during imidization, and are not suitable for this study.

Inherent viscosity, $[\eta]_{inh}$, was 0.12 dL/g and 0.45 dL/g for coordination polymer and terpolymer, respectively. The inherent viscosity of the precursor $Zr(adsp)_2$ was 0.015 dL/g. The viscosity of $Zr(adsp)_2$ and the coordination polymer are a little different from that previously published.[21] The first layers of film for each blend containing 10% (mol) Zr were homogeneous. The thickness of the first layer in each case was about 8.0 mm on average. No visible phase separation was observed. No cracks were apparent in either film after imidization. However, cracking occurred upon imidization after applying the second layer to the film in most cases.

$Zr(acac)_4$/polyimide Composite Films

The upper limit of $Zr(acac)_4$ that can be incorporated into a polyimide film and still maintain the good flexibility of the film is 10% by mole. Beyond that, the composites show an unacceptable degree of brittleness. Composite films having this composition have to be made very thin, otherwise, the films crack after imidization. The viscosity of the composite solution is another important factor for forming good films. Solutions with very high viscosity tend to form thick films which will crack after imidization; however, solutions that are too dilute do not stay in place on the substrate

well which often causes the non-uniformity of the films. Practically, for 10% by mole of $Zr(acac)_4$ composites, 1 mL of $Zr(acac)_4$ in NMP solution mixes with 1 gram of commercial polyamic acid of Kapton produces the best results. Aging of the composite solution is another important factor. Let the composite solution age for one hour before making film will help achieve better uniformity of film. Gel is formed if the composite solution is allowed to sit over 24 hours.

Plasma Ashing Test

1. Preliminary plasma ashing test at Rochester Institute of Technology

Figure 2.2 displays the mass loss per unit area versus plasma exposure time of pure Kapton and 10% (mol) $Zr(acac)_4$/polyimide composite. It is clearly seen that the mass loss of 10% (mol) $Zr(acac)_4$/polyimide composite is much slower compared to pure polyimide. Figure 2.3 is a plot of percentage of mass remaining of pure polyimide and 10% (mol) $Zr(acac)_4$/polyimide composite. About 50% of mass remains for 10% (mol) $Zr(acac)_4$/polyimide composite whereas everything was gone for pure polyimide.

After plasma ashing, white zirconium dioxide layer was observed on the surface of brown 10% (mol) $Zr(acac)_4$/polyimide composite, which retards the erosion of underlying polymer.

2. Plasma ashing test at NASA Glenn Research Center

a). Visual observation

The original 24-layer 10% (mol) $Zr(acac)_4$/PI sample has a darker brown color than pure Kapton. During first 4 days of ashing, there was no significant change on the surface. On the fifth day, chalky white tint appeared and covered the whole top surface of the sample. The sample under the white layer appeared to be darker than originally. For the next 7 days, the sample looked very similar to the 5th day. On the 13th day, the

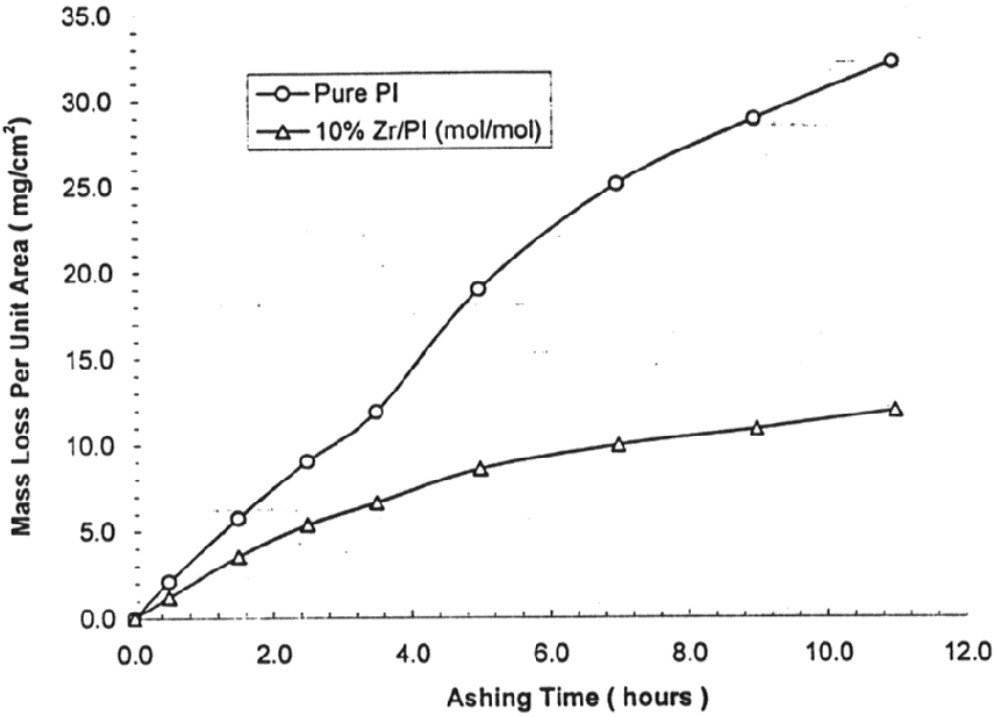

Figure 2.2 Mass loss per unit area versus plasma exposure time of pure polyimide (PMDA/4,4'-ODA) and 10% (mol) $Zr(acac)_4$/PI composite

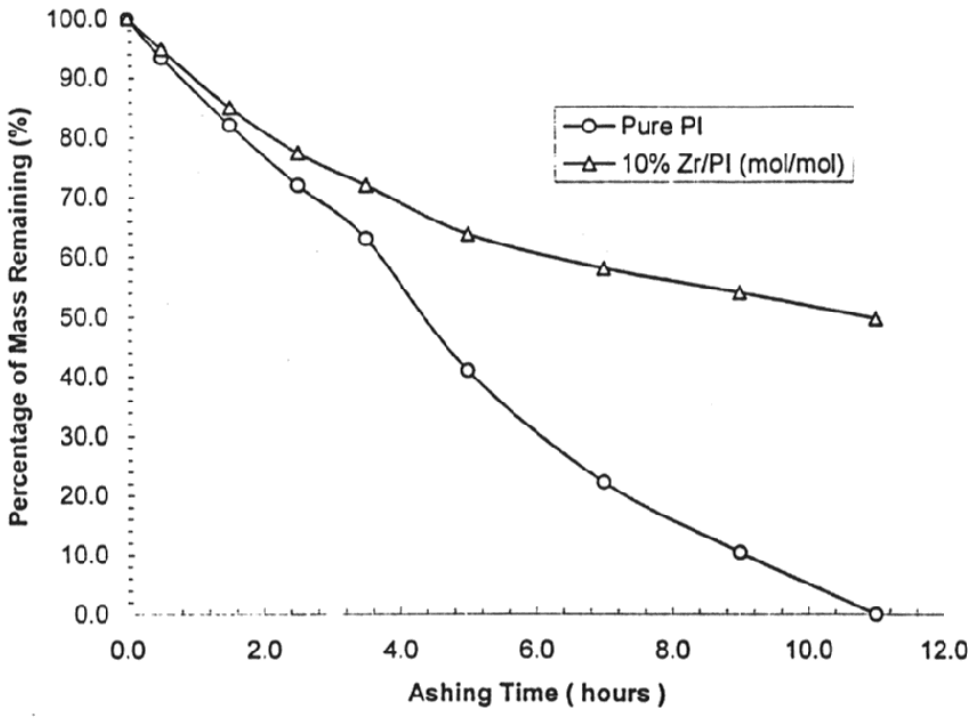

Figure 2.3 Percentage of mass remaining per unit area versus plasma exposure time of pure polyimide (PMDA/4,4'-ODA) and 10% (mol) $Zr(acac)_4$/PI composite

polymer had rough appearance around edges. On the 19th day, sample looked like before but seemed to be thinner in some areas. On the 23rd day, the sample was still dominated by a dark brown appearance with white coating, but some edge areas started to show white with no dark brown color. On the 30th day, sample showed more white on the surface, and there was no brown color left in the part of the central area. Above 90% of the area still had intense dark brown color. On the 44th day, about 75% of the area still had brown polymer under white protective layer. The ashing was continued to 106.5 days, when 80% of the area was covered by pure white layer.

b). Fluence, flux and erosion yield

Fluence is the number of oxygen atoms arriving at a unit area of sample in the plasma asher. Flux is the number of oxygen atoms per unit area per second in the plasma asher. Fluence equals to flux multiple by time. The volume of organic material oxidized per incident atomic oxygen atom is called erosion yield. The erosion yield for polyimide Kapton is 3×10^{-24} cm^3/atom.[7]

Fluence and flux of the plasma asher used at NASA was determined by using the following equations:

$$\text{Fluence} = \frac{\Delta \text{ mass}}{\text{area} * \rho_{\text{kapton}} * E_y} \qquad (1)$$

$$\text{Fluence} = \text{flux} * \text{time} \qquad (2)$$

where, Δ mass = mass loss of samples

area = exposed area of samples

ρ_{kapton} = density of Kapton (1.42 g/cm^3)

E_y = erosion yield of Kapton (3×10^{-24} cm^3/atom)

The mass of the pure Kapton sample (1" diameter) before exposure was 36.923 mg and became 11.087 mg after exposed for 180,300 seconds, i.e., 50 hours.

Change in mass of sample = 11.087 mg - 36.923 mg = -25.836 mg

= -0.025836 g

Area of exposure = Π * (1 inch * 2.54 cm/inch/2)^2 = 5.07 cm^2

Time of exposure = 180,300 seconds

According to equation (1), fluence = 1.19×10^{21} atoms/cm^2

According to equation (2), flux = 6.63×10^{15} atoms/cm^2.second

The flux value agrees well with other flux values determined experimentally using the same asher in past experiments.

The thickness of the 24-layer 10% (mol) $Zr(acac)_4$/PI composite sample measured by profilometer is 0.032 mm. The cumulative plasma exposure time and fluence on the 24-layer 10% (mol) $Zr(acac)_4$/PI composite sample is 9,205,500 seconds and 6.10×10^{22} atoms/cm^2, respectively. The erosion yield can be calculated by using equation (5) obtained as follows:

From equation (1), we have

$$\text{Fluence} = \frac{\Delta \text{ mass}}{\text{area} * \rho_{\text{kapton}} * E_y} \qquad (3)$$

Since Δ mass = area * Δ thickness * ρ (4)

From (3) and (4), we have

fluence = Δ thickness / E_y

i.e., E_y = Δ thickness / fluence (5)

From equation (5), the erosion yield of the 24-layer sample is calculated to be 5.3×10^{-26} cm^3/atom.

c). Comparison with pure polyimide Kapton

Experimentally, pure polyimide Kapton with similar thickness as 24-layer 10% (mol) $Zr(acac)_4$/PI sample was all eroded away in about 2 days in the same asher.

The actual time needed to erode pure polyimide Kapton with exactly same thickness as 24-layer 10% (mol) $Zr(acac)_4$/PI sample can be calculated as well.
From equation (2) and (5), we can get

time = Δ thickness / (E_y * flux) (6)

Therefore, time needed to erode unprotected Kapton with same thickness of the original $Zr(acac)_4$/polyimide composite sample is:

$$\text{time} = \frac{0.00324\ \text{cm}}{3\times10^{-24}(\text{cm}^3/\text{atom})*(6.63\times10^{15}\text{atoms/cm}^2.\text{second})}$$

= 162,987 seconds = 45.27 hours, about 2 days!

The pure Kapton with the same thickness can only last for less than two days, while the 24-layer 10% (mol) $Zr(acac)_4$/polyimide sample lasts for 106.5 days, the endpoint being the loss of color due to polymer. Only a white residue remained where x-ray diffraction analysis showed that minimal crystallinity was present. See Appendix B. Considering after about 40 days, the polymer around the edge was eroded away, the actual exposure area became less the than original. This would result in decreased erosion rate, however, even if we discount the total exposure time to 40 days, the $Zr(acac)_4$/polyimide sample still has improved the duration of atomic oxygen resistance by 20 times.

Solar Absorptance and Emittance

The Solar Absorptance and Emittance data for unexposed PMDA/4,4'-ODA polyimide, unexposed 10% (mol) $Zr(acac)_4$ in PMDA/4,4'-ODA polyimide, and atomic oxygen exposed 10% (mol) $Zr(acac)_4$ in PMDA/4,4'-ODA polyimide film samples are summarized in the Table.

ABSORPTANCE AND EMITTANCE DATA FOR RIT ZIRCONIUM COMPLEXES

SAMPLE	SOLAR ABSORPTANCE	EMITTANCE AT 9 μm
#1: PAA Unimidized Kapton	0.16	0.89
#2: PAA Imidized Kapton	0.34	0.88
#3: 10% Zr in Kapton	0.36	0.88
#4: 10% Zr in Kapton with 3 hrs ashing	0.39	0.88
#5: 10% Zr in Kapton with 6 hrs ashing	0.41	0.89
#6: 10% Zr in Kapton with 9 hrs ashing	0.34	0.89
#7: 10% Zr in Kapton with 16 hrs ashing	0.08	0.88

Scanning Electronic Microscopy (SEM) Study

Figure 2.4 is the SEM picture of 10% (mol) $Zr(acac)_4$/polyimide before ashing and after ashing. Although 10% (mol) $Zr(acac)_4$/polyimide doesn't have visible phase separation, there is evidence under SEM with only 320 magnifications that phase

separation may be occurring. After 3 hours plasma ashing, there is no change on the surface visually, however, the surface has been roughened dramatically as observed under SEM with 2,500x magnification.

DISCUSSION

Inorganic Component Screening

Of the total ten zirconium compounds and two coordination polymers examined, $(Cp)_2Zr(Cl)(H)$ and ZrH_2 are too reactive to form good composites with the commercial PAA of Kapton used in this study. The gelation of polyamic acid of Kapton upon the addition of $(Cp)_2Zr(Cl)(H)$ is probably due to crosslinking. ZrH_2 may act as chain scissioning reagent which lowers viscosity dramatically. The mixtures of $Zr(OBu)_4$, $Zr(ox)_2$, $ZrOCl_2$ 8H2O, $(Cp)_2Zr(Cl)(OAc)$ with polyamic acid of Kapton produce films of poor quality either because of poor thermal stability or poor dispersity. The upper concentration limit of 4% (mol) Zr in films of $Zr(dsp)_2$, $Zr(bdsp)_2$, and $Zr(dsdp)_2$ (see Figure 1.2) is not high enough to provide sufficient Zr aerial density. The protective oxide layer would form too slowly to protect the Kapton.

The inability of Zr terpolymer/PAA and coordination/PAA solutions to allow multilayer film fabrication at 10% (mol) Zr likewise prevents sufficient aerial density of Zr to be achieved in the sample for generating a protective oxide layer. SEM pictures of 10% (mol) Zr terpolymer/PI and coordination/PI films show that their surfaces are smooth, without any apparent phase separation. There exist some bubbles, probably due to solvent or water vapor formed in the imidization process. After two hours etching, the surface of coordination polymer appears roughened. There were more irregular pits on the surface of terpolymer. In addition to blend compatibility, the rate of atomic oxygen diffusion into the surface is thought to be a factor in how pits form.

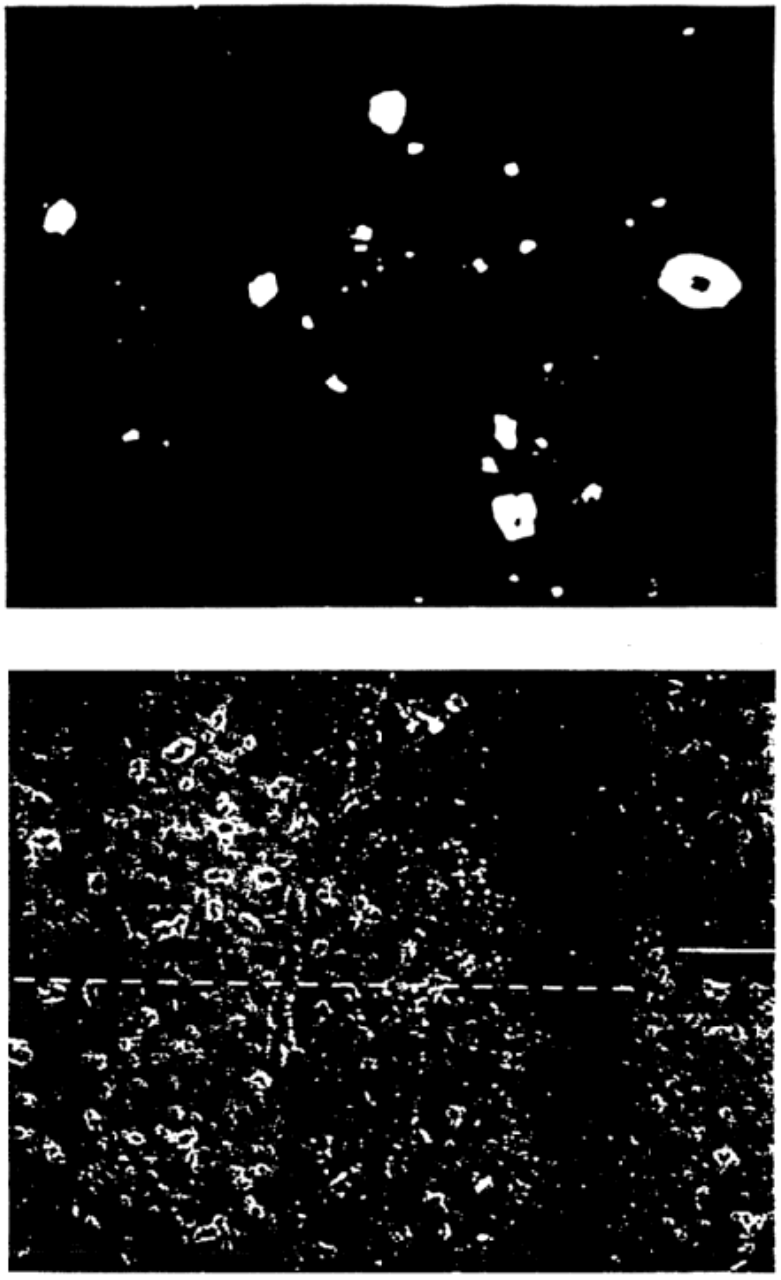

Figure 2.4. Scanning Electron Microscopy pictures of 10% (mol) Zr(acac)4/PI composite before (top) and after 3 hours plasma ashing (bottom)

The reason that $Zr(acac)_4$ is the most promising candidate tested so far may be attributed to the hydrogen bonding that is likely to occur between the acetylacetonato ligand and the polyimide.

$Zr(acac)_4$/polyimide Composite Films

It is found that $Zr(acac)_4$ has the ability to increase the viscosity of $Zr(acac)_4$/polyamic acid NMP solution. Qualitatively, the more $Zr(acac)_4$ is added into polyamic acid, the more viscous the mixture appears to be. Suitable amounts of hydrogen bonding may help the distribution of $Zr(acac)_4$ throughout polyamic acid matrix; however, excessive hydrogen bonding may increase viscosity dramatically and affect the final quality. At about one hour, a suitable amount of hydrogen bonding has been formed which gives the best $Zr(acac)_4$ distribution and optimum viscosity for film-making. After 24-hour aging, 10% (mol) $Zr(acac)_4$/polyimide forms one big chuck of gel, very likely, due to excessive hydrogen bonding.

Thick films crack during imidization. Probably, if the film is too thick, water generated from the imidization reaction becomes trapped within the film and causes local degradation at this elevated temperature (300°C). To generate reasonably thick films, the method of "multi-layers of thin film" should be employed to obtain good film quality.

Solar Absorptance and Emittance

The emittance data shows very little change. Emitance data usually does not change much upon AO exposure in an asher for materials that are already rough. This may be because the surface texture cannot be further increased, and emittance is driven more by gross surface morphology. The solar absorptance for the zirconium complex seems to be a little higher than that for the polyimide controls and increases slightly with atomic oxygen exposure until the polyimide is attacked. At 16 h of ashing, all that is left is an ash of the inorganic component which is less absorbing than the original polyimide.

Scanning Electronic Microscopy (SEM) Study

The SEM picture of 10% (mol) $Zr(acac)_4$/polyimide composite reveals its heterogeneous characteristics. $Zr(acac)_4$ reacts with water in the NMP to form clusters (see **Part II** of this NASA Technical Memorandum). After AO exposure the film surface appears roughen, as expected. What is not apparent in this SEM photograph is that the roughened surface now appears white, due to zirconium oxide formation.

PART II. Materials Science and Engineering Analysis of 10% (mol) $Zr(acac)_4$/PMDA-ODA Polyimide Films (JAB)

Chapter 1. Experimental

This chapter will include all parameters, techniques, procedures and equations used in testing the films of PMDA-ODA polyimide and $Zr(acac)_4$/PMDA-ODA polyimide composites.

Sample Preparation

Samples were made as films on a glass substrate, then peeled off for later study. Of the different substrates that could be used, glass was chosen because it provides the smoothest surface possible to make more uniform films at lowest cost. Other types of substrates could be used, such as silicon wafers. To prepare samples of sufficient size, mirrors with the back scrapped off are used. These mirrors were about 5 by 10 inches and commercially available.

Before the polymer composite solutions are made using the complex, the purity of the complex was checked using two tests. One of the tests checks the melting point of the complex, which should be 195°C.[23] The other test is that the complex dissolves completely in benzene. Particulate impurities will be seen in the bottom of the vial when dissolving in benzene since they are not soluble in the solvent.

In case the purity of the complex is not correct, that is a melting point below 195°C or it does not completely dissolve in benzene, the following procedure was used to purify the complex:

1. Weigh desired amount of the complex and dissolve in benzene.
2. Filter to remove the insoluble impurities.
3. Add hexane to the remaining solution to precipitate the complex.
4. Let the solution stand for about 3-4 hours, if necessary in a refrigerator.
5. Filter and collect the solid which is a more pure complex.
6. Verify purity. If still under desired purity, repeat procedure. This refers to melting point and impurity filtration.

Samples containing the complex were prepared as follows: the complex which is a solid was dissolved in a solvent, in our case 1-methyl-2-pyrollidinone (NMP), using the following dilution factors.

Table 1 . Dilution factors for preparing samples with $Zr(acac)_4$ complex.[19]

Percent by mass $Zr(acac)_4$ in PAA	Grams of complex $Zr(acac)_4$	mL of NMP	grams PAA solution ~ 15.5% solids
2	0.02	4.0	5.0
4	0.04	6.5	5.0
6	0.06	7.0	5.0
8	0.08	7.5	5.0
10	0.10	8.0	5.0

The amount of complex needed for preparing the solutions, using as basis 5 g of the polyamic acid, were calculated using the following 2 equations:

$$\text{Zr Mole \%} = \frac{\text{(moles Zr)}}{\text{(moles Zr + moles PAA)}} \qquad (1)$$

$$\%\ Zr(acac)_4 = \frac{\text{moles } Zr(acac)_4}{\text{(moles Zr + moles PAA)}}$$

to simplify moles $Zr(acac)_4$ = moles Zr

moles Zr = (% Zr) x (moles Zr + moles PAA)

(% Zr) x (moles PA) = moles Zr (1- % Zr)

$$\text{moles Zr} = \frac{\%\ Zr}{(1-\%\ Zr)} \times \text{(moles PAA)}$$

$$g\ Zr = \frac{\%\ Zr}{(1 - \%\ Zr)} \times \text{(moles PAA)} \times MW\ Zr(acac)_4$$

$$g\ Zr = \frac{\%\ Zr}{(1 - \%\ Zr)} \times \frac{g\ PAA}{MW\ PA} \times MW\ Zr(acac)_4$$

$$g\ PAA = (g\ solution) \times (\%\ solids)$$

Therefore:

$$g\ Zr(acac)_4 = 487 \times \frac{\%\ Zr}{(1 - \%\ Zr)} \times \frac{g\ solution \times \%\ solids}{MW\ PAA} \qquad (2)$$

Equation 2 calculates the amount of the complex in grams from the rearrangement of equation 1 and the conversion of moles to grams. The 487 is the molecular weight of the complex and the percent of solids come from the fact that the PAA is in a solution of PAA and NMP solvent, obtained from DuPont. From empirical observation, the dilution volumes include 1-2 mL of solvent to make solutions less viscous and make the films easier to prepare.[19]

After the Zr solutions are made they are added to the PAA solutions, mixed well and allowed to stand for about 30 minutes. This standing allows the solution to attain the perfect viscosity to prepare the films. After heating at 100°C for 1 hour, 200°C for 1 hour and 300°C for another hour,[22] the 2% Zr/PAA becomes 2% Zr/PI. Once the films are on the substrate, they are exposed to the imidization process.

The substrate surface is cleaned before the solution is applied to reduce the presence of dust particles or impurities that might affect the film preparation. After the surface is clean, layers of tape are applied at both sides of the substrate, making a channel in the middle of it. The amount of tape applied to the substrate determines the thickness of the film to be obtained. After the tape is in place, the polyamic acid solution is poured into the channel between the two layers of tape and spread using a glass slide that is run from side to side over the tape layer. See Figure 26. The amount of solution applied to the glass slide is close to 2 g from the 5 g prepared.

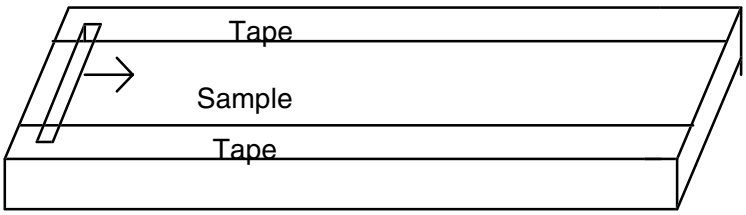

Figure 26. Technique to make films over glass substrate.

The glass slide is moved from one end to the other using a clean slide for each pass. This procedure reduces nonuniformities and removes more sample than expected due to surface tension. After the third or fourth pass the slide should be clean i.e., no polyamic acid should be observed adhering to the slide. The film produced is observed visually and when it seems to be uniform enough, the strips of tapes are removed. Then, the substrate containing the film is ready for imidization.

Some steps are needed in this procedure, such as the film has to be heated for at least one hour at each temperature and not removed from the furnace to assure its complete imidization. Also, a rack was made in order to have all samples exactly horizontal and made at the same time in order to reduce errors caused by different heat treatments of the samples.

Heating for less time will reduce the film's tensile strength properties. The time required to change from one temperature to another is not included in the heating times. Another precaution is to exercise care when removing the substrate from the furnace because sudden changes in temperature might cause the substrate to break and generate deformities or cracks in the film produced. After the samples are heated at 300°C for one hour, they are left inside the oven after the oven is turned off until the temperature drops to around 200°C.

When the film is formed it can be removed from the substrate by two methods; method one consists of soaking the sample in water. Because of the affinity of water for the glass surface, the film peels off of the mirror. Films obtained in this way are easier to handle and come off in one piece. The other technique consists of peeling the film using a razor blade. This method causes the film to roll over on itself and might cause breaks at different points. The first technique is preferred. It is observed that cutting the samples to

the desired size while they are attached to the substrate is better than preparing them from free standing films, because they are easier to handle.

To obtain the thickness of these film samples, the first method used was Infrared Analysis (IR). The instrument used was a Perkin Elmer 681IR. A film sample was put in the trajectory of the light beam and the interference pattern generated by the film was recorded in a plot. From the spectrum generated, the thickness of the film was calculated using the following standard formulas:

$$b\ (cm) = (m/2\eta)\ (1/(\sigma_1 - \sigma_2)) \qquad (3)$$

$$b\ (cm) = (m/4\pi\eta)\ (\lambda_1\ \lambda_2/(\lambda_1 - \lambda_2)) \qquad (4)$$

where m: number of fringes between σ_1 and σ_2, or between λ_1 and λ_2

η: index of refraction (1 for air, 1.6 for polystyrene).

σ: wavenumbers (cm^{-1})

λ: wavelength (μ)

First, a known sample of polystyrene is used as a standard for calibration. Since we know the value of the thickness for the polystyrene film any correlation factors can be determined for the unknown before it is analyzed.

A second method for measuring the thickness of films is the gravimetric method. Here a film of known dimensions is placed in a beaker full of water. Since the film is more dense than water it goes to the bottom. Another solution is prepared that has a density higher than water and higher than the film's.

The solution made was one of potassium iodine (KI). When the solution of KI is added to the beaker with water and the film, the film will start floating in the solution until the density of the film equals the density of the solution. At this moment the film will be suspended in the solution. Mathematically the thickness of the film can be determined from the following equations:

$$\rho_f = \frac{mass_f}{vol_f} = \frac{mass_f}{w*l*h} \quad (5)$$

where: ρ_f = density of the film

w = width of the film

l = length of the film

h = height of the film

$$\rho_f = \frac{mass\ solution}{vol\ solution} \quad (6)$$

$$\frac{mass_f}{w*l*h} = \frac{mass\ solution}{vol\ solution} \quad (7)$$

Rearranging we obtain:

$$h = \frac{vol\ solution\ x\ mass_f}{mass\ sol\ x\ l\ x\ w} \quad (8)$$

A third method, and the preferred one, was profilometry, because it is faster and very accurate. Once the films are obtained, their thickness is measured using a profilometry instrument. See Figure11. A Sloan Dektak is used. This is an instrument for measurement of surface profiles and surface elevations from a minimum of 25 A° up to a maximum of 1,000,000 A°. In this method, films on a substrate are placed over a movable platform, where a stylus lays on top of the film. When the platform moves it will cause the spindle to move over the film surface until it reaches its edge and falls onto the substrate surface. There is no special sample preparation other than to have a nice cut edge in the film.

The fall over the edge is recorded on a chart and the reading is then converted to the thickness of the film using the appropriate conversion factors. Several points are taken all over the film to observe its thickness variation.

Once the films were prepared and their thickness measured, they were cut using the following dimensions: six inches long by half an inch wide. These dimensions were the required size for mechanical testing and convenient for plasma ashing.

The best time to cut the samples is while still adhered to the substrate. Using a sharp razor blade the film is then cut to the desired dimensions. After the samples were cut, they were stored in vials to avoid water absorption. Before any testing is done the films were placed in a vacuum for 24 hr to remove any water collected in the surface of the films.

Error Propagation for Film Thickness[24,25]

No matter how well the measurements are taken, there are always uncertainties in the final results due to a wide range of errors. Some of these errors are systematic and others are random.

Systematic errors are due to equipment setup or procedure and it shows when a value is far from the others. The only way to see this is when you compare the value with a theoretical one.

Random errors, on the other hand, can be measured and are usually a good measure of the range of reasonable values associated with a measurement or calculation.

In most experiments you measure more than one parameter, some errors might cancel out while others are additive. Since the primary goal of most experiments is to calculate the final result from the experimental measurements, the error must be propagated along with the experimental value, so that the final answer contains an uncertainty value.

Some measures of random errors are: instrument limit error, estimated uncertainty and estimated uncertainty in repeated measurements. In our set of experiments, the error can be either instrumental or estimated uncertainty in repeated measurements.

This error can be calculated by taking half the difference from the extreme values taken, like maximum or minimum values.

$$\text{Error(uncertainty)} = 1/2(x_{max}-x_{min}) \qquad x\text{:variable in question} \qquad (9)$$

This error was seen when taking the film thickness using the profilometer. The systematic error comes from lifting and releasing the needle for the multiple measurements. For our case, the error will be:

$$\text{Error(uncertainty)} = 1/2(x_{max}-x_{min})\mu m \qquad (10)$$

Mechanical Testing

Sample sizes follow ASTM standards and industry testing techniques used by Dupont. Distance between grips is not less than 1 in, chart speed and rate of elongation are set to 20 mm/min and 2 mm/min. Sample dimensions are 0.5 in width, between 4 and 6 inches in length and thicker than 1 mil. Parameters used resemble also the ones found in the literature.[26]

Pneumatic grips were used to provide a superior grip. A minimum of 3 samples for each different film concentration were analyzed. The values for the three samples of each concentration were then averaged to obtain the values of tensile strength and ultimate strength.

The following equations were used to calculate the stress and strain of the films:

$$\text{stress} = \text{load} / \text{area} = \text{load(lb)} / (\text{thickness}_f * \text{width}) \qquad (11)$$

$$\text{strain} = \Delta l / l_0 \qquad \Delta l = \text{change in length}, \; l_o = \text{original length} \qquad (12)$$

$$\text{strain} = \text{reading(in)} / 50.8 \qquad (13)$$

$$\text{stress} = (\text{kg}) * 2.2 / (\text{width} * \text{thickness}) = x\ (\text{lb}) / (w * t) \qquad (14)$$

Plasma Ashing

The operation of the plasma asher consists of loading the object to be processed, evacuating the reaction chamber, applying the process gas and applying the energizing RF power. The RF amplifier must be resonated and power level adjusted to the appropriate level to give a stable, high flux plasma. Upon completion of the process, the

RF power switch is turned off. The power must remain on in order to return the chamber to atmospheric pressure.

The films were cut as coupons of about 0.5 x 0.5 inches and placed on the center of a quartz boat on top of glass slides. The position of the samples in the boat corresponds to the locations of greatest plasma uniformity in the chamber, which is 1 inch away from the door and provides the best exposure to atomic oxygen. The gas used was oxygen.

Samples were exposed to the atomic oxygen plasma and monitored at different intervals of time. After these intervals the films were placed for 5 minutes in a vacuum desiccator to remove water absorbed in their handling, and then promptly weighed. Analyses were performed in triplicate to compare the behavior of films containing 2-10 % (mol) complex and to correlate this behavior to that of commercial film. The weights and times used in the Results Section were based on:

weight : weight sample - weight glass slide (15)
time: minutes

Normalization (due to different original weights):

weight : weigh sample / original weight (16)
time: minutes

Scanning Electron Microscopy and Energy Dispersive Techniques

For Scanning Electron Microscopy and Energy Dispersive Spectroscopy, films of 1 cm diameter were prepared and mounted onto a stub that is coated with a silver paint. The mounted films were placed in a furnace for 15 minutes to evaporate the solvent in the paint and then sputtered with gold to obtained a coating of about 100A^{o} thick on top of the film to make it conductive. For the normal scan the instrument was set at

Beam voltage:	30 Kev
grain size:	500 μm
line time:	64 msec
# lines:	500
SED:	10x volts
Grid:	+275 volts
Gain:	700 volts

Brightness and contrast were set visually to obtain a good balance in shades for taking the pictures.

For the X-ray analysis, the sample was tilted 30^{o} in order to collect a better distribution of rays coming out of the sample. The energies per channel were set at 40 volts. The Dewer chamber was filled with fresh liquid nitrogen (LN2) at least four hours before performing the experiment. The energy range used was of 20 KeV and the data was collected for about 200-500 seconds.

To obtain the energies of certain peaks, the cursor was positioned upon the peak of interest and the required key in the instrument was pressed. Also, when a certain element of interest is entered to the computer, the software will identify the peaks related to that particular element. This was done particularly for Zr and Au. Using the data group function, the spectrum of the film containing the additive was compared to the one with no additives. Peak identification was accomplished using an energy-versus-element chart.

Optical Microscopy

Samples for Optical Microscopy do not need any special preparation, but handling it with gloves is necessary not to leave fingerprint marks in the surface. The samples were observed at about 100x magnification and under brightfield and darkfield conditions. Films tested were imidized polyamic acid with from 2-10% (mol) complex. Images were scanned and stored. No manipulation in colors was made.

Atomic Force Microscopy

For Atomic Force Microscopy, small films were mounted on glass slides and taped at the edges to reduce misplacement when the instrument is operating. Samples of 2-10% (mol) complex were also studied under tapping mode. Areas of 100 μm x 100 μm were scanned. Roughness studies were performed in the smooth and feature areas of the films.

Chapter 2. Results

Data, and results from mathematical manipulation of raw data (equations and graphical representation of particular techniques), are presented. The intent of the chapter is only to show the data obtained during the work in a manner which will facilitate their interpretation. For any description or discussion of these results please go to Chapter 3.

Film Thickness

After preparing the films of $Zr(acac)_4$/PI, three techniques were used to measure their thickness:

i) Diffraction (from IR spectra)

ii) Gravimetric

iii) Profilometric

Diffraction from Infrared (IR) Spectra

From the spectra collected for the standard and unknown samples, the number of fringes were counted and the thickness calculated from equations (3) and (4).

For the standard,

σ_1: 2000

σ_2: 1600

m: 5

η: 1.6

so, from $b\ (cm) = m/2\eta - 1/(\sigma_1 - \sigma_2)$,

b = 0.0039 cm = 0.039 mm.

The reading was supposed to equal 0.040 mm from information on the manufacturer's label, only a 0.001 mm difference.

For unknown:

σ_1: 2000

σ_2: 1600

m: 3

η: 1.6

so, from $b\ (cm) = m/2\eta - 1/(\sigma_1 - \sigma_2)$,

b = 0.0023 cm = 0.023 mm

+ 0.001mm correction = 0.024 mm

See Figures 27 and 28 for spectra.

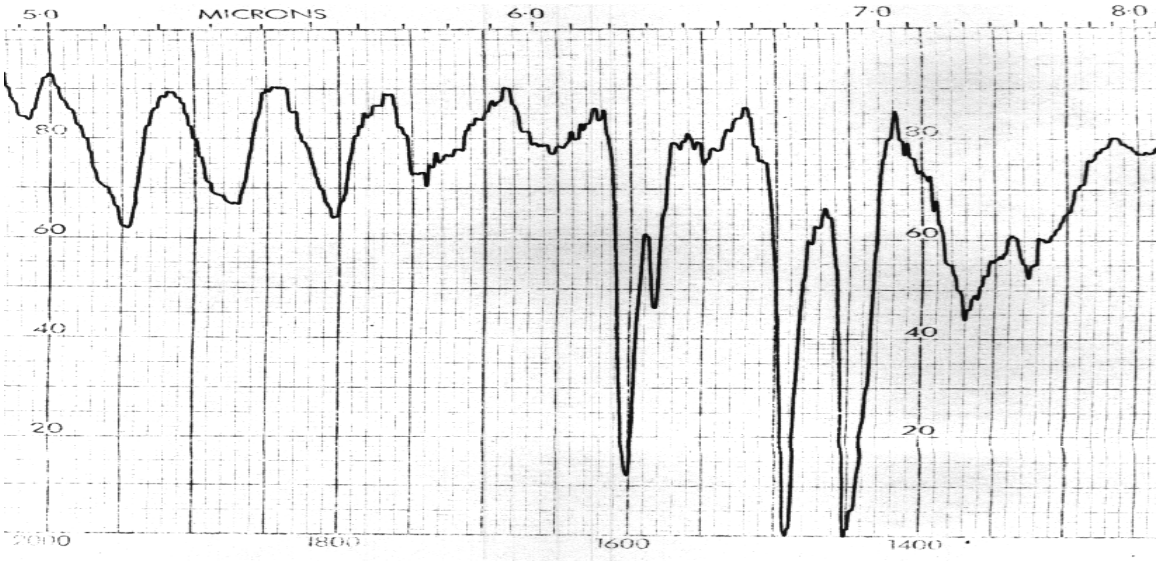

Figure 27. IR Spectra of Polystyrene from 2000 –1300 cm^{-1}.

Figure 28. IR spectrum of Zr/Pl film from 2400-2300 cm^{-1}

Gravimetric method

This technique is more accurate than the IR method since it takes into account all the dimensions and weight of each film.

Using equations 5 to 7 and the data below,

$$\rho_f = \text{mass}_f / \text{vol}_f = \text{mass}_f / w*l*h \quad (5)$$

$$\rho_{fsolution} = \text{mass}_{solution} / \text{vol}_{solution} \quad (6)$$

$$\rho_{fsolution} = (\text{mass}_{beaker+solution} - \text{mass}_{beaker}) / \text{volume}_{solution} \quad (7)$$

beaker mass:	62.78 +/- .001 g
dimensions of film (w, l):	1.8 cm x 1.9 cm
mass of film:	0.023 g +/- .001 g
mass of beaker plus solution:	203.26 +/- .1 g
volume of solution:	225 mL

$\rho_{fsolution}$ = (203.26 - 62.78) / 225 = 1.12 +/-.01 g/cm^3

and, for $\rho_{fsolution} = \rho_f$,

h = 0.023 g / (1.12 g/cm^3*1.8 cm*1.9 cm)

= 0.0060 +/- .0001 cm = 0.060 +/- .001 mm

Profilometry

For this technique a standard was run first. The standard consisted of a gold pattern of known thickness of 9.11 kAº. From the instrument:

1.8 div * (5000 Aº / div) = 9.0 kAº

This is a discrepancy of about 1% which represents a good accuracy for the instrument.

Results for variation in 20 readings in one film for the profilometer measurements:

average:	72.84 μm
error propagation:	3.8 μm
thickness:	72.84 +/- 3.8 μm = 0.0728 +/- .0038 mm

The thickness result for the same film analyzed by gravimetric method, 0.060 mm, was in reasonable agreement with this method.

Scanning Electron Microcopy

The SEM study of the films was divided in four parts. The first was to look at the surface of film without additive (pure) and films containing 2-10 % (mol) of the additive.

1. Surfaces of pure films look very smooth and featureless. See Figures 29 and 31. The right side of Figure 29 shows the smooth film and the left side shows the conductive silver coating on the film. Figure 30 shows a top view of the film at 80X. The white features on top are flakes from the reference cross etched on the film surface. A flake in the film crack resembles very much the rest of the film.

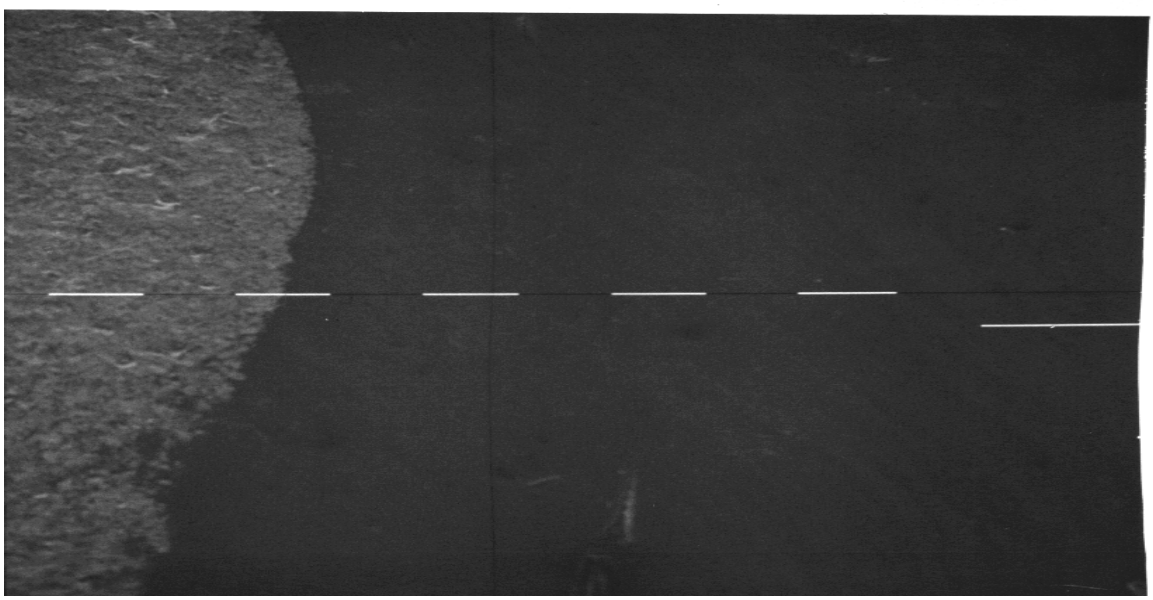

Figure 29. SEM picture at 80x and 30° tilt of pure film. The left side shows silver paint coating

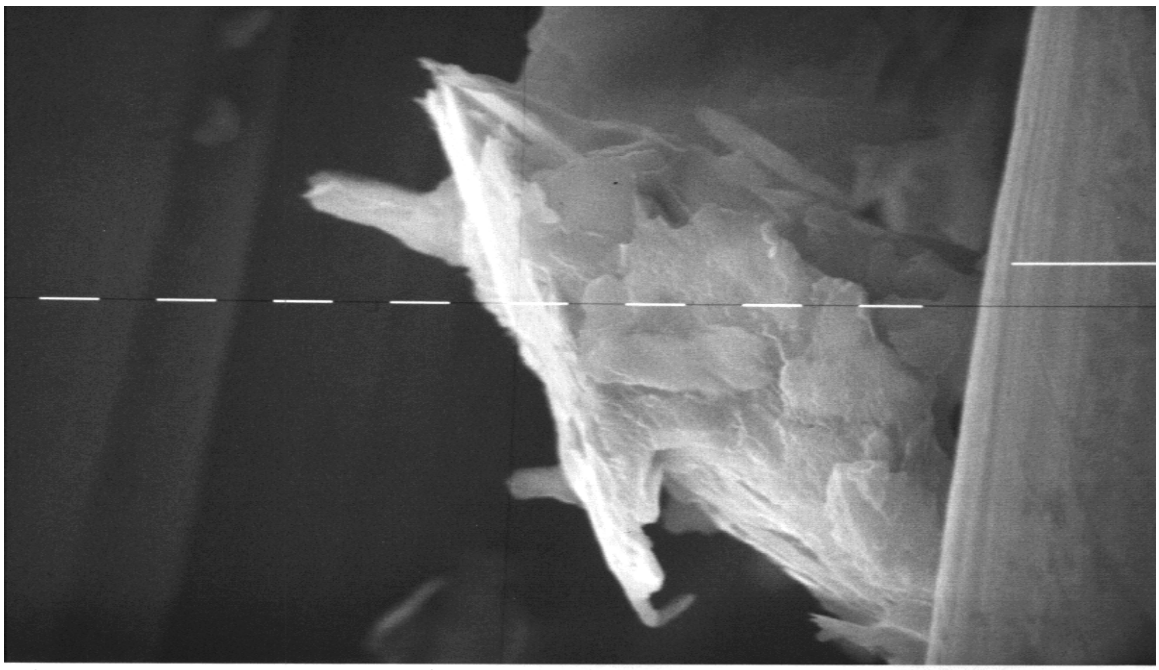

Figure 30. Flake at a crack on a pure film at 80x, 0° tilt

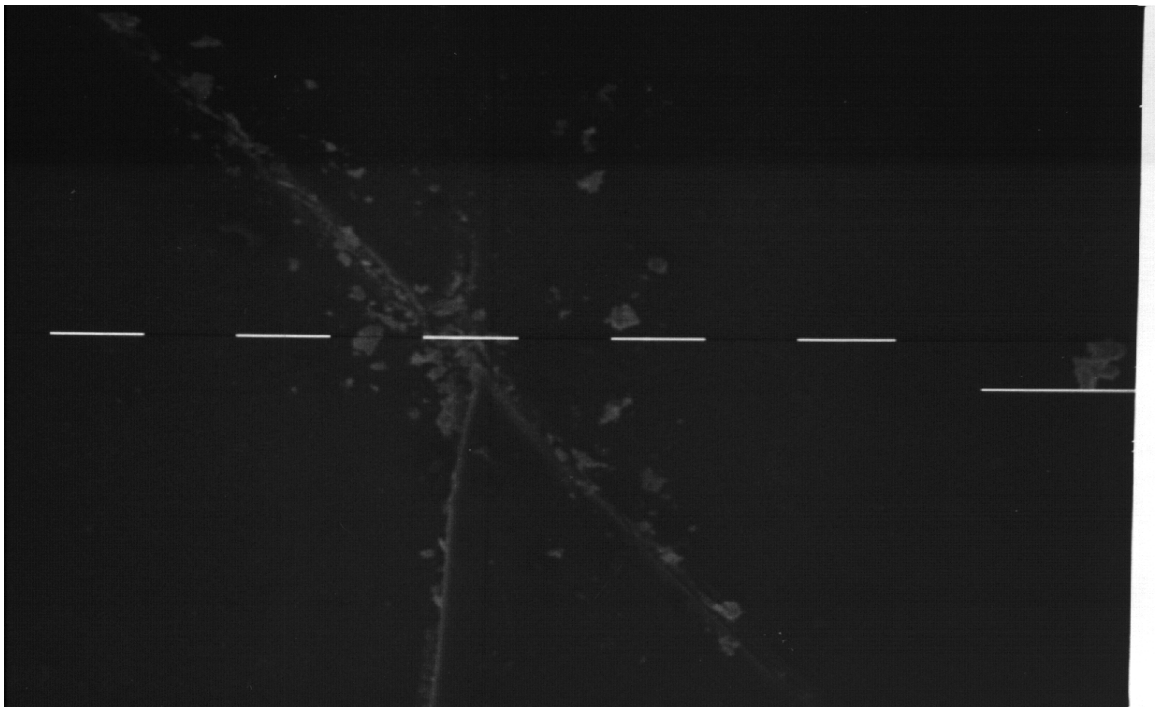

Figure 31. Top view of a pure film at 5000x and 30° tilt

2. For films of two percent additive, some features start to develop. These features are dispersed in the surface of the film. See Figure 32. From Figure 33, the features seem to have a spherical shape, but from Figure 34, they resemble an agglomeration of features.

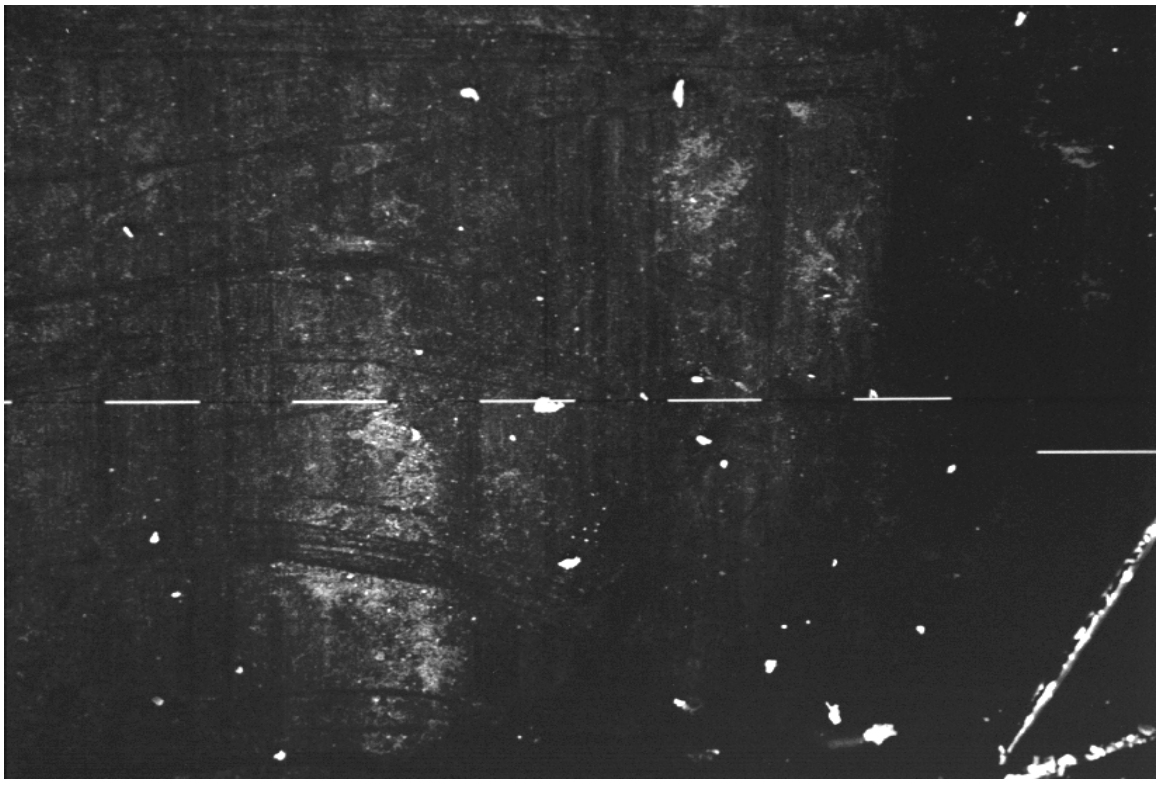

Figure 32. Surface view of a 2% $Zr(acac)_4$/PI film at 80x

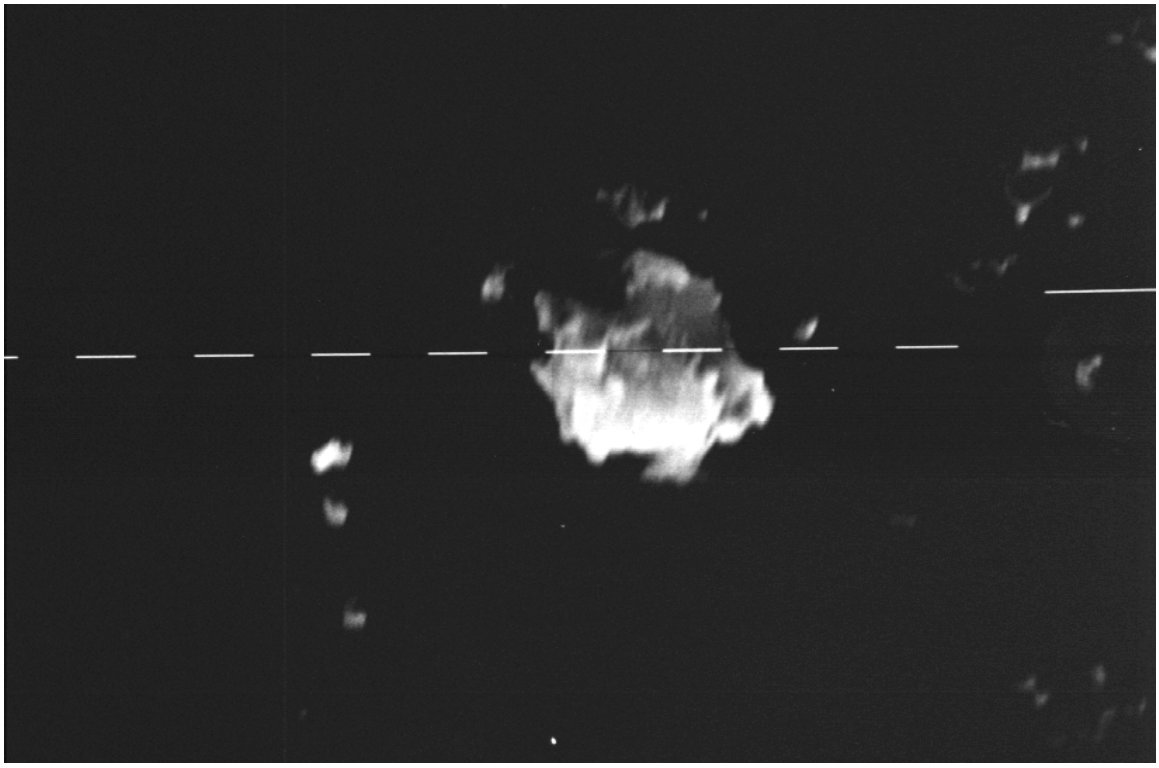

Figure 33. 1250x and 30° tilt picture of feature in 2% $Zr(acac)_4$/PI Film

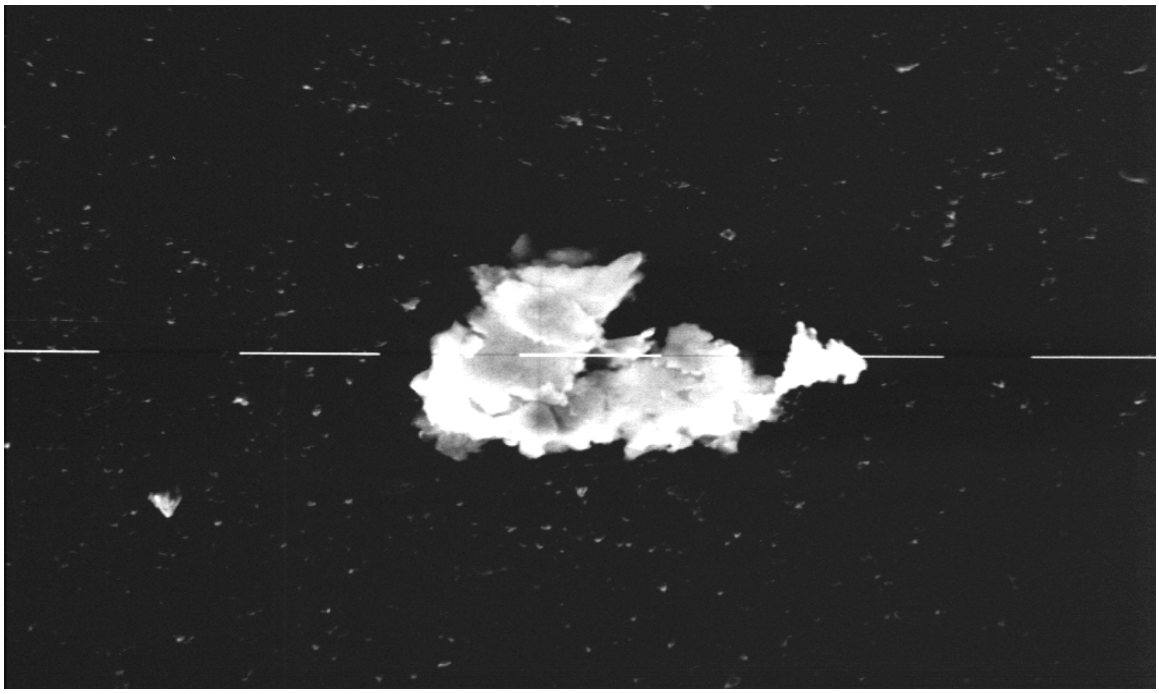

Figure 34. Picture of a clustered feature in a 2% (mol) Zr(acac)4/PI film at 1250x and 30°

3. Films of four mole percent additive shows the same type of features as the two mole percent, but a bit smaller and surrounded by a more smooth surface. Figure 35 shows the surface of the film and Figure 36 shows the features. Figures 37 shows another view near a crack.

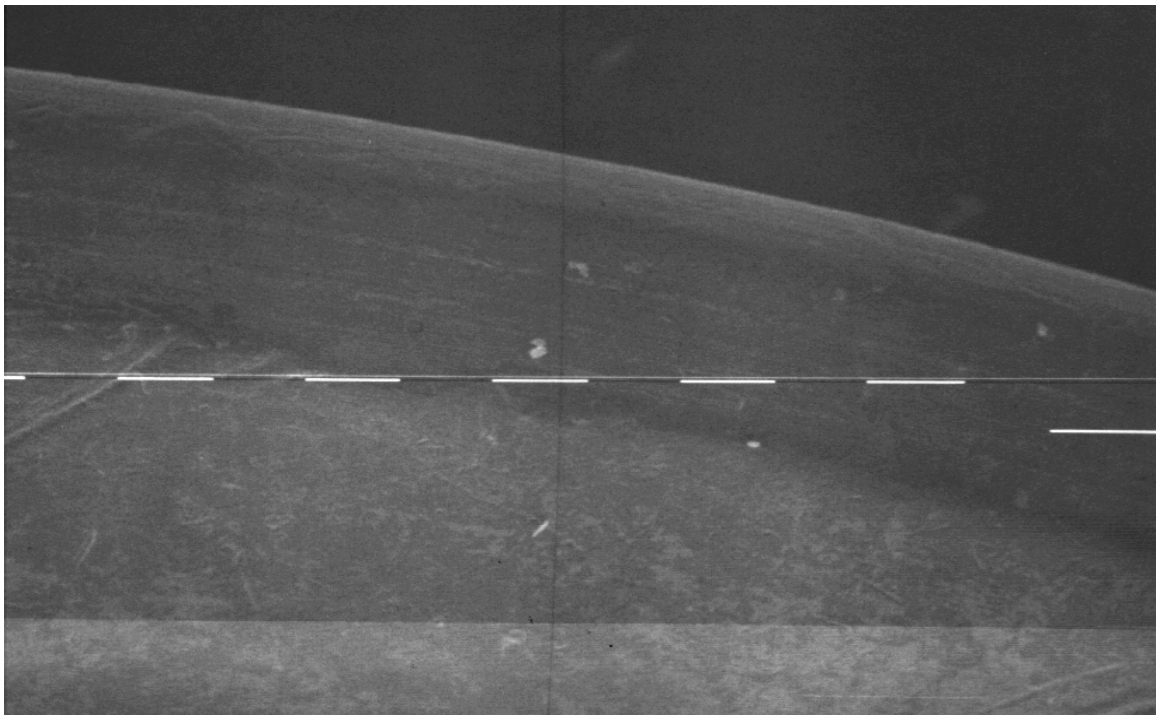

Figure 35. Surface view of a 4% (mol) $Zr(acac)_4$/PI film at 80x

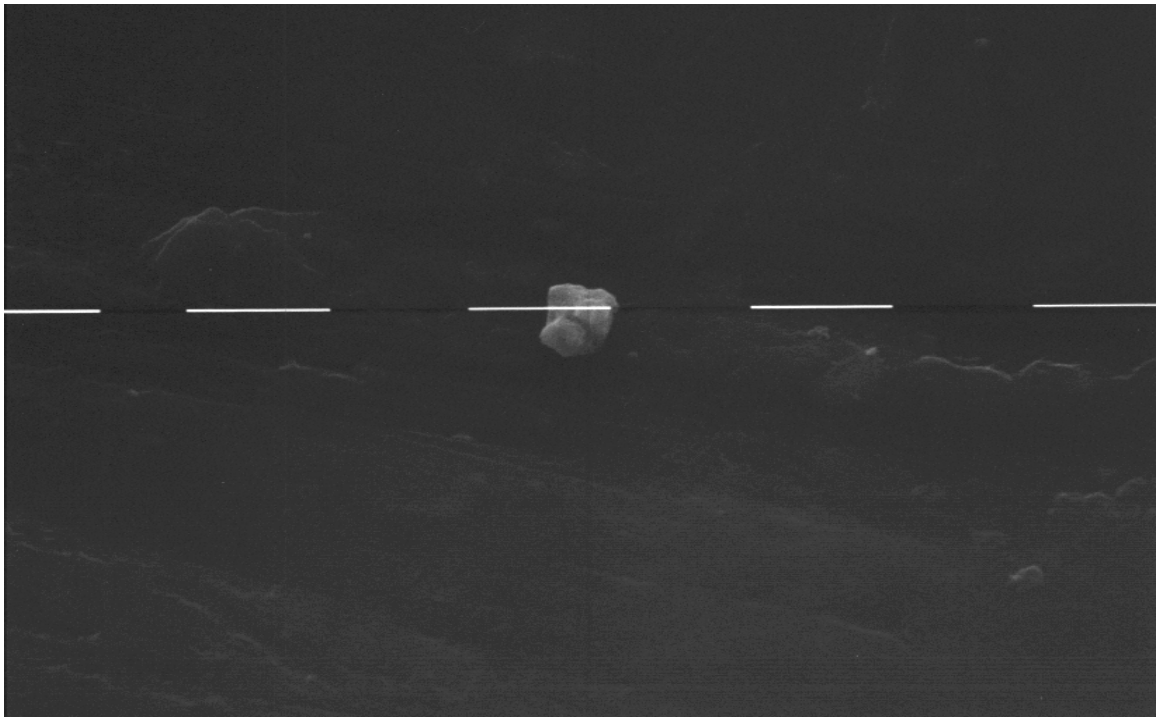

Figure 36. Picture of a feature on surface 4% (mol) $Zr(acac)_4$/PI film at 1250x and 30°

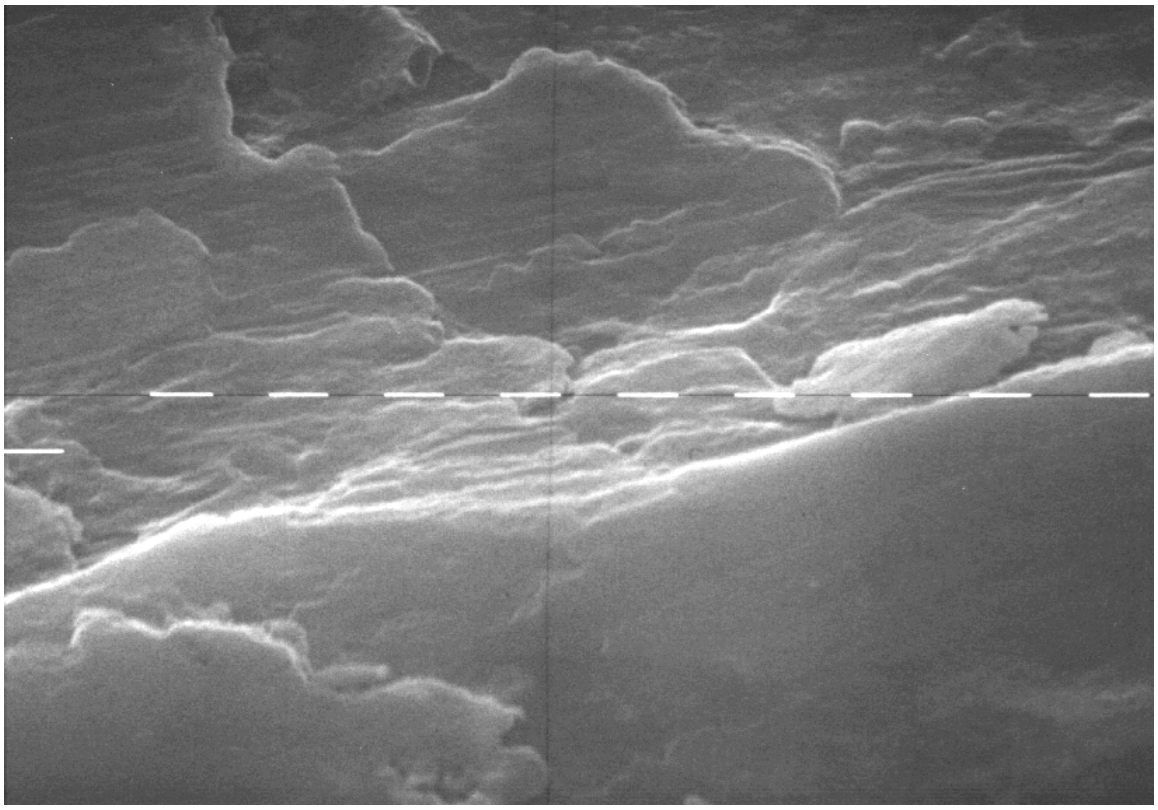

Figure 37. Surface view of a 4%(mol) $Zr(acac)_4$/PI film at 5000x and 30° tilt

4. Films of six mole percent additive have the same behavior as the last two, but the number of clusters is higher. Figure 38a shows the surface of the film with a scratch along the lower right corner. The surface is smooth with the features on top of it. Figure 38b shows a closer look at an area with cluster features and flakes of film.

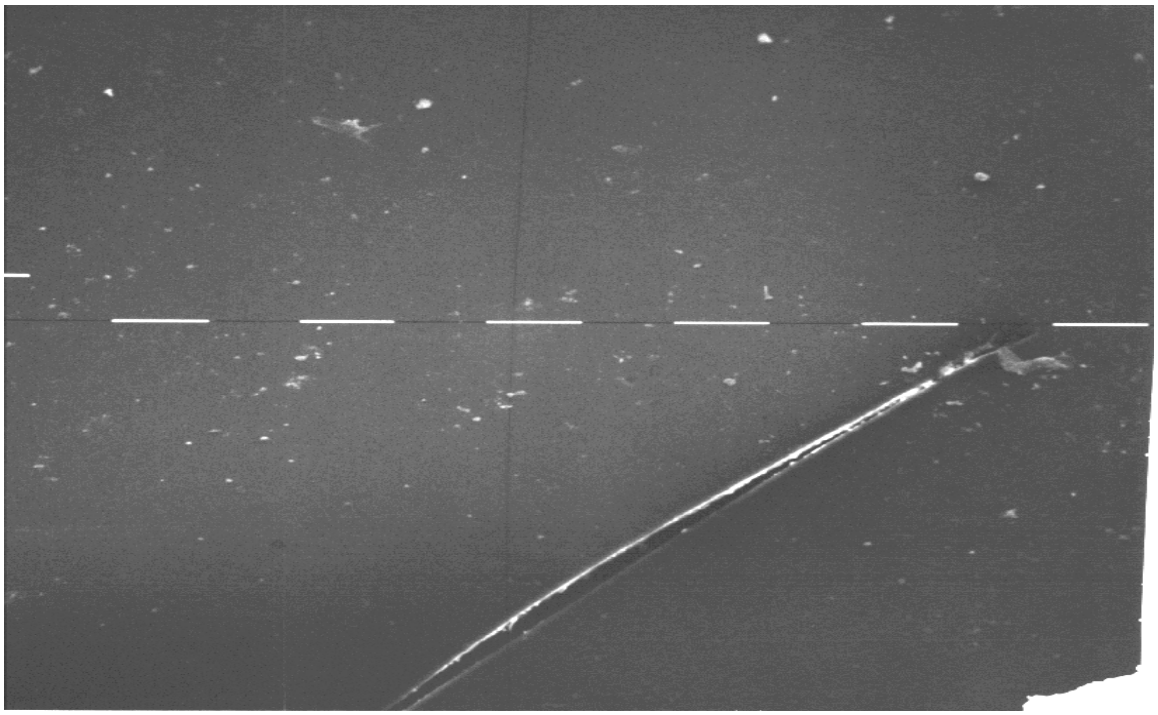

Figure 38a. Surface view of 6% (mol) $Zr(acac)_4$/PI film at 80 x and 30° tilt

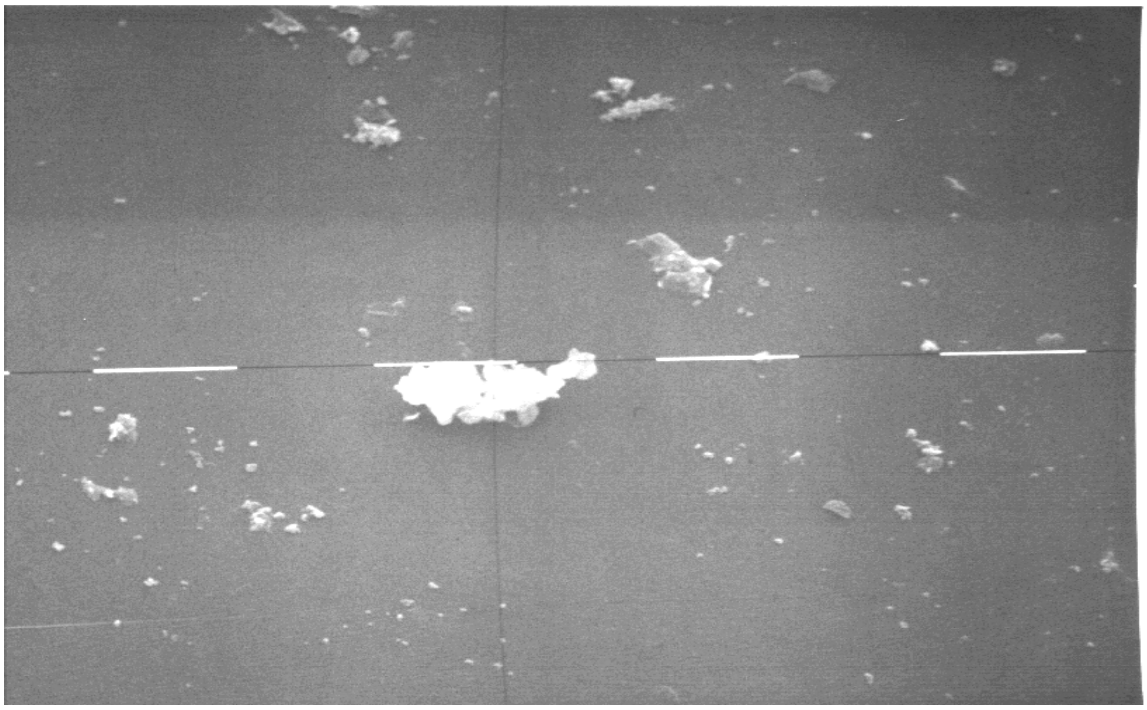

Figure 38b. Feature on a 6% (mol) $Zr(acac)_4$/PI film surface at 1250x and 30° tilt

5. For eight mole percent films, looking into areas similar to the other films, quite similar behavior to the four mole percent films is seen. See Figure 39. The feature shape is quite spherical and only a small number of features are present per unit area. A crack flake resembles the one seen for the pure film, but is smaller and brighter. See Figure 40. Figure 41 is a surface view.

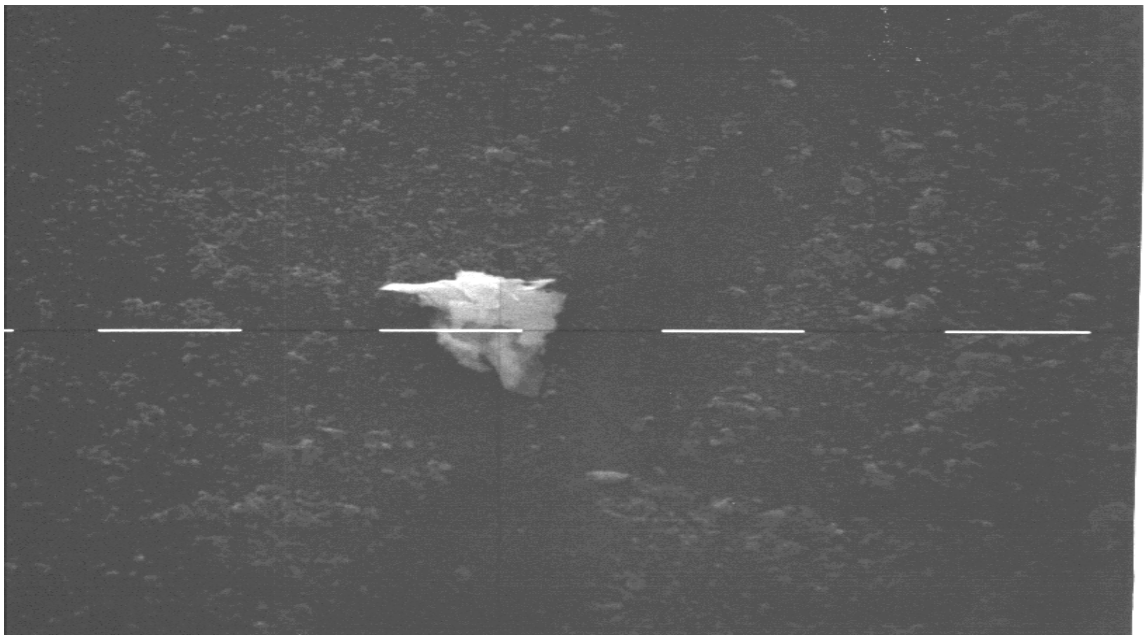

Figure 39. Particle on top of a 8% (mol) $Zr(acac)_4$/PI film at 1250x

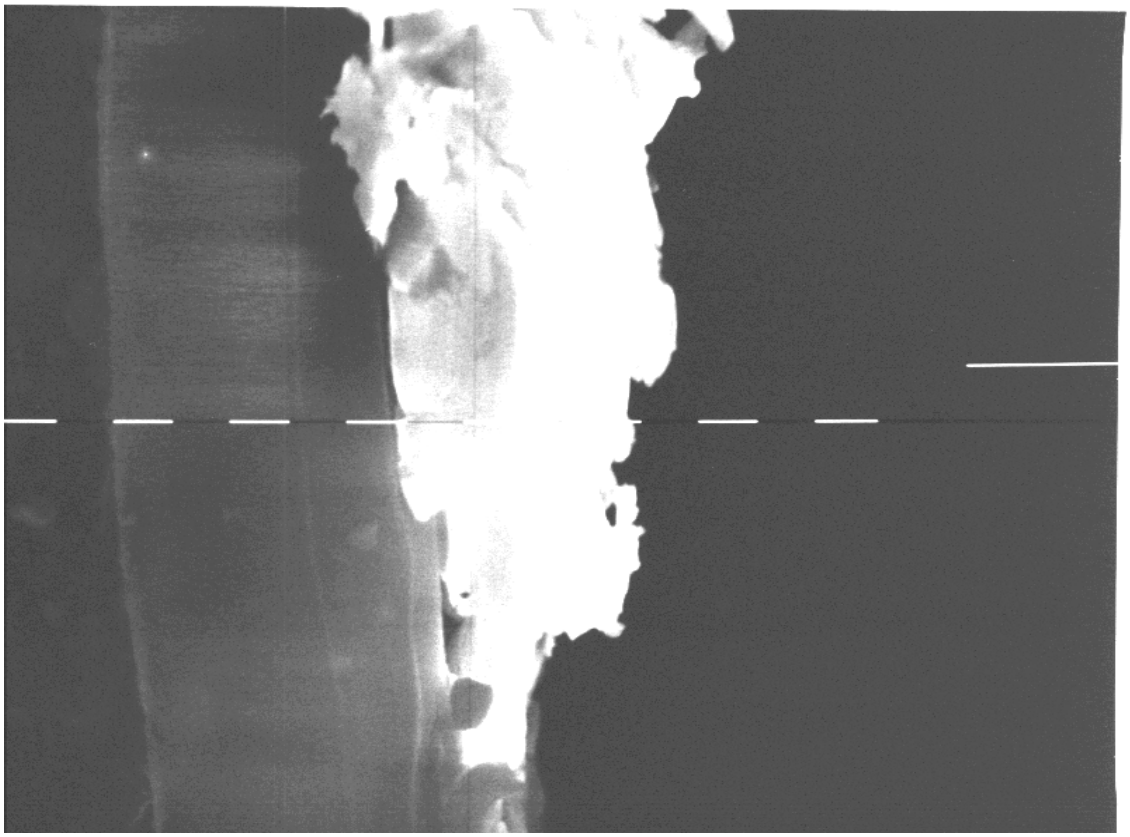

Figure 40. Flake on a crack of a 8% (mol) $Zr(acac)_4$/PI film at 80x and 30° tilt

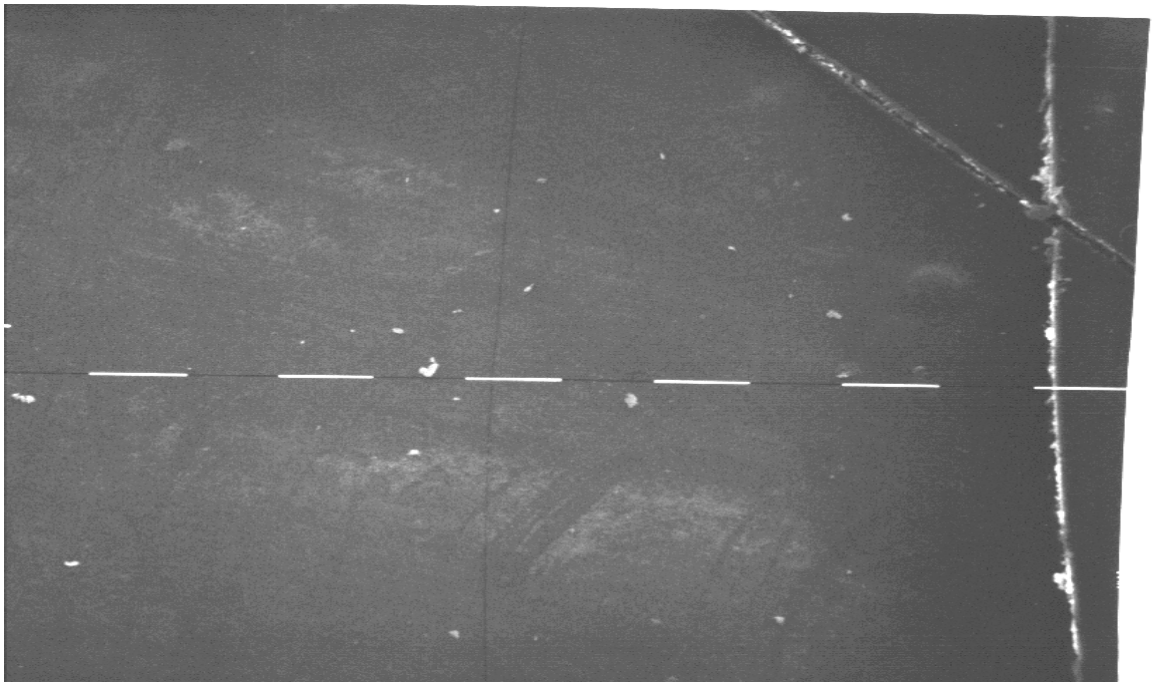

Figure 41. Surface view of a 8% (mol) $Zr(acac)_4$/PI film at 80x and 30° tilt

6. The ten mole percent films, the highest concentration of additive tested, shows a larger, spherical feature tapered at one end. See Figure 42a. Figure 42b is a surface view and shows a very smooth featureless area, more than for the films with lower percentages of additive. Figure 43 is a view of a crack.

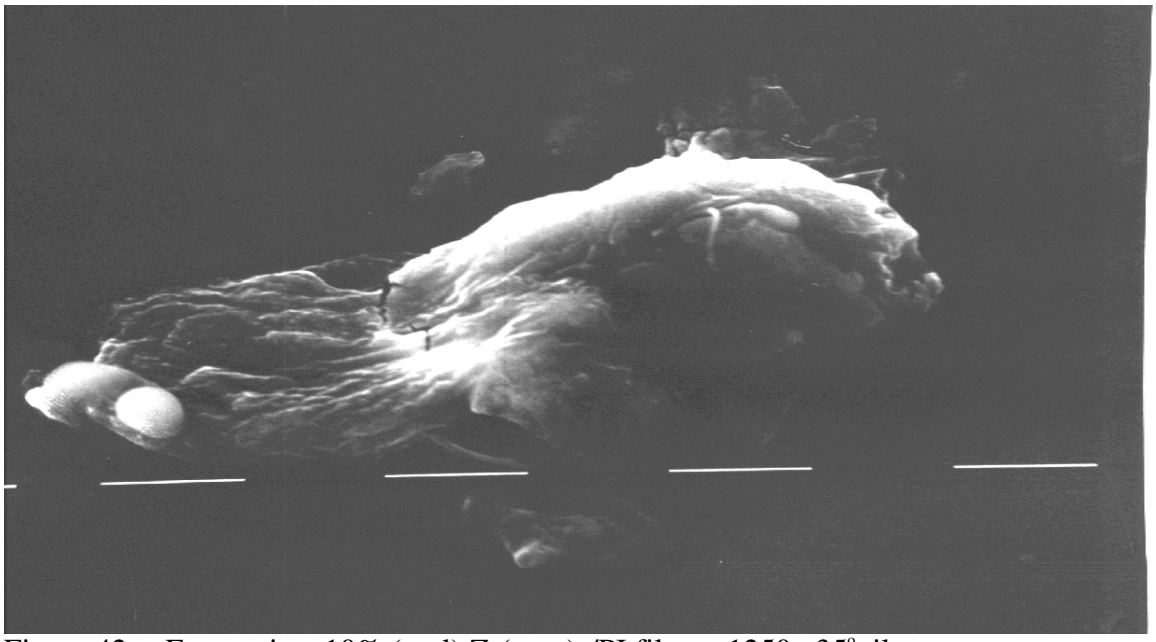

Figure 42a. Feature in a 10% (mol) $Zr(acac)_4$/PI film at 1250x 35° tilt

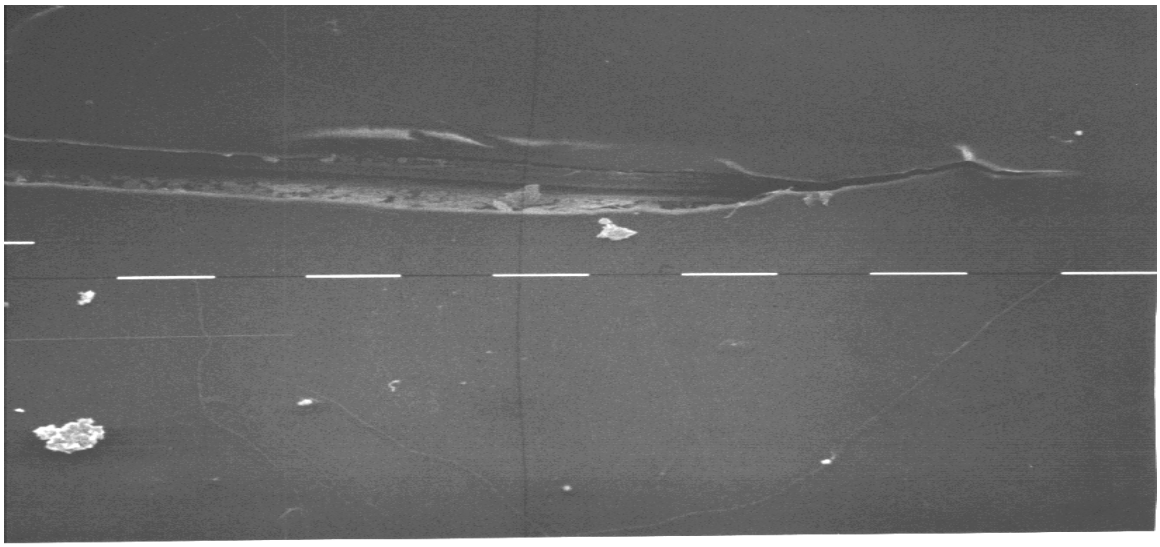

Figure 42b. Surface view of a 10% (mol) Zr(acac)4/PI film at 80x and 30° tilt

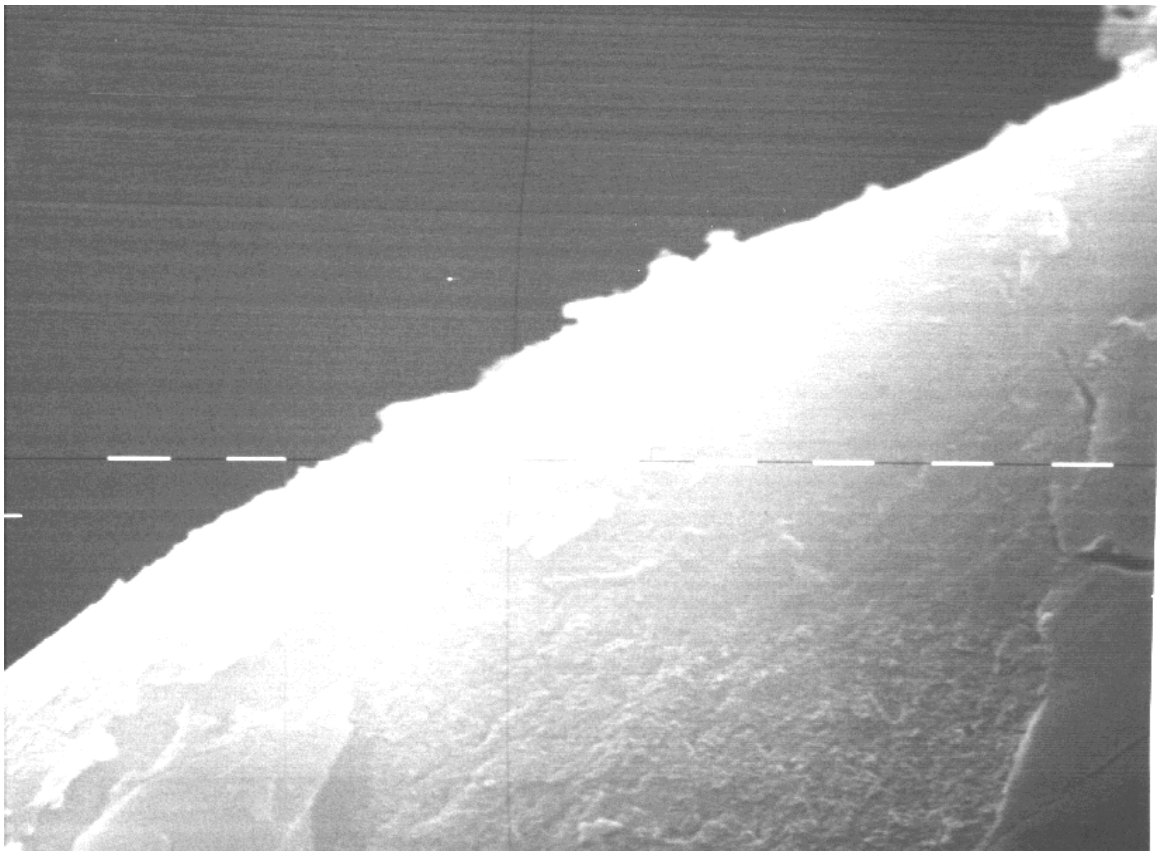

Figure 43. View of crack area in a 10% (mol) $Zr(acac)_4$/PI film

A second study using the SEM was to look at the top and bottom surfaces of the films and notice any differences. See Figures 43 to 45. The results shows no difference between them and that the top and bottom have similar amounts of particulate conglomeration present.

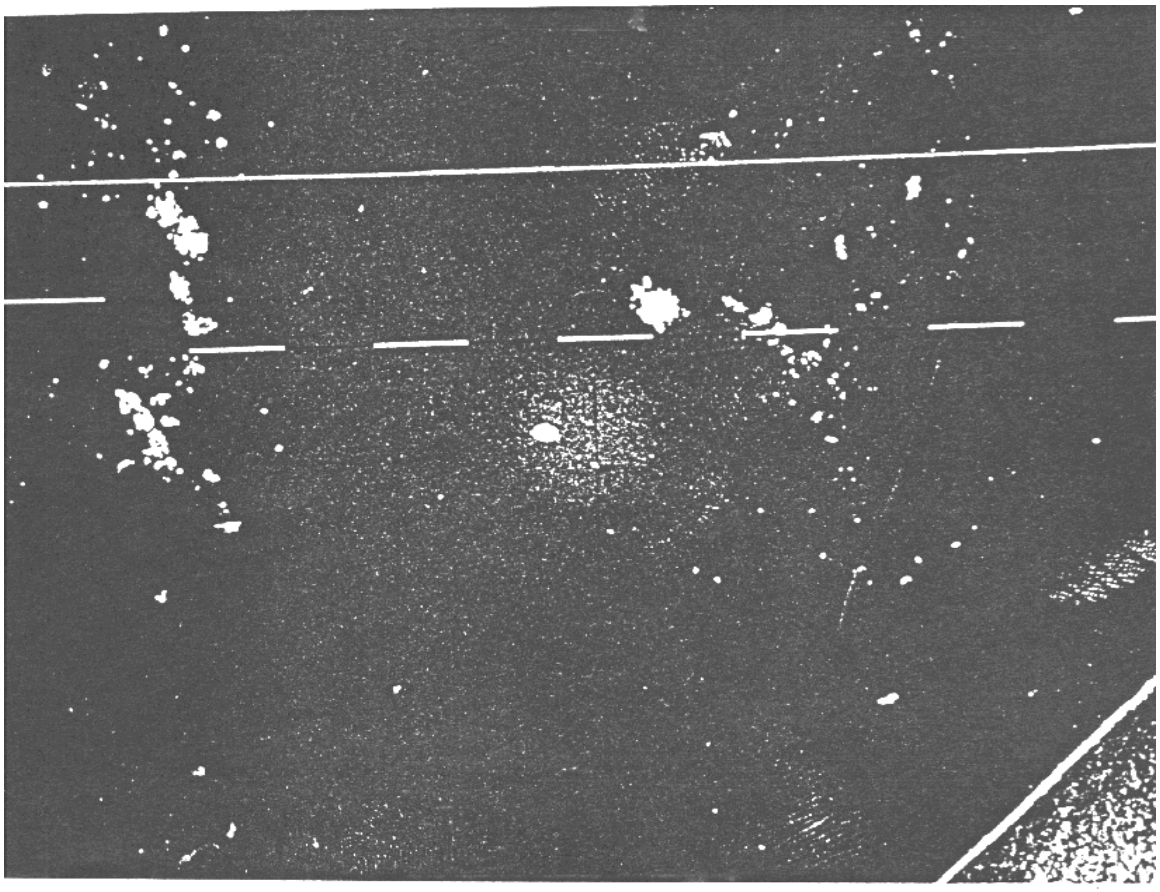

Figure 44. Bottom view of the surface of a 10% (mol) $Zr(acac)_4$/PI film at 80x

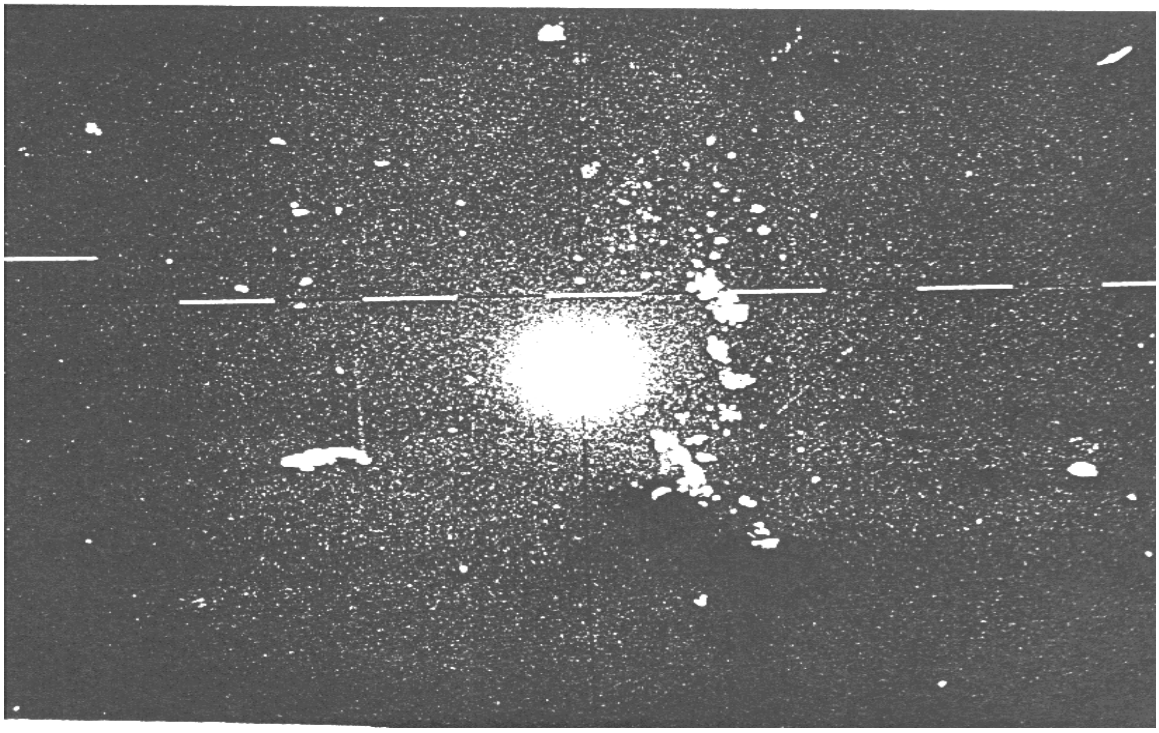

Figure 45. Bottom view of the surface of a 10%(mol) $Zr(acac)_4$ film at 80x and 0° tilt

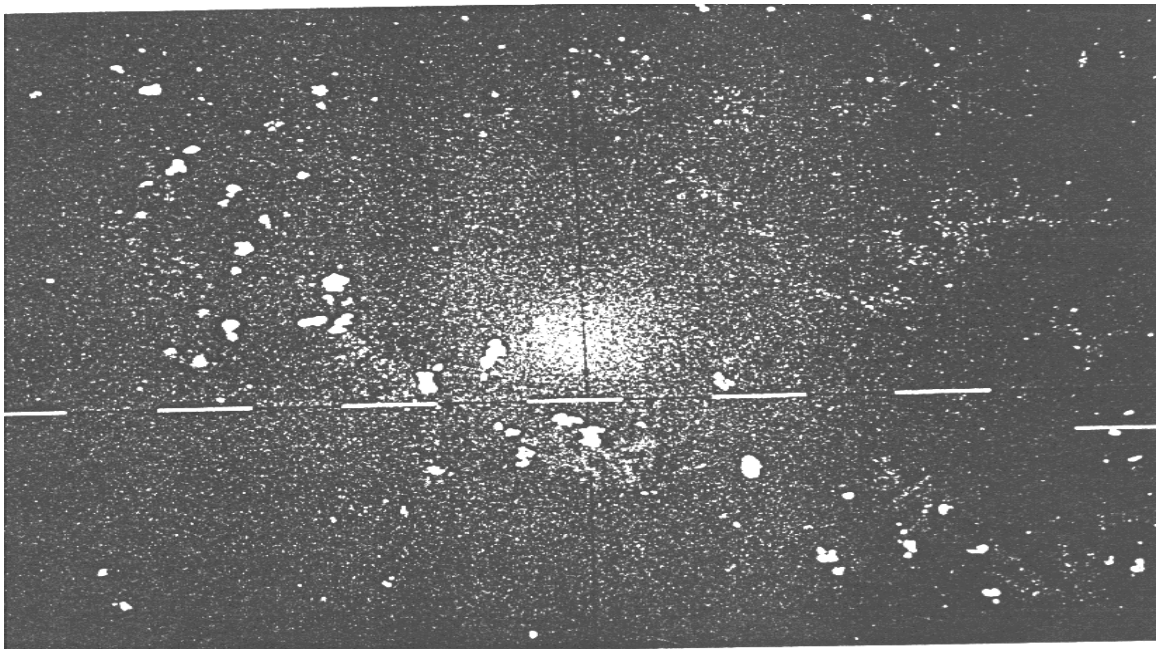

Figure 46. Top view of a 10% (mol) Zr(acac)4/PI film at 80x

The third study was to determine the size and number of features per area of film.

Table 2. Results of feature size and number study on $Zr(acac)_4$/PI films for a fixed area of film.

% (mol) $Zr(acac)_4$/PI	Sizes features	Quantity	Comment
Pure	0	0	smooth surface
2	4um	16	biggest feature
4	5-6um	3	
6	10-12um	6	
8	12um	8	
10	40um	4	

The EDS X-ray analysis involves determination of the elements present in a film of 10% (mol) $Zr(acac)_4$/PI in a smooth area and in one with a feature, both in the same film. See Figures 46 to 48. The elements determined to be present were obtained by superimposing the feature area spectra over the smooth one.

Table 3. Elements present on a 10 % (mol) Zr(acac)4/PI film in a feature area after superimposing over an area with no features

Energies intensities (Kev)	Elements on feature
1.26	Mg
1.52	Al
1.76	Si
2.14	Zr or Au
2.64	Cl
3.34	K
3.70	Ca
4.54	Ti
7.52	Fe
8.06	Cu

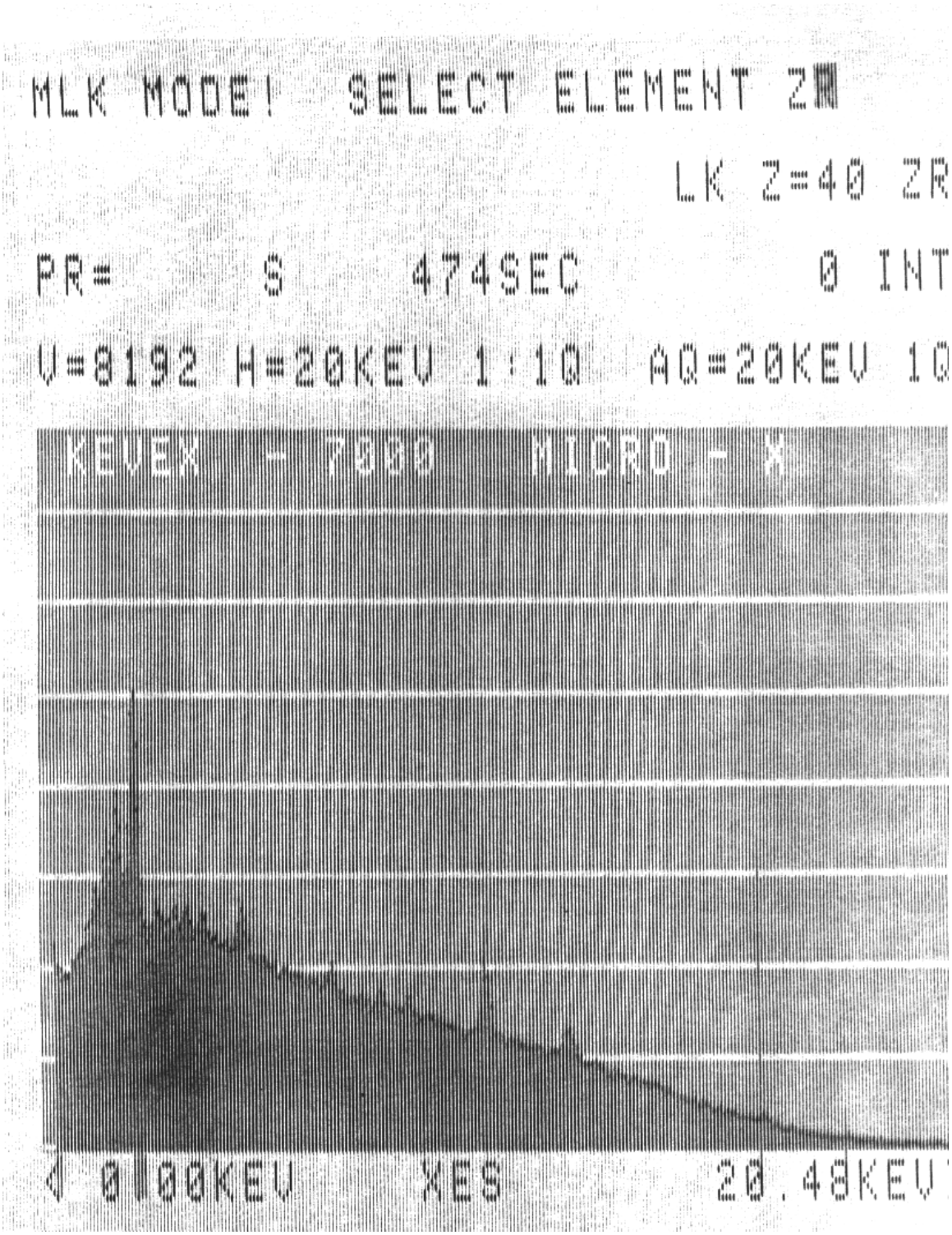

Figure 47. Spectrum of PI film containing 10% (mol) $Zr(acac)_4$ additive in feature area showing Zr peaks

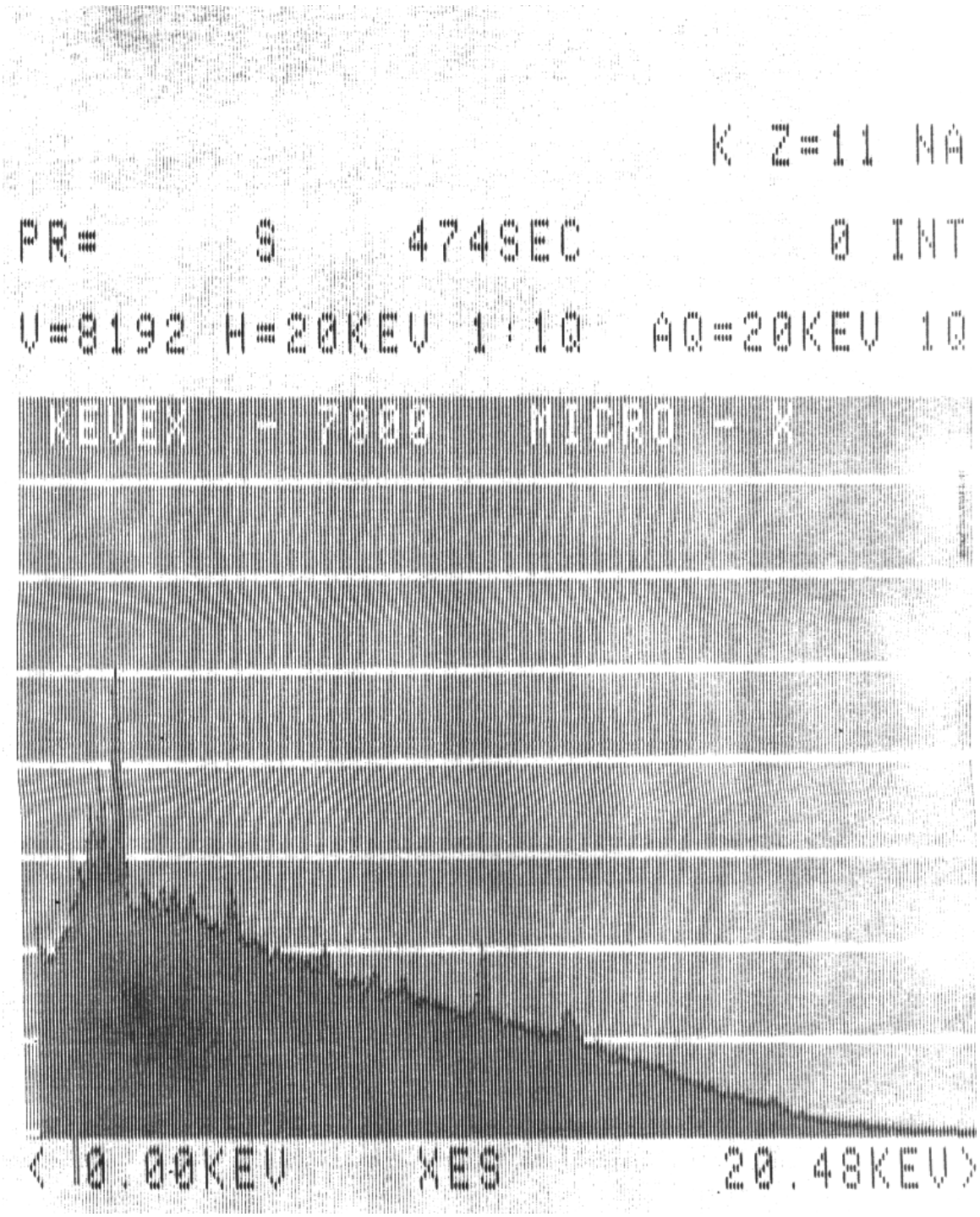

Figure 48. Spectrum of PI film containing 10% (mol) $Zr(acac)_4$ additive in feature area

Figure 49. Spectrum of 10% (mol) $Zr(acac)_4$/PI film over spectrum of pure film

Optical Microscopy

The optical microscopy study involved the observation of films at different steps during the imidization process. The films were photographed under bright and darkfield conditions. Heating steps were:

1. Films heated at 100°C. See Figure 49 for pure PAA film, and Figure 50 for 10% (mol) $Zr(acac)_4$/PAA film.
2. Films heated at 300°C. See Figure 51 for pure PI film, and Figure 52 for 10% (mol) $Zr(acac)_4$/PI film.
3. For 2% (mol) $Zr(acac)_4$/PI film see Figure 53, 4% film see Figure 54, 6% film see Figure 55, 8% film see Figure 56.

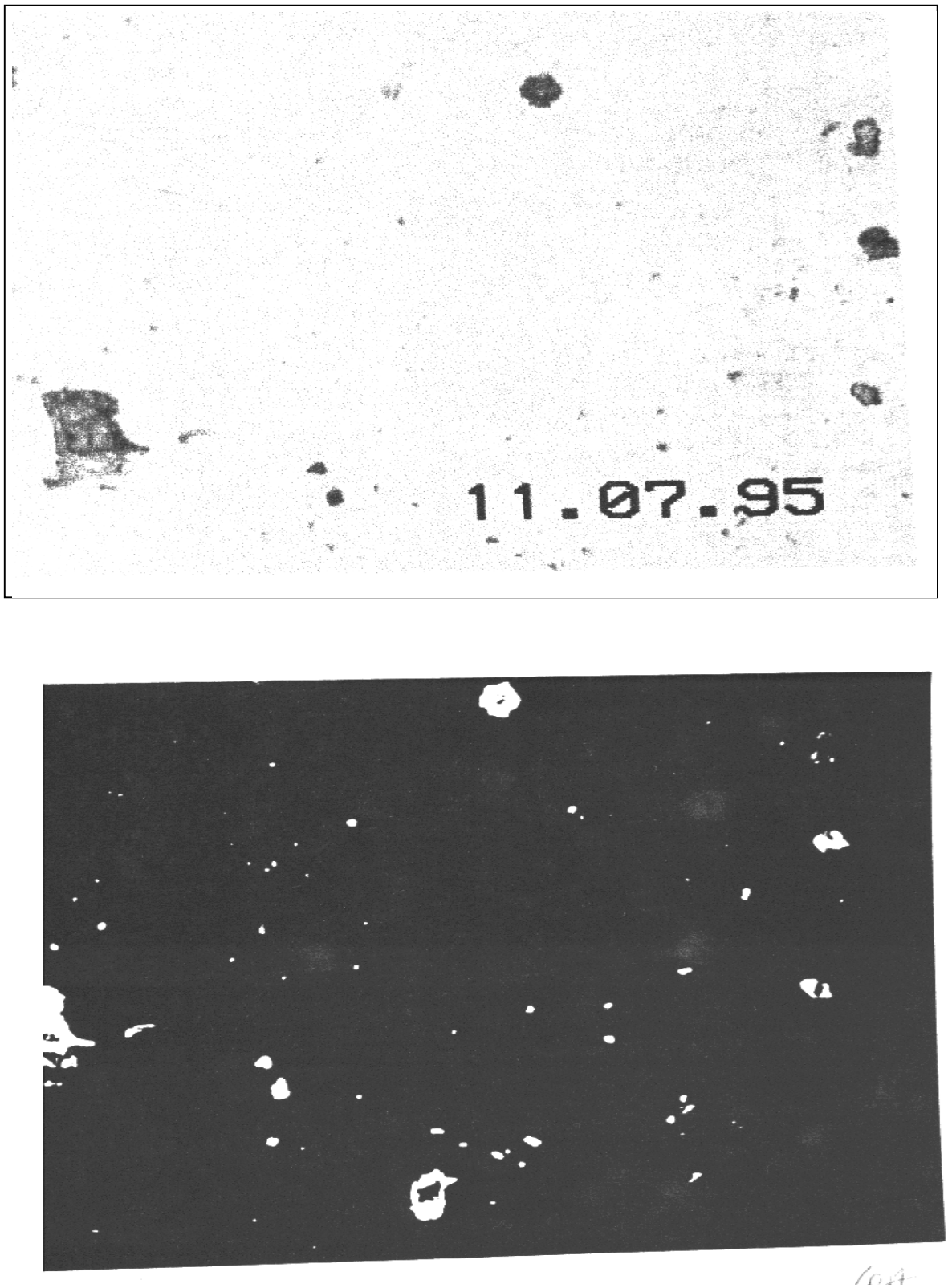

Figure 50. Optical microscopy picture of a film without additives previously heated at 100°C (top: brightfield, bottom: darkfield)

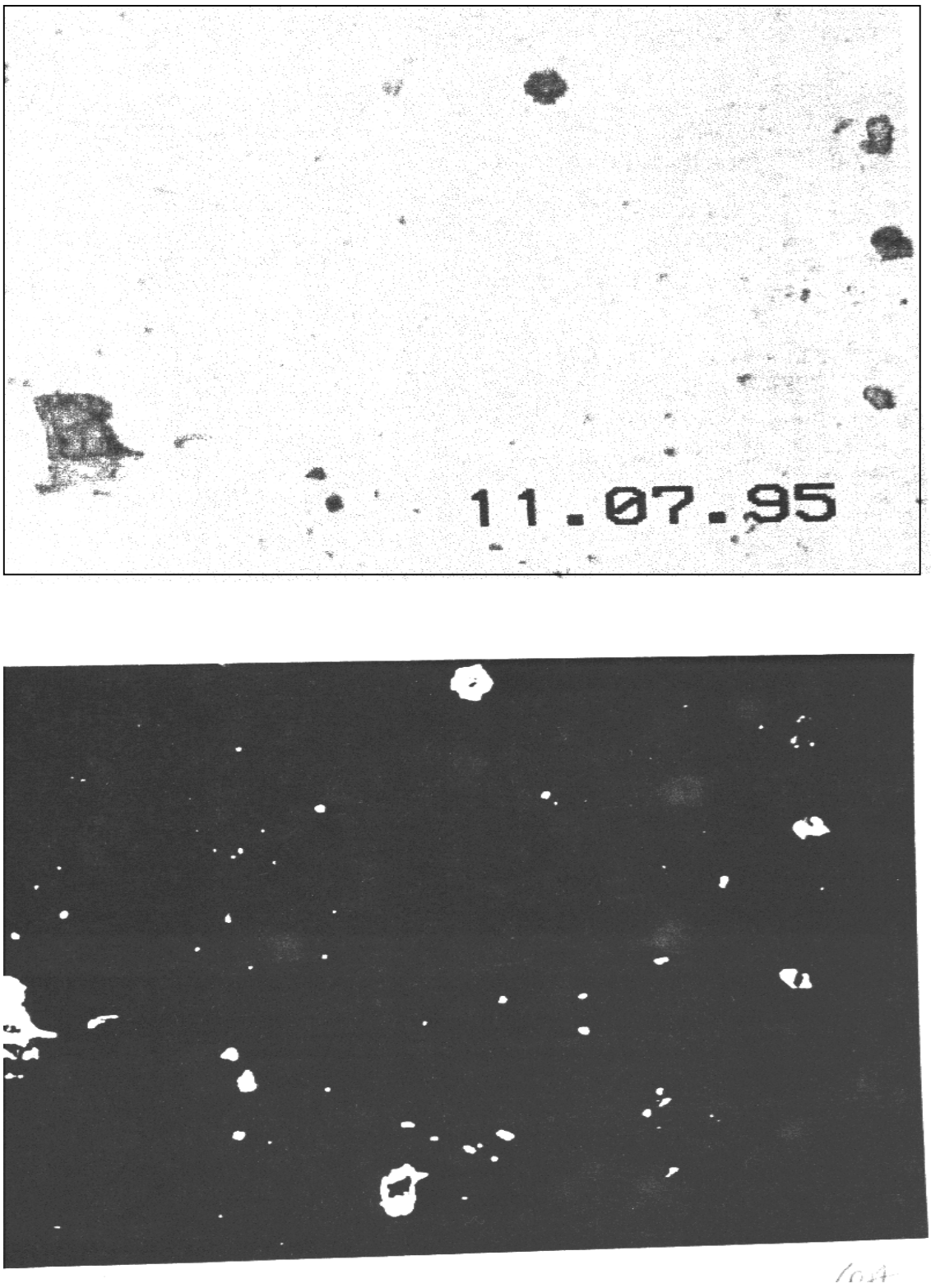

Figure 51. Optical Microscopy picture of a PAA film with 10% (mol) $Zr(acac)_4$ previously heated at 100° C (top: brightfield, bottom: darkfield)

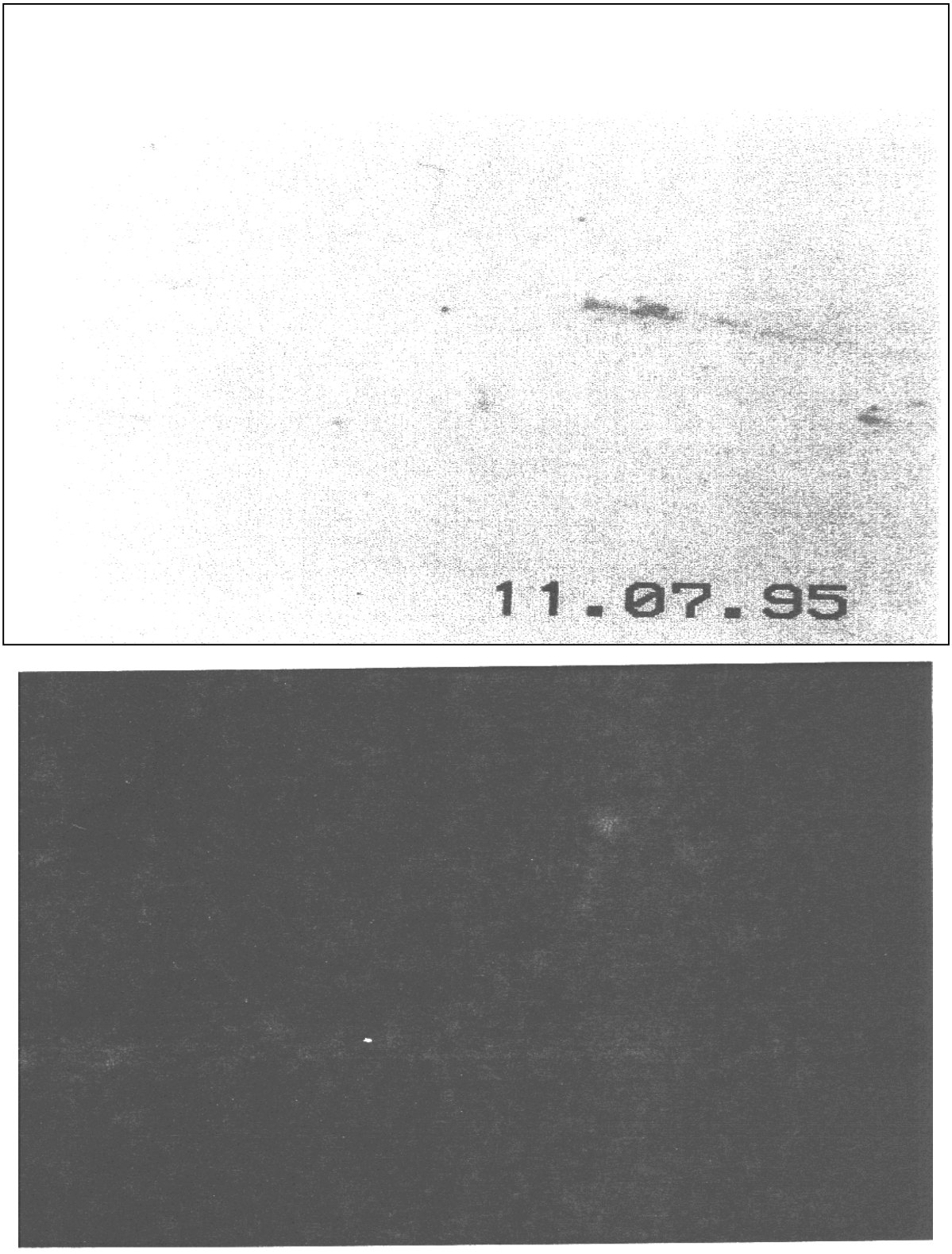

Figure 52. Optical microscopy picture of a PI film without additives previously heated at 300°C (top: brightfield, bottom: darkfield)

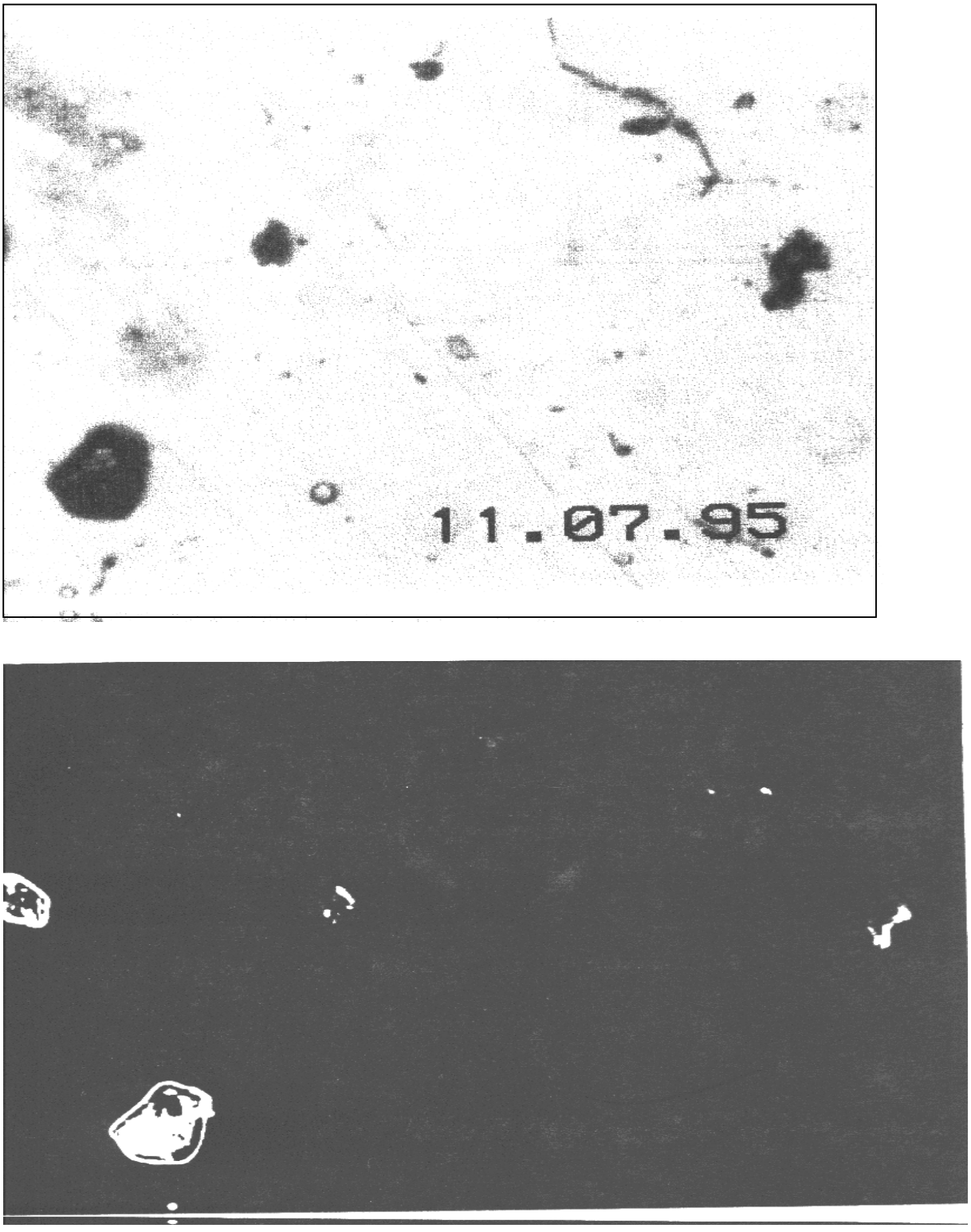

Figure 53. Optical microscopy of a 10% (mol) Zr(acac)4/PI film previously heated at 300°C (top: brightfield, bottom: darkfield)

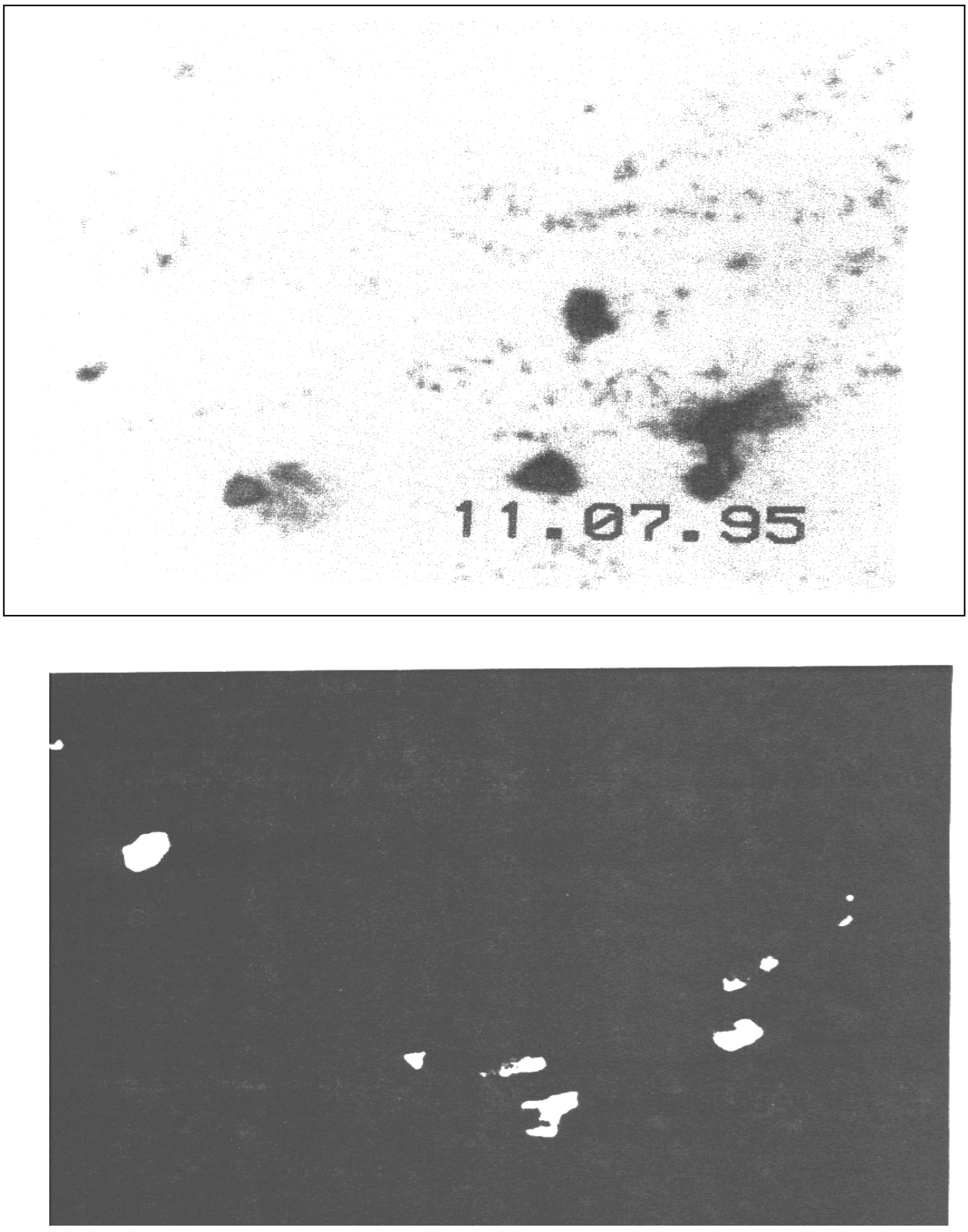

Figure 54. Optical microscopy picture of a 2% (mol) $Zr(acac)_4$/PI film (top:brightfield, bottom: darkfield)

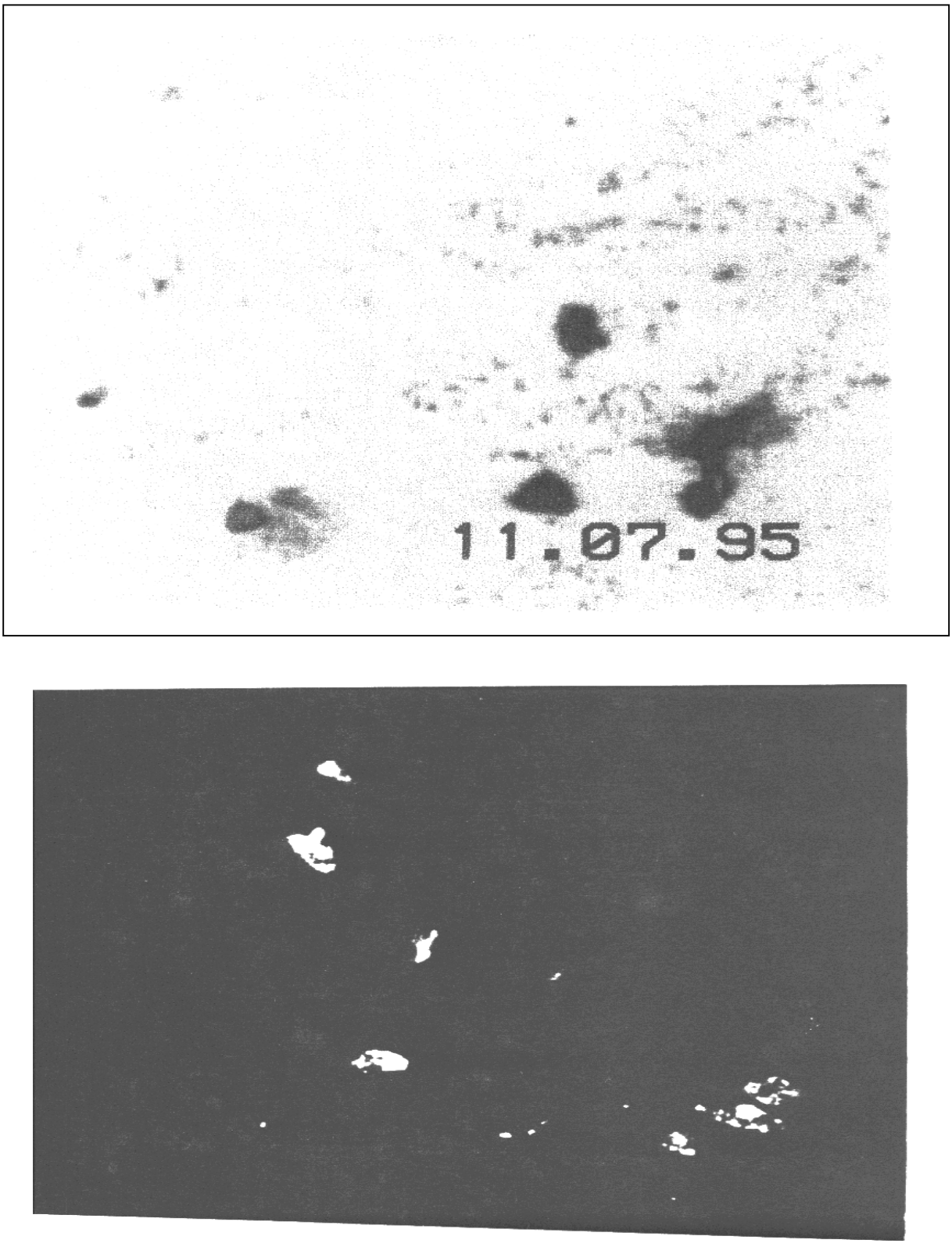

Figure 55: Optical microscopy picture of a 4% (mol) $Zr(acac)_4$/PI film (top: brightfield, bottom: darkfield)

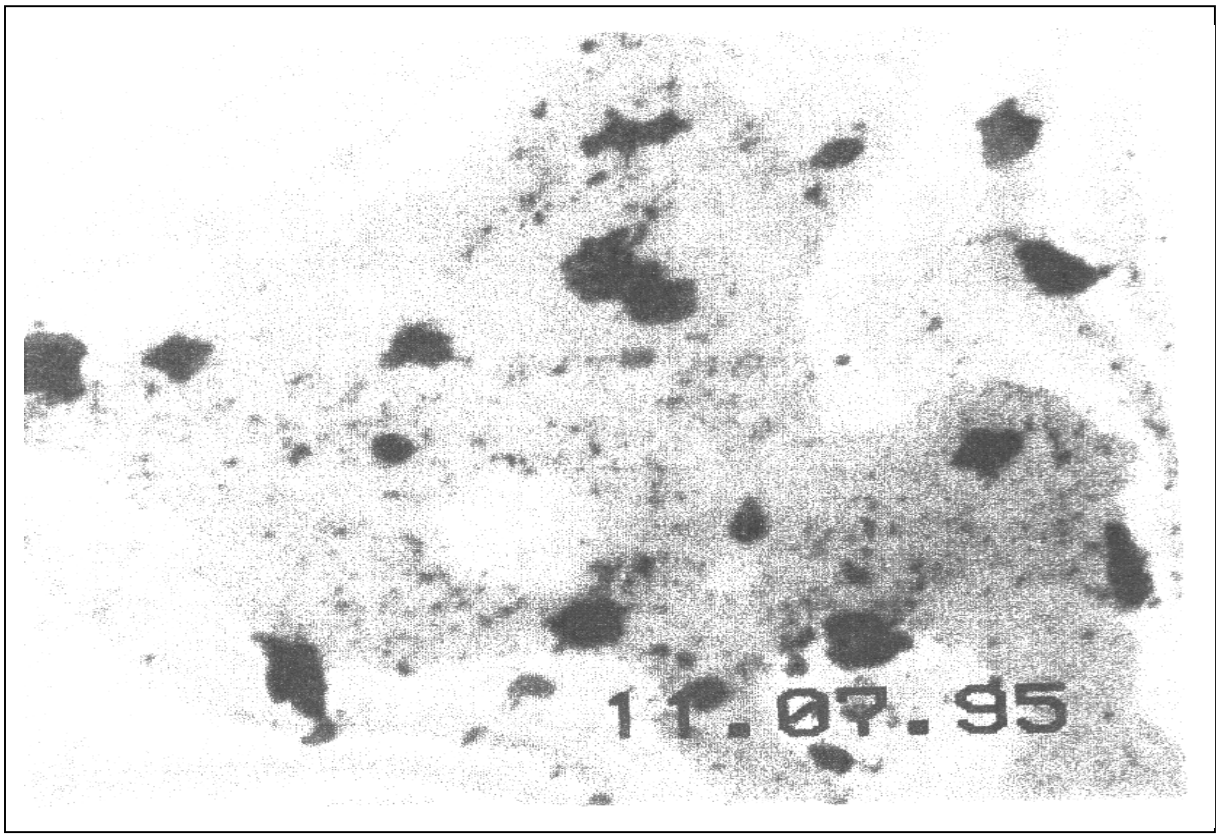

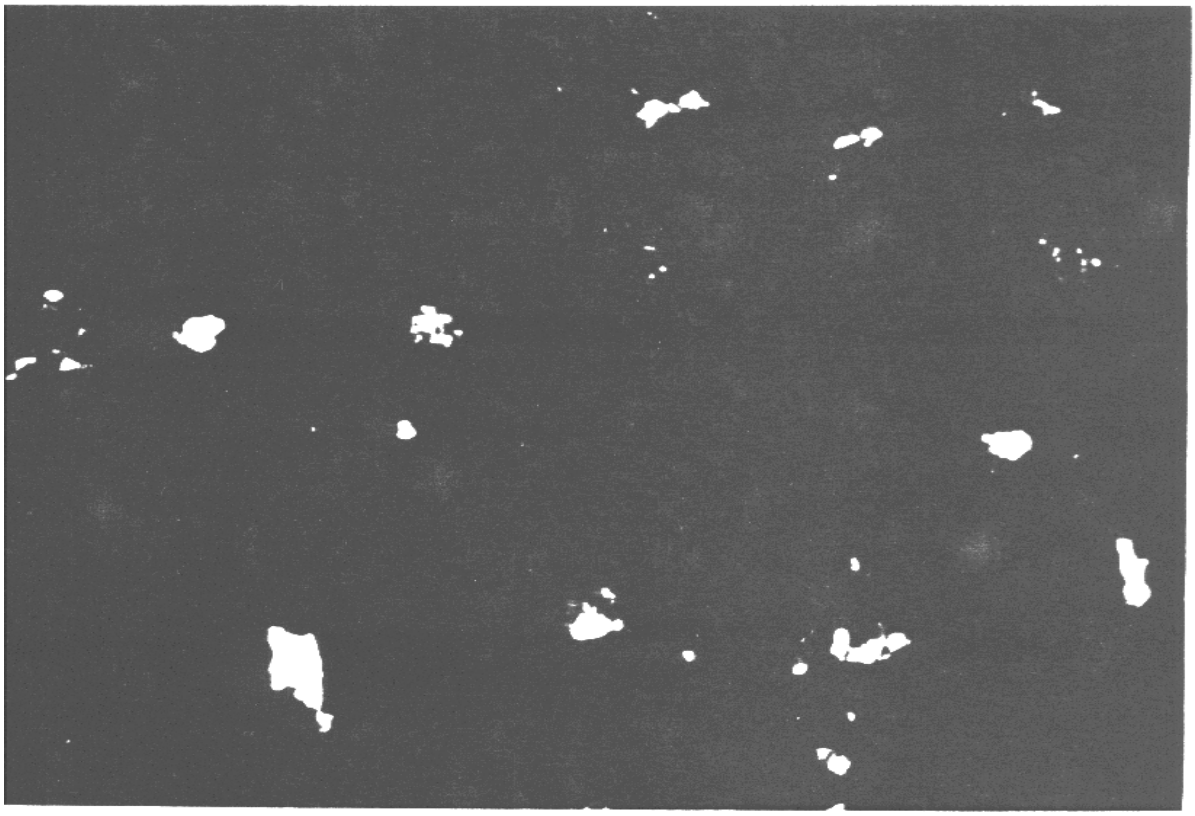

Figure 56: Optical microscopy picture of a 6% (mol) $Zr(acac)_4$/PI film (top:brightfield, bottom:darkfield)

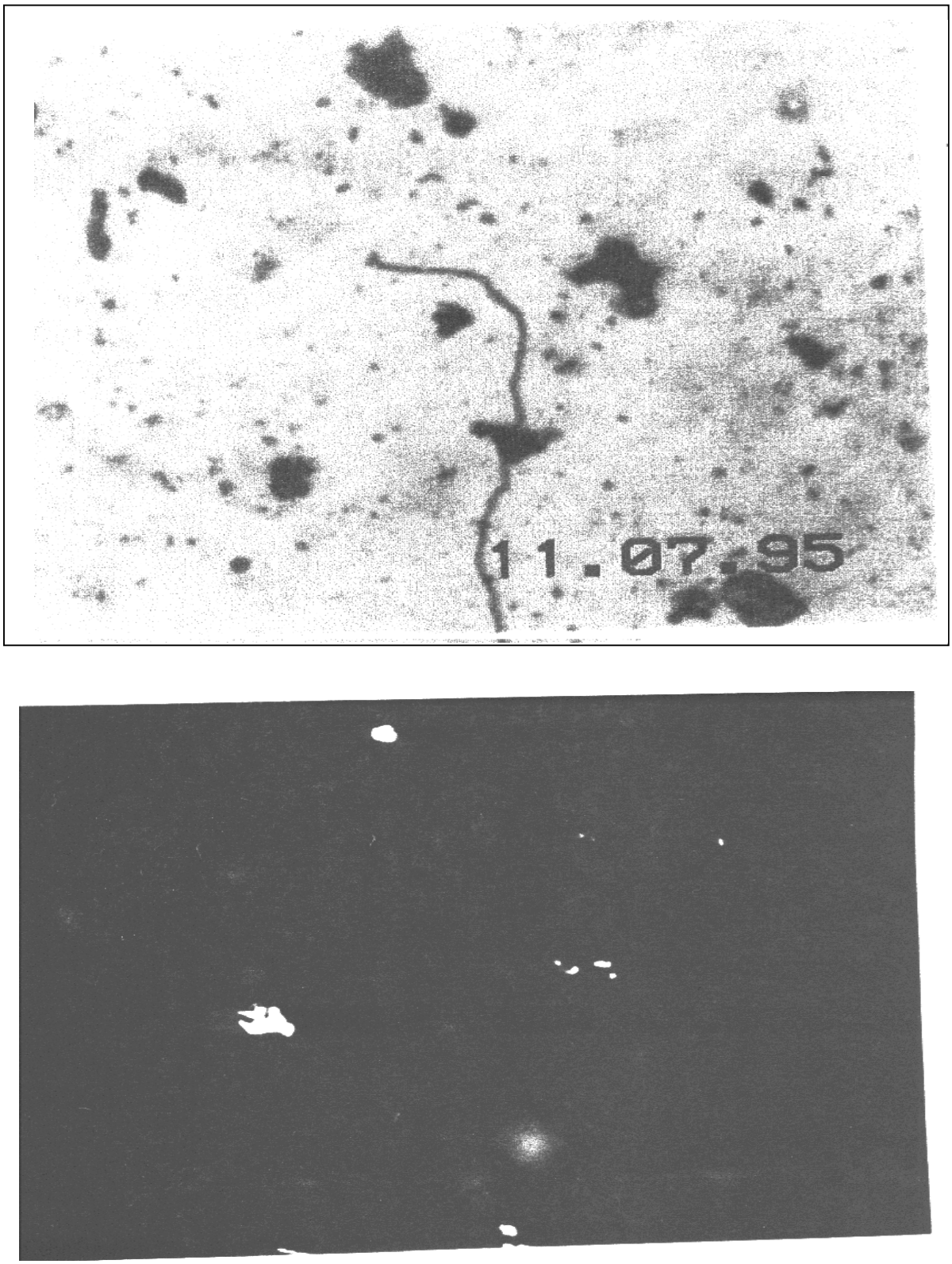

Figure 57. Optical Microscopy picture of a 8% (mol) $Zr(acac)_4$/PI film (top: brightfield, bottom: darkfield)

Atomic Force Microscopy

The study involves PI films of 4-10% additive as well as pure PI film. The images are of the top surface of the film and also include a roughness analysis of the surface.

1. For 4% (mol) Zr(acac)4/PI film, see Figure 60.
2. For 6% (mol) Zr(acac)4/PI film, see Figure 59.
3. For 8% (mol) Zr(acac)4/PI film, see Figure 61.
4. For 10% (mol) Zr(acac)4/PI film, see Figure 62.
5. For pure PI film, see Figure 58.

Table 4. Roughness analysis of films using AFM.

Percent of $Zr(acac)_4$	Image roughness (nm)
Pure	5.98
4	47.191
6	806.47
8	923.69
10	268.67

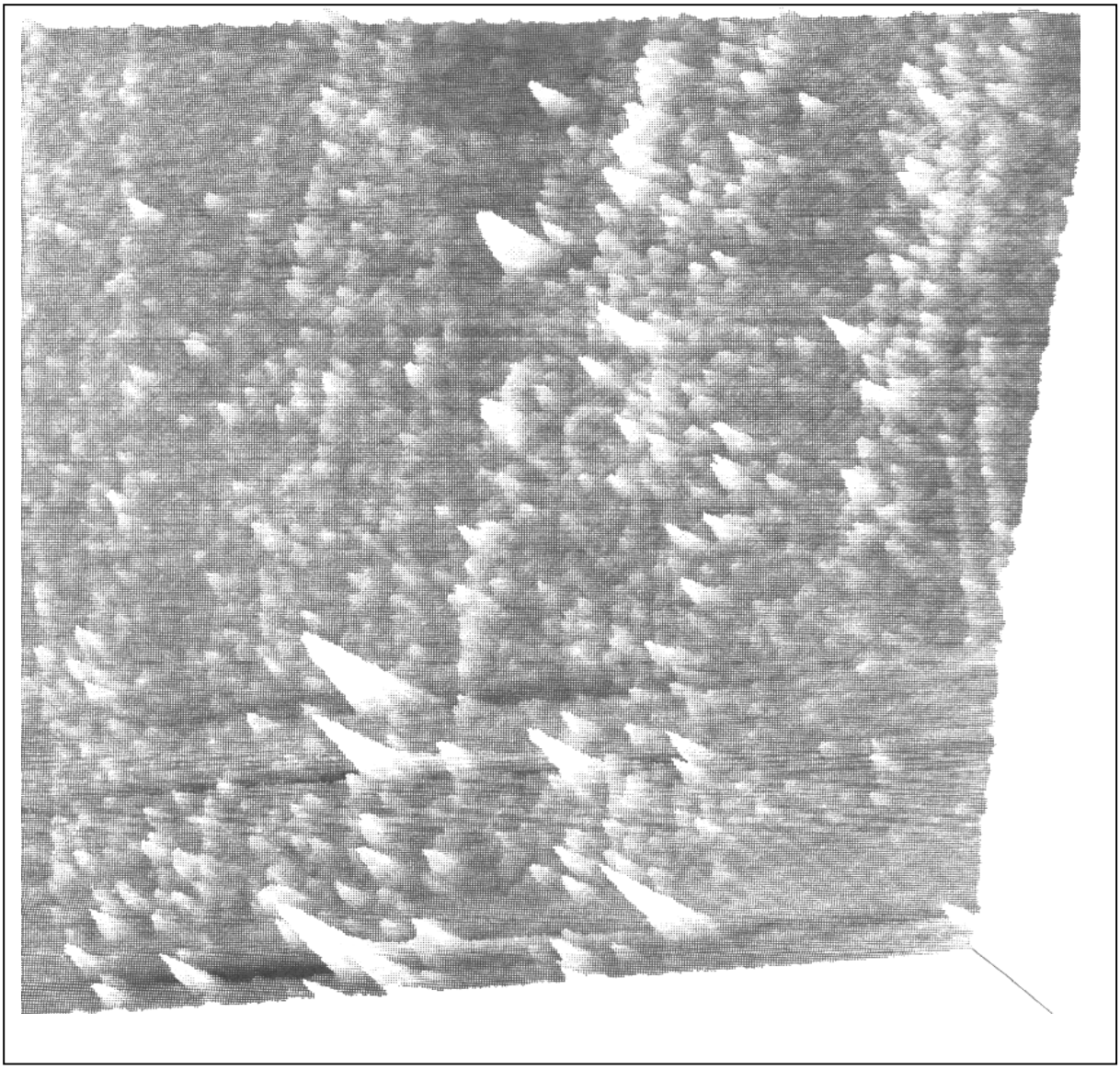

Figure 58. Surface image of a pure PI film without additives

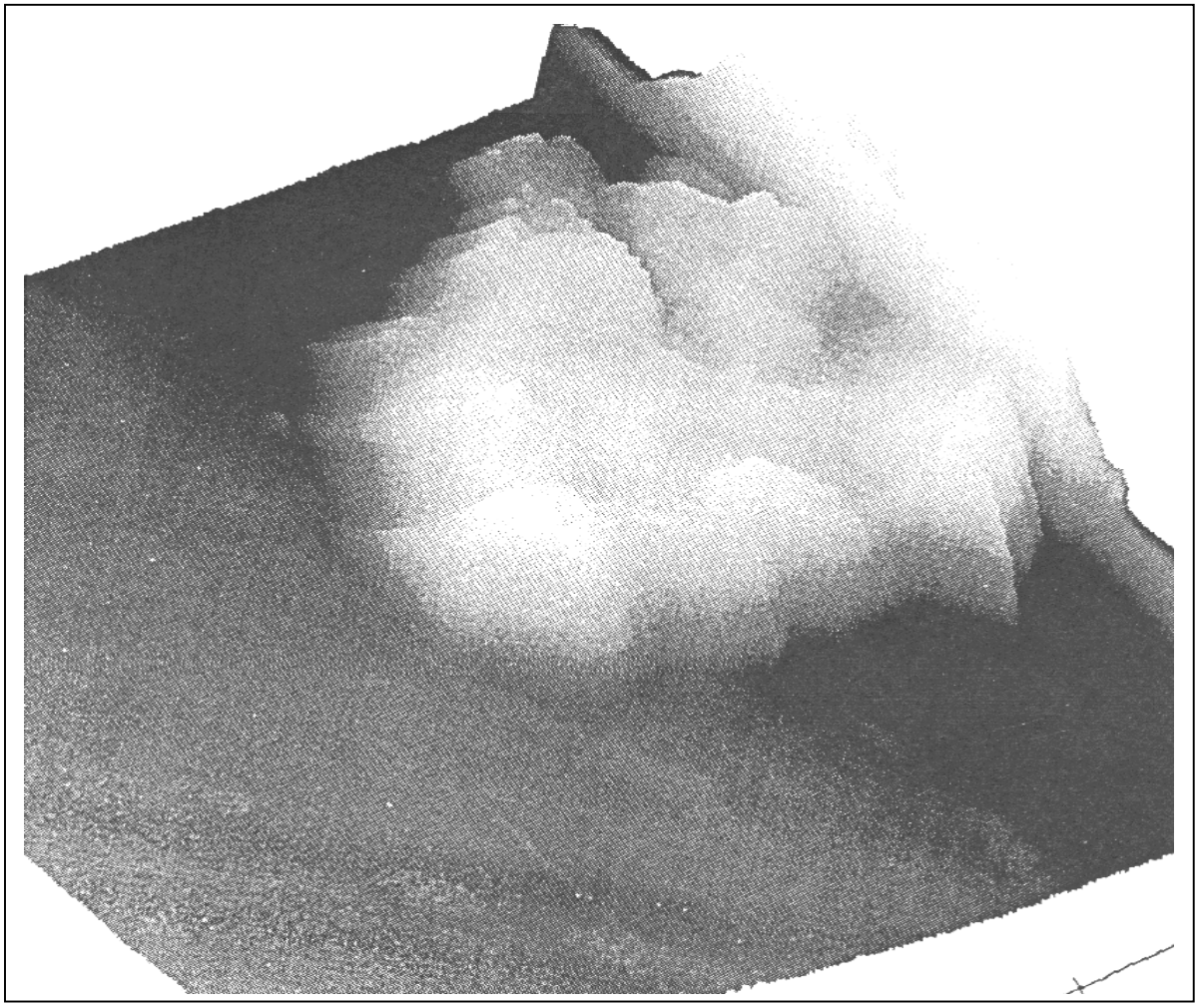

Figure 59. Image of a 6% (mol) Zr/PI film surface

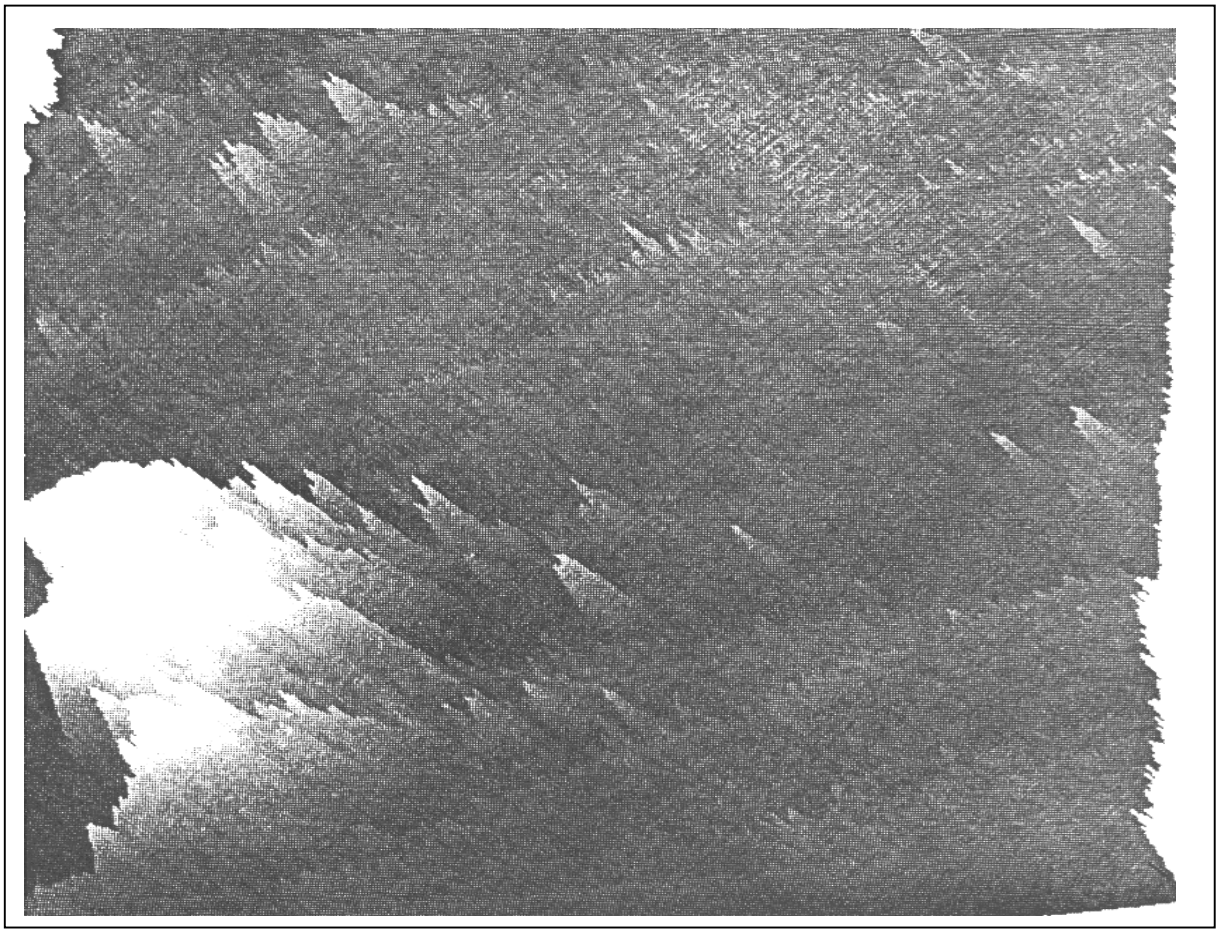

Figure 60. Surface image of a 4% (mol) Zr/PI film

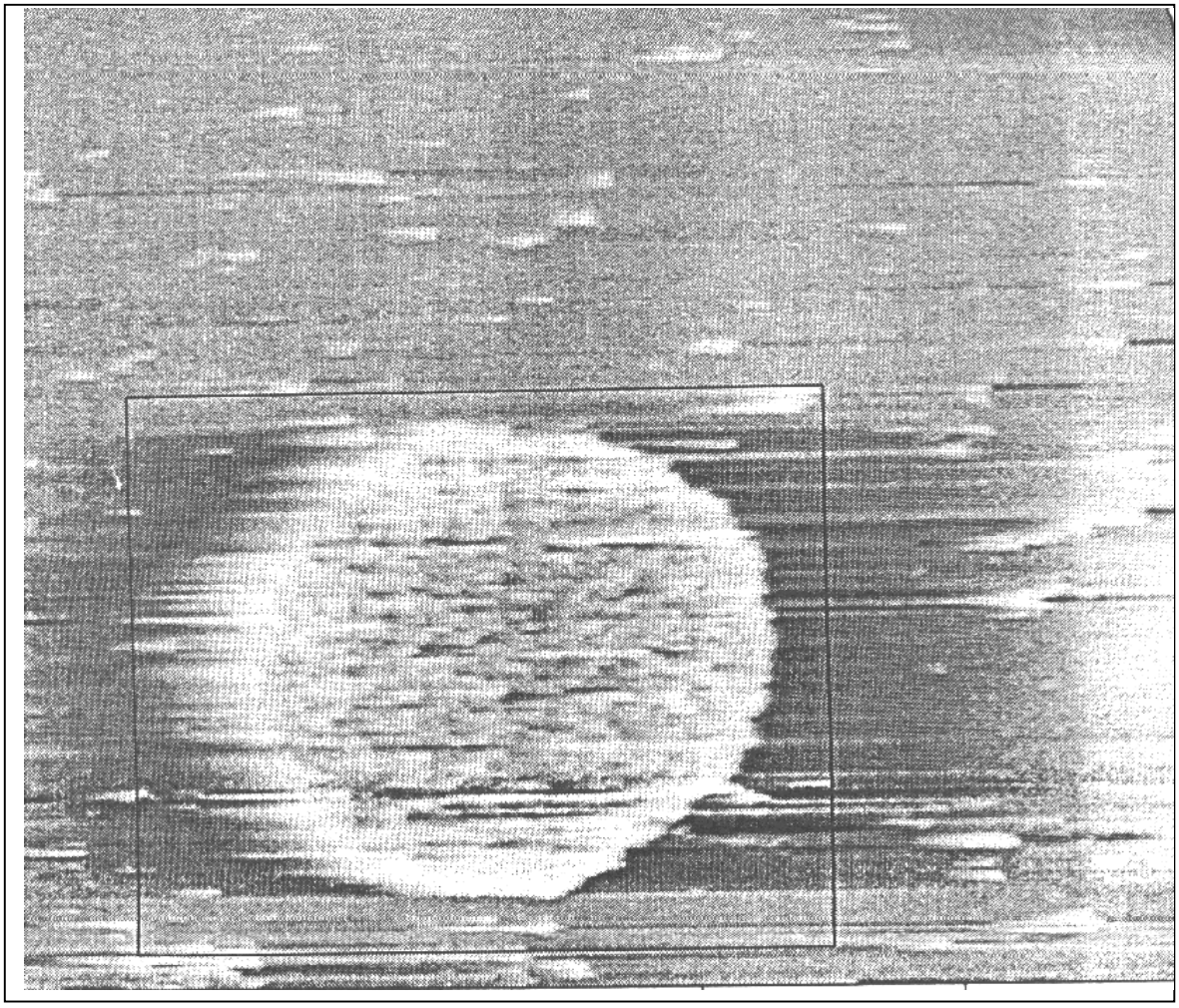

Figure 61. Surface image of a 8% (mol) Zr/PI film

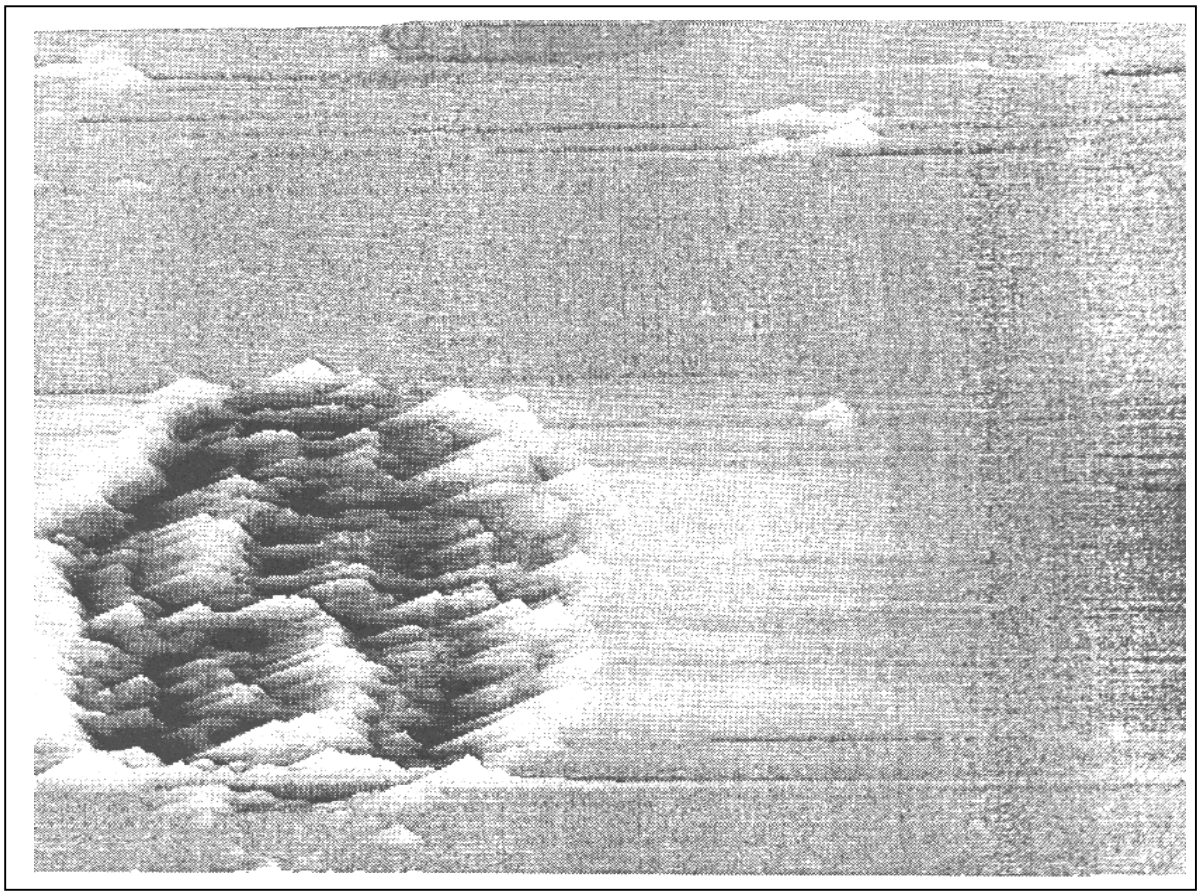

Figure 62. Surface image of a 10% (mol) Zr/PI film

Oxygen Plasma Resistance

The data and results are for the following experiments:

1. Comparison of home made film with commercial films. See Figure 63.
2. Behavior of 2-10% films. See Figures 64a, 65.
3. Behavior of pure films. See Figure 64b.

The first thing we were able to do with the films was to compare a commercial film with the pure ones made in house. From these results we see that the erosion of the commercial films is very similar to the ones made in house. The erosion of the films containing the $Zr(acac)_4$ shows the formation of a white layer over the 2-10% films. The white layer gets denser as the percent of the additive increase.

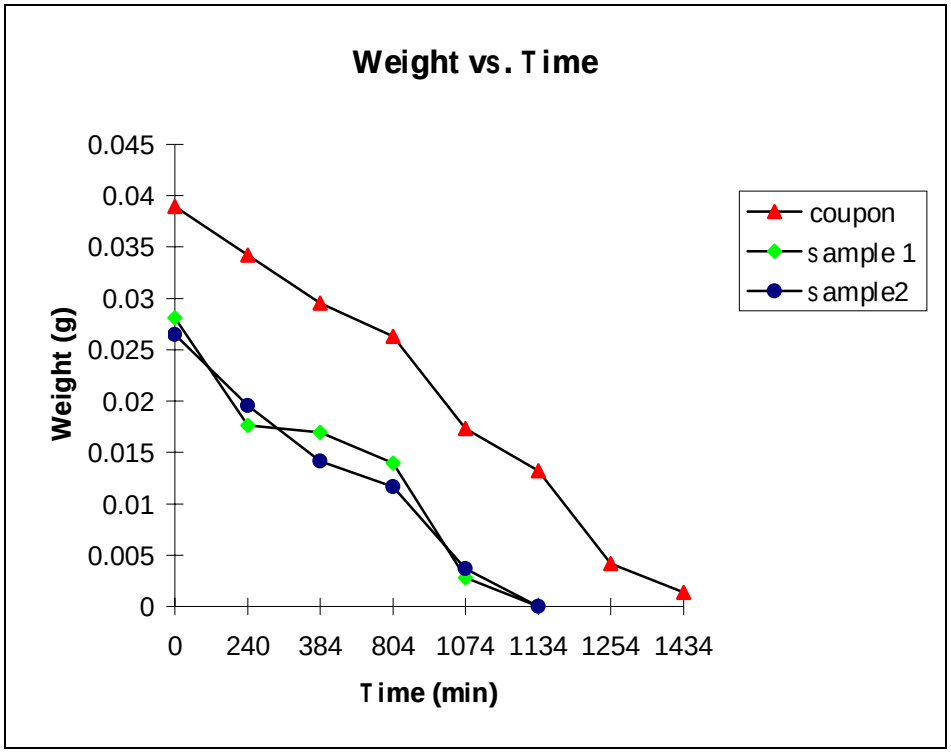

Figure 63. Atomic Oxygen erosion behavior of in house film vs. commercial films. Coupon means commercial made and sample means a particular run.

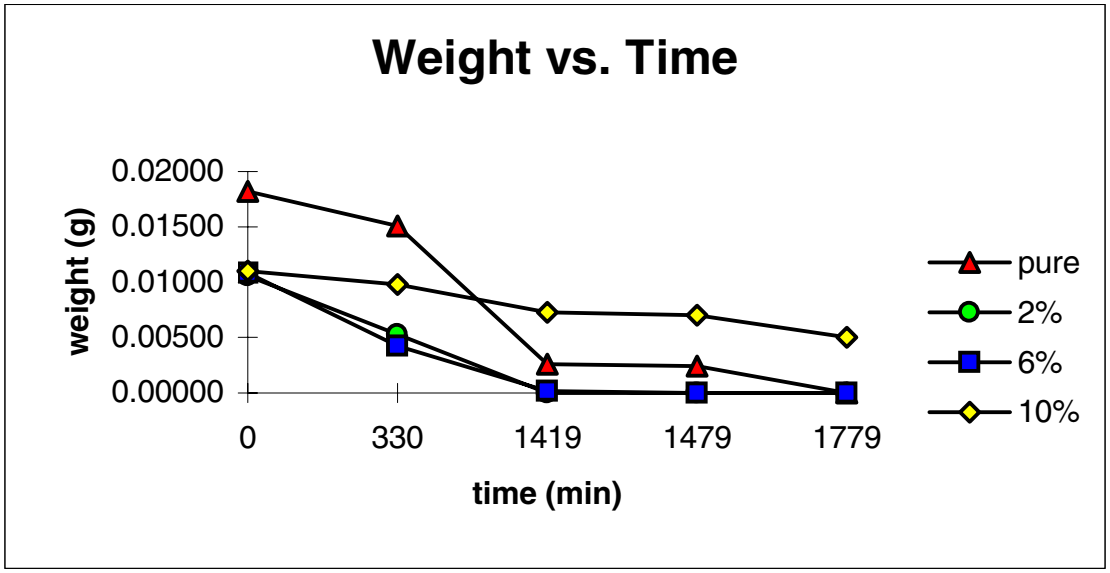

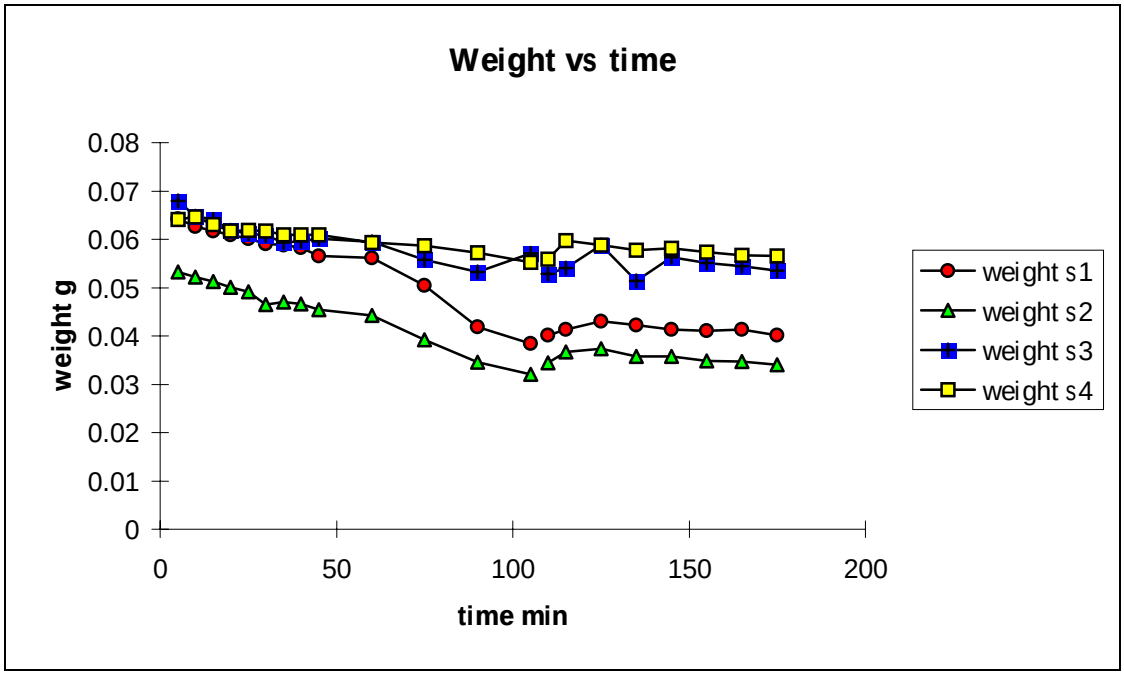

Figure 64. (a) Atomic oxygen erosion behavior of 0-10% (mol) Zr/PI films; (b) Atomic oxygen erosion for 4 different runs of a pure film

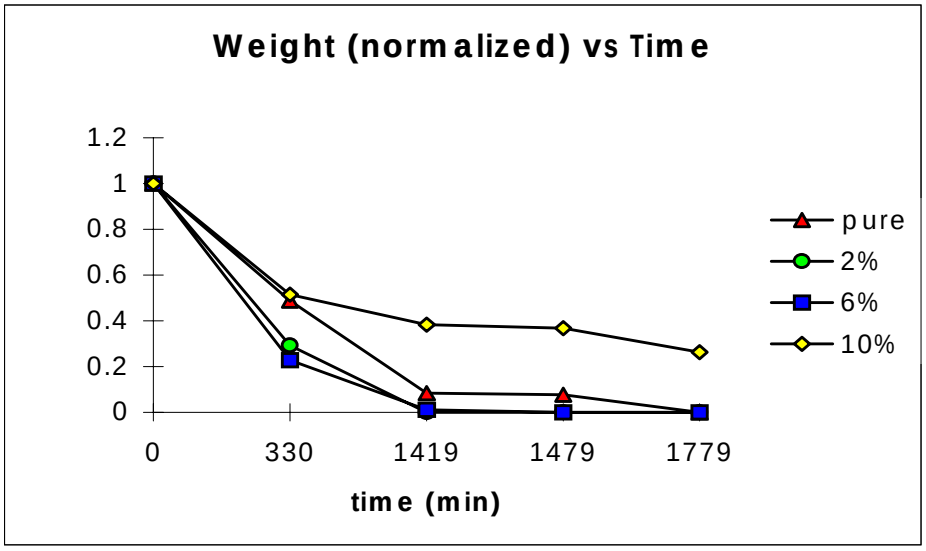

Figure 65. Behavior of 0-10% (mol) Zr/PI films. Weight normalization

Mechanical Testing

Here, three different types of analysis were performed:

1. Pure in-house prepared films, tensile strength behavior. See Figure 66.
2. Behavior of 2-10% (mol) additive films. See Figure 67.

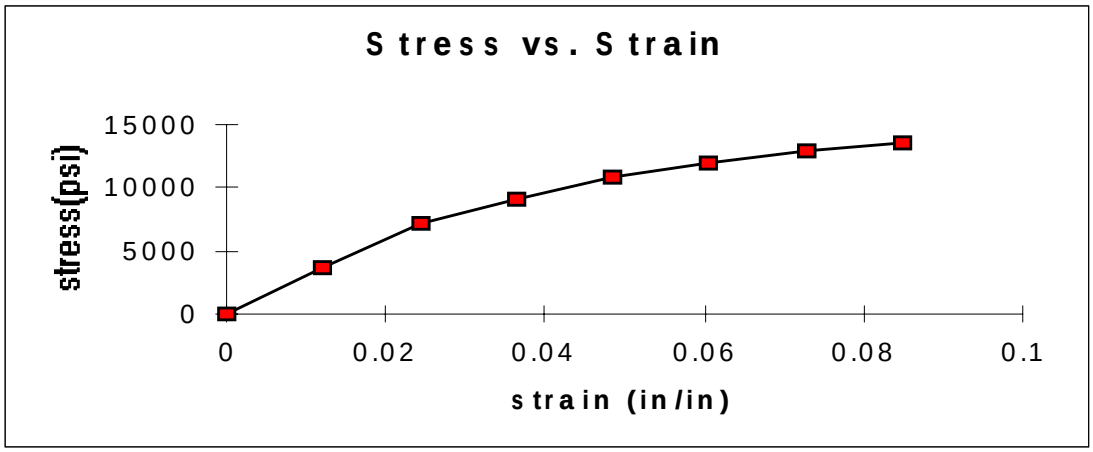

Figure 66. Mechanical behavior of an in-house made pure film

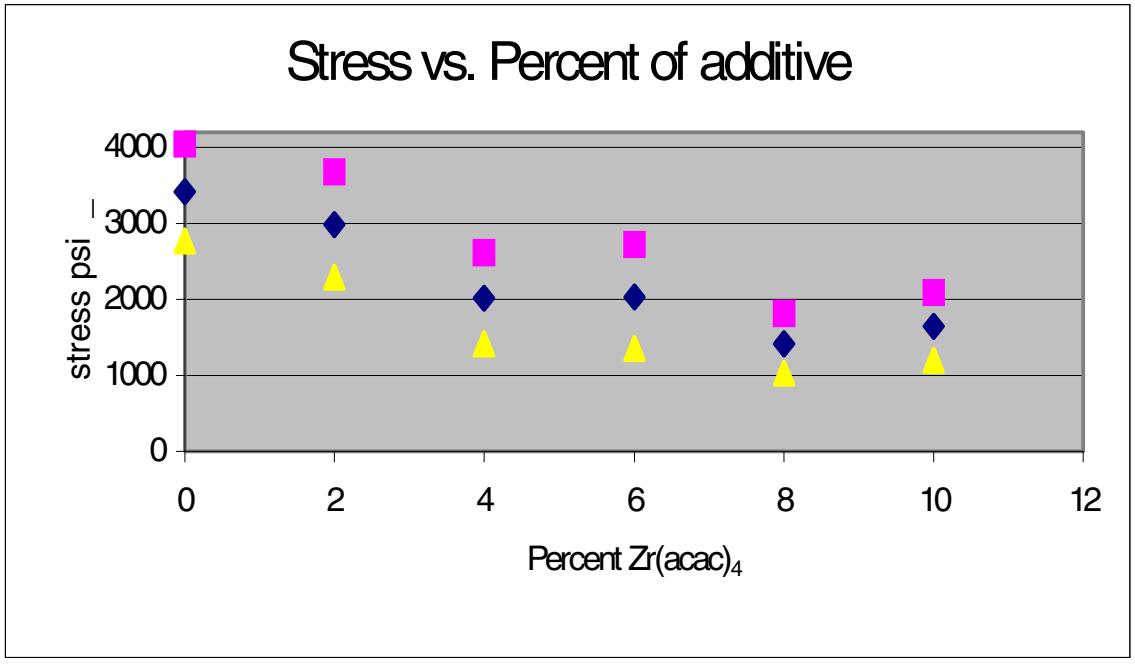

Figure 67. Chart of tensile strength vs. percent of additive. The squares represent the upper error limit, the triangles the lower error limit, and the diamonds the average value for each particular percent of additive.

3. Heat treatment third step (300°C) at 1hr, 1hr 20min, 1hr 35 min. See Figure 68.

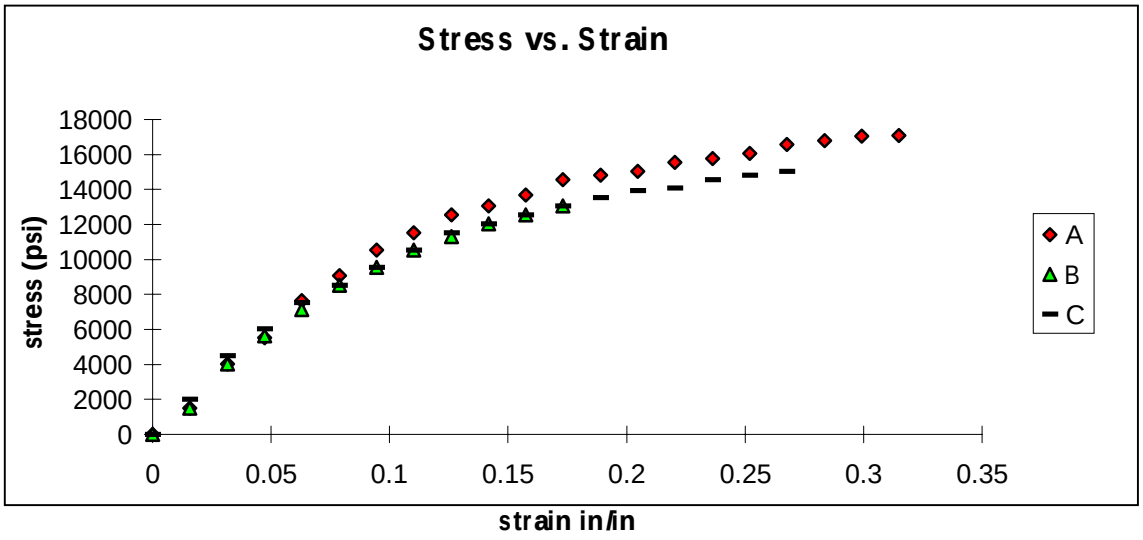

Figure 68. Mechanical behavior of heat-treated pure film (300°C) after (a) 1hr, (b) 1hr 20 min, and (c)1 hr 35 min.

Comparing the tensile strength of the in house prepared pure film with the commercial ones we see a noticeable difference in the strength. It is about 40% lower than the value obtained from Dupont literature,[27] a value of 21 kpsi vs. 15 kpsi for home made films. We observed that when we add the $Zr(acac)_4$, the tensile strength of the films decrease. One point to observe is that the values of tensile strength are lower than those obtained in earlier runs. Repetitions were made and the same tensile strength values obtained.

Chapter 3. Discussion

This chapter covers the discussion of results of the techniques presented in Chapter 2. It also includes an interpretation of these results.

Sample Preparation

The most important step in the testing of film samples with and without the $Zr(acac)_4$ complex is the way the samples are prepared, and that is why the following precautions were taken. All samples were made in the same way. A rack was made so all samples could be imidized at the same time. After the imidization process was finished and samples were cold, they were cut to the required dimensions using a new blade for each substrate and then, for the peeling process, samples were submerged under water for about 10 minutes. Since films have more affinity for the water than for the substrate, they peel off by themselves without any problem. Once the samples with the required dimensions were obtained, they were stored in vials to reduce the probability of absorbing moisture from the atmosphere. Several techniques were used to determine the thickness of the prototype films, but only profilometry was performed on each film sample because of its ease of operation and reliability. Gravimetric techniques correlate with profilometry values. Due to inconsistency in determining peaks from the IR technique, these results were discarded. The problems with IR were due to the nonuniform film thickness.

Mechanical Testing

The following observations can be made based on the data collected for mechanical testing:

1. Forty percent (40%) lower strength observed for in-house prepared film vs. DuPont prepared Kapton. This can easily be attributed to the way the films were made. Based on conversations with DuPont,[26] they prepare films in a different way than we do. They add an extra heating step of 400°C for one extra hour after the 300°C one and then they anneal the resulting film. The films

made at home all measure to an average value of tensile strength of 12.5 kpsi.

2. Changes in tensile strength with increasing mole percent of the additive were examined for the in-house samples, despite the difference noted above for the DuPont samples. Comparing the values, a 10% of $Zr(acac)_4$ additive causes a decrease of tensile strength of about 50%. It is noticed that the tensile strength of films of 4% and 8% are a little higher than for those of 6% and 10%. See Table 5. The decrease in tensile strength can be attributed to the interaction of the additive with the polymer chains of the PI film, as we see when we introduce impurities to a polymer.

Table 5. Tensile strength of films with $Zr(acac)_4$

% $Zr(acac)_4$	Tensile strength (psi)	% decrease strength
Pure	3409 +/- 633	--
2	2982+/- 695	12
4	2010+/- 599	41
6	2035+/-681	40
8	1422+/- 391	58
10	1646+/- 447	51

In conjunction with observation #1, a time/temperature study was conducted (before knowing the way DuPont made their films). By increasing the time of the 300°C step by 20 and 35 minutes, and comparing the resulting film strength with the regular one hour imidization, we see that the duration of the last imidization step doesn't increase the tensile strength of the films significantly.

Plasma Ashing

1. The difference in plasma AO erosion rates results from the difference in how the films were made, i.e. the extra heating/annealing step used to affect imidization. This is because the annealed films are more uniform than the in-house made ones.

2. We can observe that as we increase the percent of the additive, the rate of film erosion decreases, and more film is left after about 1480 minutes on later runs. Because of all the precautions and careful handling, the later run is more representative of the behavior of the films with additives.

Table 6. Comparison of atomic erosion on films 0-10% $Zr(acac)_4$ additive.

% (mol) $Zr(acac)_4$	Weight (g) after 1149 min.		Percent Erosion	Erosion
	Beginning	End		rates (g/min)
Pure	.02930	.0053	99.18	2.50e-5
2	.03015	.0210	69.70	2.62e-5
6	.00970	.0028	28.90	8.44e-6
10	.00800	.0020	25.00	6.96e-6

3. We can observe that as we increase the mole percent of the additive, the rate of erosion decreases and more film is left after about 1480 minutes on later runs.

Scanning Electron Microscopy and Energy Dispersive Microscopy

The first surface tests of the films were SEM and EDS. This study was to determine how the film surfaces change, what elemental composition the films have, and to see if the films have a uniformly dispersed concentration of the $Zr(acac)_4$ additive all over the film or if it is localized.

We expected to see a smooth surface on the films made with and without the additive before we started AO testing of the films, that is what we saw. It is only when we AO exposed the films of 2-10% $Zr(acac)_4$ that we saw the surfaces had become not so smooth. A particulate feature conglomerate is observed randomly distributed on the surface of the film. These features do not have definite shape but in some cases resemble a sphere. The logical thinking was that if something changed it must be the addition of the additive and that the number of features must increase as the additive concentration increases. Since that is not the case, because in some cases the higher $Zr(acac)_4$

concentration films seem to have lower number of features than the lower concentration ones, there must be another phenomenon occurring.

Knowledge of the elemental composition of the films and features was expected to increase the understanding of what is happening. From the EDS analysis (as shown in Figure 46-48) we see that the features contain Zr as well as other elements not present in the composition of the complex (presumed to be contamination). The smooth areas of the film contain the Zr but not the other elements. Knowing the features' origin is very important and crucial to understand the changes in properties of the PI material. One thing believed to be taking place, is that the features come from either the reaction of the $Zr(acac)_4$ with water produced in the reaction process of converting the PAA into PI (see Figure 68), with water already present in the NMP solvent, or by impurities present in the complex. Since we know that the complex had to pass a purity check and that no impurity was seen in the smooth area of the film, the third alternative was discarded. One other possibility is that the impurity is introduced during film preparation, e.g. from the ovens or it is present in the glass slides.

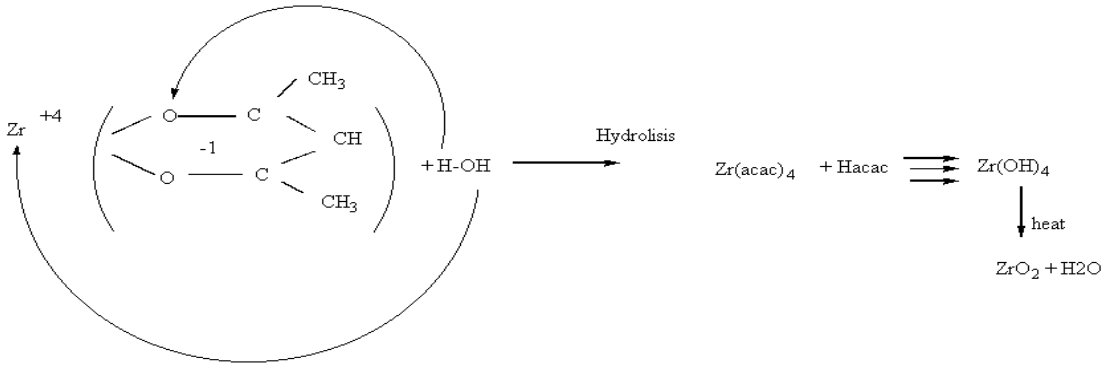

Figure 69. Reaction of water with $Zr(acac)_4$ complex

A SEM/EDS study of the top and bottom part of pure PI and 10% Zr/PI film was conducted to see if there was any difference between them. Since there was no apparent difference in the number of features on the top and the bottom of these films, whatever is causing this feature formation is occurring all through the film regardless of its location. This observation favors the hydrolysis of $Zr(acac)_4$ vs. the ovens or glass slides as sources of contamination.

From the SEM/EDS study it was not clear why this feature formation is occurring. Other possibilities come to mind. One possibility is that the impurities come from the solvent since it is only 99.9% pure; and another is that the elements' peaks overlap with one another, and we are confusing elements not present with others that should be, including dust and substrate impurities. The impurity present seems to be related to the precipitation and nucleation of the complex, since impurities accelerate precipitation.

Optical Microscopy

Films were made to see if the features form before or after the imidization process. For this the optical microscope was used. From this experiment it was observed that the features are present even after heating at the lower temperatures, and there is practically no change upon going to the higher temperatures at which imidization occurs. The only noticeable change caused by the higher temperature heating was in the color of the films, but that was expected from the reaction that was occurring. This observation suggests that hydrolysis of $Zr(acac)_4$ occurs from water in the solvent reacting with the complex, and not water produced by imidization. Films without the additive show that they are very smooth (visually) and no change is observed following the lower or higher temperature heating steps.

The dark features observed in the 10% Zr/PI films show that the features present at 100°C get darker in color at 300°C. This darkening could be due to the initial Zr hydrolysis product forming Zr oxide, or to the features becoming embedded in the organic material during imidization.

Darkfield pictures show that the features which scatter light are different than the polymeric material and are rough. The rest of the films look black because they have smooth surfaces. The white spots in the black areas show that the features have some type of crystalline formation.

Atomic Force Microscopy

Using Atomic Force Microscopy gives a different surface analysis of the films and a quantitative measure of the films' roughness. From this analysis we see that the surface of a "smooth" pure film has a 5.98 nm roughness. Also, the surfaces show lines that run from side to side and are due to the way films were prepared. This accounts for

some of the roughness measured for the "smooth" films. Films containing additives show features which correspond to the ones observed in SEM studies, and which look very circular and spherical in 3-D view. This shape suggests that the additive is surrounded by the polymer, i.e. the PI. Also we see that there are small features that are not spherical in shape, but seem to be coming from the additive too.

From the roughness study we see that pure films are very smooth, and that if they had been prepared better (using DuPont techniques) they would have been featureless. As we increase the concentration of additive, the roughness also increases until we get to a 10% (mol) additive where the roughness drops. This observation suggests that the roughness of the film is not exclusively related to the amount of feature present.

CONCLUSION

The objective of this research is to improve the atomic oxygen resistance of PMDA-ODA polyimide (PI), which has the structure of Kapton™, while retaining or enhancing the desirable properties of the pure polymer. Toward this end, zirconium-containing complexes and polymers were used to make composites and blends.

Part I. Tetra(acetylacetonato)zirconium(IV), $Zr(acac)_4$, which is commercially available, was identified as the best zirconium-containing complex for enhancing the atomic oxygen resistance of polyimide composites of the 10 complexes screened. Films prepared from the commercially-available polyamic acid (PAA) of PMDA-ODA (DuPont) have good uniformity, flexibility and tensile strength. A 24-layer 10% (mol) $Zr(acac)_4$/ PI composite film showed significant improvement (ca. 20 fold) of atomic oxygen exposure duration over the pure polyimide. However, 10% (mol) $Zr(acac)_4$ represents an upper concentration limit, above which films undergo cracking upon thermal imidization.

In order to increase the Zr complex concentration in PMDA-ODA PI films, while retaining good film properties, $[Zr(adsp)_2\text{-PMDA}]_n$ coordination polymer [bis(4-amino-N,N'-disalicylidene-1,2-phenylenediamino)zirconium(IV) - pyromellitic dianhydride] and $[Zr(adsp)_2\text{-PMDA-ODA-PMDA}]_n$ terpolymer were synthesized, respectively. The initial concentrations used for the two polymers in the PAA were 10% (mol) Zr.

However, even at this concentration, which is not an increase over the maximum $Zr(acac)_4$ concentration described above, preparation of multi-layer film samples was only possible up to a small number of layers. Both a relatively high concentration of Zr, and a large number of layers (to produce a reasonably thick film), are necessary in order to provide sufficient aerial density of zirconium to form an adequate ZrO_2 layer for protecting the rest of the underlying polymer.

Part II. From the experimentation and results obtained upon the addition of $Zr(acac)_4$ additive to the polyimide polymer, the following can be concluded:

- The addition of the $Zr(acac)_4$ to the polyimide polymer does in fact change its physical properties. Taking as reference the 10% (mol) $Zr(acac)_4$ addition we see that its tensile strength is reduced about 50% and that its resistance to monatomic oxygen erosion is increased about 70-75%.
- The addition of the inorganic additive causes the formation of some type of feature which contains Zr. The additive also is found in the rest of the film, where the features are not present, as shown in the EDS study. This means that the additive is well dispersed into the polymer matrix.
- The origin of the features seems to have to do with water in the solvent, and possibly from the polymer during imidization. These impurities seem to cause nucleation of the additive causing the features to form.
- The addition of the inorganic additive does not determine how rough the films are, but evidence suggests that it is a factor. The way films are prepared also affects the roughness in the films, as demonstrated in film preparation section.

This work could be followed by more SEM/EDX on $Zr(acac)_4$-PI films before and after AO exposure, and the features could be characterized more using EXAFS to determine Zr's chemical environment by comparison to data for known Zr compounds.

REFERENCES

1. Baraona, C.R. " The Space Station Power System", NASA TM-88847, Fifth Conference on Photovoltaic Generators in Space, Noordwijk, Netherlands, 1986.
2. Banks, B.A. " Protection of Solar Array Blankets from Attack by Low Earth Orbital Atomic Oxygen", ISSN:0160-8371, Proceedings of the 18th Photovoltaic Specialists Conference, Las Vegas, Neveda, October 21-25, 1985.
3. Banks, B.A.; Rutledge, S.K. " Low Earth Orbital Atomic Oxygen Simulation for Materials Durability Evaluation", Proceeding of the 4th International Symposium on Spacecraft in the Space Environment, Toulouse, France, September 6-9, 1988.
4. Leger, L.J.; Visentine, J.T. " A Consideration of Atomic Oxygen Interactions with the Space Station", Journal of Spacecraft and Rockets, 1986, 23(5), 505-511.
5. Leger, L.J. " Oxygen Atom Reaction with Shuttle Materials at Orbital Altitudes", NASA TM-58246, 1982.
6. Rutledge, S.K. " The Effect of Atomic Oxygen on Polysiloxane-polyimide for Spacecraft Applications in Low Earth Orbit", Space Operations, Appplications and Research Symposium, Albuquerque, NM, June 26-28, 1990.
7. Visentine, J.T.; Leger, L.J.; Kuminecz, J.F.; Spiker, I.K."STS-8 Atomic Oxygen Effects Experiment", AIAA Paper 85-0415, AIAA 23rd Aerospace Science Meeting, Reno, Nevada, January 14-17, 1985.
8. Golub, M.A. " ESCA Study of Kapton Exposed to Atomic Oxygen in Low Earth Orbit or Downstream from a Radio Frequency Oxygen Plasma", Polymer Communication, 1988, 29.
9. Bank, B.A. " SiOx Coatings for Atomic Oxygen Protection of Polyimide Kapton in Low Earth Orbit", Coating Technologies for Aerospace Systems Materials Specialist Conference, April 16-17, 1992, Dallas, TX.
10. Banks, B.A. "Ion Beam Sputter-Deposited Thin Film Coating for the Protection of Spacecraft Polymers in Low Earth Orbit", Aerospace Science Meeting, Reno, Neveda, January 14-17, 1985.
11. Rutledge, S.K. and Olle, R.M. " Durability Evaluation of Photovoltaic Blanket Materials Exposed on LDEF Tray S1003", The First LDEF Post-Retrieval Symposium, Kissimmee, Florida, June 2-8, 1991.

12. Banks, B.A.; Auer, B.M.; Rutledge, S.K. " Monte Carlo Modeling of Atomic Oxygen Interaction with Protected Polymers for Projection of Material Durability in Low Earth Orbit", MRS Spring Meeting'92, San Francisco, CA.

13. Banks, B.A.; Rutledge, S.K. " The implication of the LDEF Results on Space Station Freedom Power System Materials", 5th International Symposium on Materials in a Space Environment, Cannes-Mandelieu, France, September 16-20, 1991.

14. Illingsworth, M.L.; Banks, B.A.; Smith, J.W.; Jayne, D.; Garlick, R.G.; Rutledge, S.K.; de Groh, K.K., "Plasma and Beam Facility Atomic Oxygen Erosion of a Transition Metal Complex", *Plasma Chem. and Plasma Proc*., **1996**, *16(2)*, 209.

15. Handbook of Chemistry and Physics, CRC, 74th edition, **1993 - 1994**.

16. John Emsley, The elements, 2nd edition, Oxford University Press, **1992**.

17. Aldrich catalogue, 1994 - 1995.

18. Chen, Y. "Zirconium-Containing Polymeric Materials", MS project, RIT, August, **1996**.

19. He, L. "Atomic Oxygen Resistant Zirconium-Containing Polyimides", MS Thesis, RIT, June **1996**.

20. Betancourt, J. A. "Characterization of Kapton Polymer with an Inorganic Additive", MS Thesis, RIT, November, **1998**.

21. Illingsworth, M. L.; Rheingold, A. L. "Synthesis and Molecular Structure of the Eight-Coordinate Complex Bis(4-amino-N, N'-disalicylidene-1,2-phenylenediaminato)zirconium(IV), a New Reagent for Preparing Coordination Polymers", *Inorg. Chem.* **1987**, *26*, 4312.

22. Polyimides: Synthesis, Characterization and Applications. Vol. 1; K. L. Mittal, Ed.; Plenum, New York **1984**.

23. Handbook of Inorganic Compounds, D. L. Perry and S. L. Phillips, Eds.; CRC, **1995**.

24. "Error Determination and Propagation", Chemistry 484, University of Nebraska-Lincoln,Wwish.un1.edu/chem484/error/errorhelp.html.1997

25. "Error Propagation" ,Kyle Snow, University of California Fresno,1997 WWW.engr.csufresno.edu/~4sight/error.html.

26. J. Edman (DuPont; Circleville, OH), private communication, June 1996.

27. Kapton Polymer Empirical Data Sheets (provided by DuPont).

Appendix A.

Yang Chen, MS Project, "Zirconium Containing Polymeric Materials"

Introduction

Low Earth Orbit (LEO) atomic oxygen interacts with exposed polymers, resulting in loss of material due to oxidation.[1] The National Aeronautics and Space Administration (NASA) has interest in the use of materials which are inherently durable to atomic oxygen (AO) or are provided with protective coatings to prevent exposure of underlying materials which could be subjected to oxidation.

Polyimide Kapton (Figure 1) was the material originally selected for the structural support the Space Station Freedom (SSF) photovoltaic array blanket.[2] Its low density, flexibility, strength and thermostability make it an ideal material for this application.[3] The volume of organic material oxidized per incident atomic oxygen atom, called the erosion yield, was found to be 3.0×10^{-24} cm^3/atom for polyimide Kapton.[i] However, the atomic oxygen flux requirement for the anti-solar facing surface of the array blanket is sufficiently high (1.14×10^{14}/atoms/(cm^2/sec)) that the array would be oxidized in six months, in spite of its 15-year durability requirement. [4]

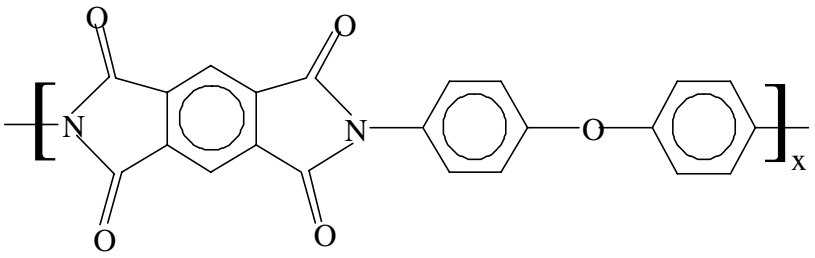

Figure 1. The structure of polyimide Kapton

In order to increase polyimide Kapton's durability in atomic oxygen environment, Kapton was coated with metal oxides, such as SiO_2, fluoropolymer filled SiO_2, and Al_2O_3 films, which have been demonstrated in both ground and space testes to be effective in protecting polyimide Kapton from oxidation by LEO atomic oxygen. [4 - 6] Although the coatings themselves are durable to atomic oxidation, defects in the coating can still allow atomic oxygen to attack the

underlying Kapton (Figure 2) and results in gradual mass loss of the solar array blanket.[7]

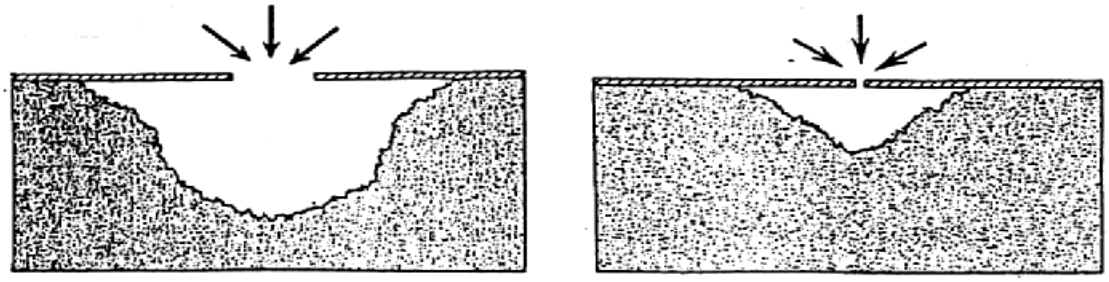

Figure 2. Plasma asher atomic oxygen interaction at narrow and wide crack defect site on protected Kapton

To overcome the shortcoming of SiO_2-coating Kapton, an Atomic Oxygen Resistant (AOR) Kapton was proposed as a back up materials for the SSF solar array design.[8] The ground-based plasma asher tests showed a significant improvement of AOR Kapton over pure Kapton.

However, when tested on the Long Duration Exposure Facility (LDEF), these silicon-containing polymers produced a volatile substance.[9] The deposition of a dark contaminant film on adjoining surface has potential for causing diminished solar illumination of the solar cells, which would greatly reduce the operating life of spacecraft.

Zirconium-containing materials proposed by Dr. M. L. Illingsworth have the potential to offer comparable AO resistance to the silicon-containing materials, without formation of volatile substance and without the need for a metal oxide coating.[10] A zirconium oxide protective layer can be formed upon AO exposure of a zirconium-containing polymer composite. The advantage of ZrO_2 is its standard formation free energy of ΔG_f^0 = -1042 KJ/mol,[11] making it one of the most stable metal oxides.

The goal of this research is to integrate zirconium complexes with polyimide (PI) Kapton, and produce an enriched ZrO_2 layer upon exposure to AO. The oxide layer will be protective of the polymer beneath it.

Zr-containing PI Kapton were prepared via two routes. In the first route, zirconium complexes, bis(4-benzoyl-N,N'-disalicylidene-1,2-phenylenediamino)zirconium(IV), $Zr(bdsp)_2$, bis(N,N'-disalicylidene-1,2-phenylenediamino)zirconium(IV), $Zr(dsp)_2$, and bis(N,N'-disalicyclidene-3,4-diaminopyridino)zirconium(IV), $Zr(dsdp)_2$, were mixed respectively (Figure 3) with commercial polyamic acid of Kapton (PA) cast into film and heated at 100°C, 200°C, and 300°C for one hour each to obtain Zr complex/polyimide Kapton composite films. The concentration limit for the complexes was determined to be 4% by mole Zr, above which the mechanical properties of the composite films degrade.

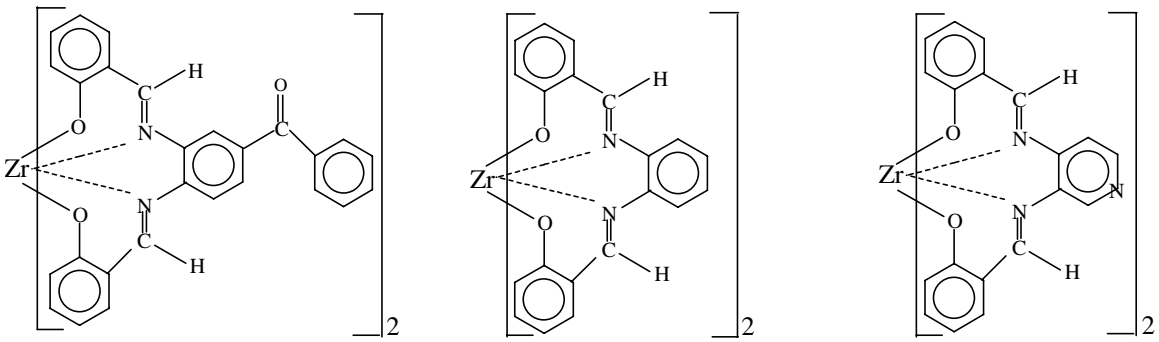

Figure 3. Structure of $Zr(bdsp)_2$ (a), $Zr(dsp)_2$ (b) and $Zr(dsdp)_2$ (c)

In order to increase the Zr complex concentration in PA, a second route was pursued, where $[Zr(adsp)_2\text{-PMDA}]_n$ coordination polymer [bis(4-amino-N,N'-disalicylidene-1,2-phenylenediamino)zirconium(IV) - pyromellitic dianhydride] and $[Zr(adsp)_2\text{-PMDA-ODA-PMDA}]_n$ terpolymer [where ODA is oxydianiline] were synthesized and blended with the commercial PA, respectively (Figure 4-6), and treated as above. The concentration for the two polymers in Kapton PA was 10% by mole Zr.

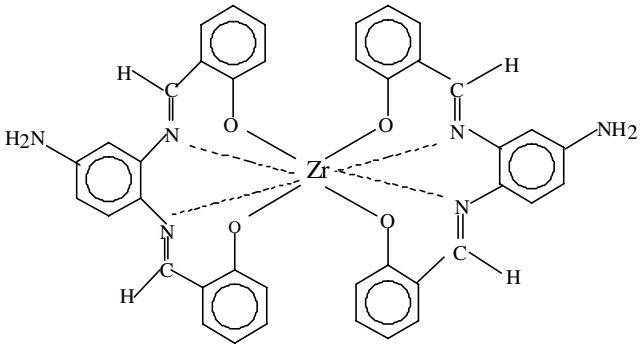

Figure 4. Structure of $Zr(adsp)_2$

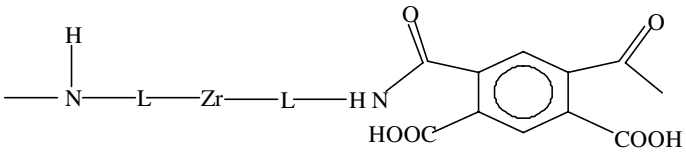

Figure 5. Structure of $[Zr(adsp)_2\text{-PMDA}]_n$ polyamic acid coordination polymer

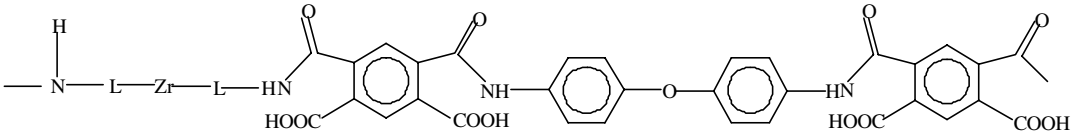

Figure 6. Structure of $[Zr(adsp)_2\text{-PMDA-ODA-PMDA}]_n$ polyamic acid terpolymer

Experimental

Zirconium complexes, bis(4-benzoyl-N,N'-disalicylidne-1,2-phenylenediamino)zirconium(IV), $Zr(bdsp)_2$, bis(N,N'-disalicylidene-1,2-phenylenediamino)zirconium(IV), $Zr(dsp)_2$, and bis(N,N'-disalicylidene-3,4-diaminopyridino)zirconium(IV), $Zr(dsdp)_2$ were mixed, respectively, with commercial PA to form three Zr composites.

Preparation of Zirconium Complexes

$Zr(bdsp)_2$ and $Zr(dsp)_2$ were prepared by previous workers.[12, 13] $Zr(dsdp)_2$ was prepared according to the following procedure developed by Todd Browning (private communication) and futher refined in this research:

N,N'-disalicylidene-3,4-diaminopyridine, H_2dsdp.[14] 3,4-diaminopyridine 2.000g (0.01833 mol) was dissolved in 100 ml absolute ethanol; 4.00 mL (0.0375 mol) salicylaldehyde was added to the suspension; the mixture was heated and maintained at reflux for 5 hours. Completion of the reaction was established by TLC using a silica gel plate and a 10:1 mixture of carbon tetrachloride and methanol. No spot corresponding to known starting materials was observed in the TLC of the reaction solution. After drying over night, 5.49 g of yellow Schiff base was obtained with 94% yield. H_2pdsp was crystallized by using hot ethanol. Melting points varied (see result and discusson). Elemental analysis (EA) was obtained as a verifying factor for H_2pdsp. For $C_{19}H_{16}N_3O$, Calc'd : C, 71.90; H, 5.07; N, 13.24. Found: C, 71.44; H, 4.88; N, 13.50.

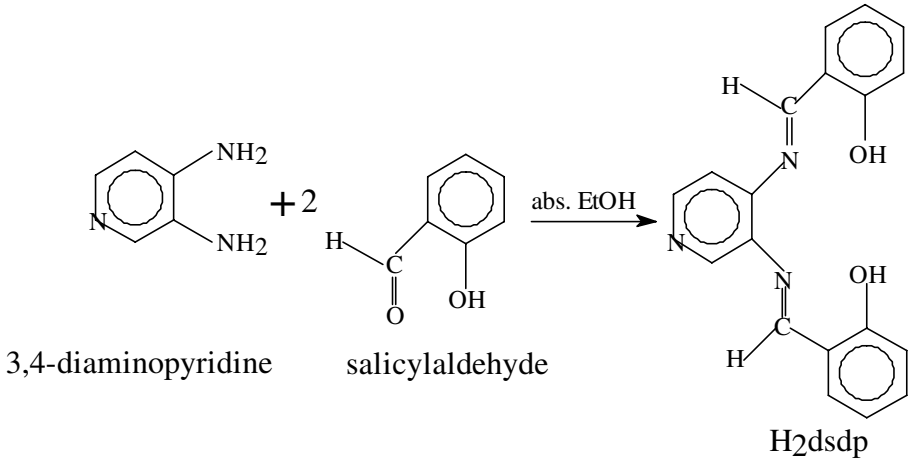

Figure 7. Synthesis of H_2dsdp

Bis(N,N'-disalicylidene-3,4-diaminopyridino)zirconium(IV), $Zr(dsdp)_2$ H_2dsdp 0.400g (0.00133mol) was suspended in 60.0 mL absolute ethanol. In a nitrogen atmosphere (glovebag) 0.290 mL (0.633 mol) of 80% tetra (n-butoxide) zirconium(IV), ($Zr(OBu)_4$), was added to the round bottom flask. The flask was stoppered and removed from the glovebag, and fitted with a condenser to which

a drying tube had been attached and set to reflux overnight. After 19 hours of reflux, the contents of the flask were suction filtered while while still hot, and the powdery yellow product was collected with 50% yield. Completion of the reaction was confirmed by TLC with the same chromatography system described above. Its identity was confirmed by EA, FT-IR and ^{1}H-NMR.

Zr complex / polyimide composite films

Three Zr complexes, Zr(bdsp), Zr(dsp) and Zr(dsdp) were separately dissolved in a small amount of solvent (NMP) and mixed with commercial polyamic acid (PA) of Kapton in NMP (Dupont).[15] For example, 0.0556g of $Zr(bdsp)_2$ in 2.00 ml NMP was mixed with 4.000g of PA (15% solids) in NMP to make 4% by mole Zr solution. Films were prepared from these three solutions on glass substrates, and then imidized by baking at 100°C, 200°C and 300°C for one hour[16] each to produce the Zr-PI composites. The amount of each complex was increased up to 4% by mole before the films cracked upon imidization.

Synthesis of coordination polymer and terpolymer containing $Zr(adsp)_2$ complex

Bis(4-amino-N,N'-disalicylidene-1,2-phenylenediamino)zirconium(IV), $Zr(adsp)_2$. $Zr(adsp)_2$ was prepared following the procedure described in Ref. 17. Before hydrogenation, purification was required for $Zr(adsp)_2$. $Zr(adsp)_2$ was dissolved in THF, and recrystallized twice with decolorized carbon, and precipitate with hexanes.

$[Zr(adsp)_2$-PMDA$]_n$ coordination polymer. The commercial monomer reagent 1,2,4,5-benzenetetra-carboxylic anhydride, PMDA, was purified by sublimation. The $[Zr(adsp)_2$-PMDA$]_n$ coordination was prepared by adding $Zr(adsp)_2$ to PMDA in equal molar amounts. For typical reaction at 0°C, 0.290g (1.33 mmol) PMDA was partially dissolved in 2 mL of dried NMP (Aldrich). 1.00g (1.33 mmol) $Zr(adsp)_2$ was dissolved in 3.0 mL NMP at room temperature. The

red $Zr(adsp)_2$ solution was added slowly into PMDA solution at 0°C with stirring. $Zr(adsp)_2$ container was rinsed with 2.2 mL fresh dried NMP. The rinse solution was added to the red polymerization solution. The resultant brown solution was stirred at 0°C overnight. Polymerization was established by TLC using silica gel plate and a 1:1 mixture of methylene chloride and ethyl acetate. No spot corresponding to known $Zr(adsp)_2$ was observed in the TLC of the polymer solution. Some of the polymer was isolated by pouring the solution into 80ml of rapidly stirred anhydrous ether. After several minutes, the yellow precipitate was suction filtered, and vacuum dried.

$[Zr(adsp)_2$-PMDA-ODA-PMDA$]_n$ terpolymer. In addition to the reagents used to prepare the above coordination polymer, oxydianiline, ODA, was purified by sublimation. $[Zr(adsp)_2$-PMDA-ODA-PMDA$]_n$ terpolymer was prepared by mixing $Zr(adsp)_2$, PMDA, and ODA in 1:2:1 mole ratios. For typical reaction at 0°C, 0.5817g (2.66 mmol) PMDA was dissolved partially in fresh, commercial anhydrous NMP. 1.00g (1.33 mmol) $Zr(adsp)_2$ and 0.2670g (1.3333 mmol) ODA were dissolved in fresh anhydrous NMP at room temperature, separately. The total amount of NMP used was 11 mL. The red $Zr(adsp)_2$ solution and colorless ODA solution were added slowly into PMDA solution at 0°C at the same time with stirring. Then the obtained red solution was stirred over night at 0°C. Polymerization was established by TLC with same chromatography system described above. Some of the terpolymer was isolated by pouring the solution into 80 mL of rapidly stirred anhydrous ether. After several minutes, the yellow precipitate was suction filtered, and vacuum dried.

The structures of the above two yellow products were confirmed to be $[Zr(adsp)$-PMDA$]_n$ and $[Zr(adsp)_2$-PMDA-ODA-PMDA$]_n$ by elemental analysis, FT-IR and ^{1}H-NMR. TGA was performed at RIT. Viscosity for dilute solutions (0.1 g/dL) was measured in N-methylpyrrolidone (NMP) at 30°C by using an Ubbelohde No. 1 viscometer. Gel permeation chromatography (GPC) analyses in NMP at 60°C were performed at NASA Langley.

Blended polymer film formation

The two polymers were dissolved in NMP respectively to make 15 wt.% solutions and mixed with commercial PA in NMP also 15 wt%. The Zr mole percentage of the two polymer blends was 10% by mol for both solutions. The preparations of the solutions are described below.

One gram of coordination polymer (mer unit molecular weight Mw = 968) was dissolved in 5.7 mL NMP, yielding a 15 wt.% solution. The solution was then mixed with 26 gram 15 wt.% commercial polyamic acid Kapton to obtain a 10% mol Zr blend polymer solution to be used in film formation.

10% mol Zr = moles of mer unit coord.polymer / [moles of mer unit coord. polymer + moles of mer unit PA]

= (1/968)/[1/968 + (0.15)(x)/418]

where, x = 26 g, the weight of commercial PA solution used.

In the same way, for one gram terpolymer (repeat unit Mw = 1386), 5.7 mL NMP and 18 gram PA were used to make 10 % mole Zr blend polymer solution to be used in film formation.

The two types of polymer blend films were formed by uniformly spreading the above polymer solutions on glass plates using strips of tape on either side of the polymer solution and dragging clean glass edge over the solution surface two or three times in the same direction. Using a standard imidization procedure,[16] the films were heat-treated at 100°C, 200°C, and 300°C for one hour each. This film preparation procedure was repeated to make multilayer film samples until crack formation was observed.

The thickness of the films was measured using a profilometer (Dektak M-611 see lab notebook YC-II-30). The surface of the single layer coordination polymer blend and terpolymer blend which contain 10% Zr by mole were examined by SEM (Philips 501 scanning electron microscope) before and after

two hours of plasma ashing. Samples were coated with approximately 100 angstroms of gold. KV setting is 30kv and the magnification is 10,000 specifically.

Result and Discussion

Preparation of Zr complexes

There are two feasible routes to synthesize the ligand H_2dsdp. In the first route, absolute ethanol was used as solvent in the reaction of 3,4-diaminopyridine and salicylaldehyde. In the second route, salicylaldehyde is used as a solvent, as well as a starting material. Since excess salicylaldehyde was needed in the second route, and is hard to remove from the product (b.p.: 197°C from vender). Due to this problem, the first route was employed.

The TLC showed no spot corresponding to known starting materials, but there were two spots on the TLC plate. Impurities in the product was first expected to be the reason. Recrystalization was used to purify the product, but, unable to eliminate the second spot. It is possible that tautomerization of H_2dsdp (Figure 8) contributes to the two spots in TLC, and interferes with consistent melting points. Also, tautomerization would not affect the elemental analysis.

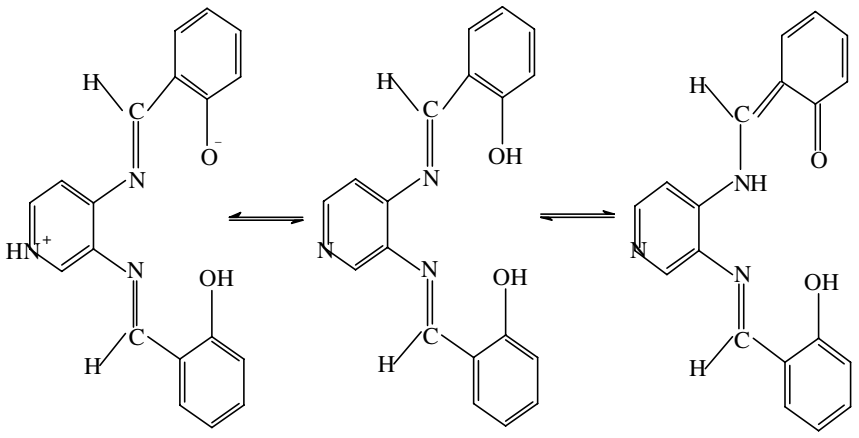

Figure 8. Possible tautomers of H_2dsdp

The Schiff-base complex $Zr(dsdp)_2$ was prepared from $Zr(OBu)_4$ and the premade Schiff-base ligand H_2pdsp according to the following reaction:[13,14,17]

$$Zr(OBu)_4 + 2H_2dsdp \rightarrow Zr(dsdp)_2 + 4HOBu$$

Characteristic FT-IR peaks (Figure A-1 Appendix) are: 1607, 1317, and 596 cm^{-1} assigned to (C=N)-Zr stretching, (Ph-O)-Zr stretching, and pyridine bending, respectively.[18] For the ^{1}H-NMR spectrum in d^2-$MeCl_2$ (Figure A-2, Appendix) the most notable peaks are a singlet at 8.7 ppm and a doublet at 7.3 ppm, which represent aromatic peaks ortho and meta to the pyridine nitrogen in $Zr(dsdp)_2$, respectively.[18] Elemental analysis was also performed and calculated for $C_{38}H_{26}N_6O_4Zr$: C, 63.22; H, 3.64; N, 11.64. Found C, 62.65; H, 3.81; N, 11.65. Deviations are most likely due to the solvents in the sample that appear in the ^{1}H-NMR spectrum.

The IR and ^{1}H-NMR spectra of the product confirms that $Zr(dsdp)_2$ was successfully prepared.

Zr complex/polyimide composite films

Films were examined visually for cracks, which determine the film quality. The onset of cracks in a film is controlled by the concentration of the complexes and thickness of the polymer layer. The highest concentrations of the three complexes that could be mixed with commercial PA solution and give high film quality is 4% by mole. Beyond the limit, films cracked extensively upon imidization.

However, 4% Zr concentration is not high enough to form an effective protective layer when plasma etched. In order to raise the concentration limit, chemically bonding the complex to a polyimide polymer and blending with PA is considered. With this idea, a terpolymer and coordination polymer were developed with functional groups suitable for the incorporation of $Zr(adsp)_2$ complex.

Polymer synthesis and characterization

For preparation of a polyamic acid between an aromatic organic diamine and an aromatic dianhydride, 0°C or room temperature is usually sufficient for a high degree of polymerization.[19,20] However, the viscosity obtained for the product from room temperature polymerization (0.34dL/g) was lower than that from 0°C polymerization product (0.45dL/g).[21] Therefore, subsequent polymerization in this study was performed at 0°C.

The data of IR, ^{1}H-NMR and EA are collected in Table I-III. In FT-IR spectra for both of the polymers (Figure A-3 and A-4, Appendix), characteristic peaks of the Zr pendant group at 1611 and 1309 cm^{-1} are assigned to (C=N)-Zr and (Ph-O)-Zr stretching.[17] There is another peak at 1219 cm^{-1} in the terpolymer spectrum. This peak is attirbuted to (Ph-O-Ph) stretching (Figure A-5 appendix).[22]

Table I. FT-IR spectral assignments

assigned	coordinate polymer (cm^{-1})	terpolymer (cm^{-1})	$Zr(adsp)_2$ (cm^{-1})
O-H N-H	3500 - 3000 3500 - 3000	3500 - 3000 3500 - 3000	 3300-3410
C=O (carb. acid) C=O (amide)	1719 1656	1719 1656	/ /
(C = N)-Zr	1611	1611	1612
Ph-O-Zr	1307	1309	1318
Ph-O-Ph	absent	1219	/

The ^{1}H-NMR spectra for the two polymers are shown in Figure A-6 and A-7 Appendix. The peak interpretation is shown in Table II. The number of protons was assigned through the intergration profile. The total integration of the two

polymers matches the number expected. From ref. 17 for $Zr(adsp)_2$, imine proton was assigned at 8.5ppm aromatic proton in the range of 7.4 - 6.1 and 5.8 - 5.45 ppm.

Elemental analysis was also performed and results were shown in Table III. Calculation was based on the repeat unit $C_{50}H_{32}O_{10}N_6Zr$ and $C_{72}H_{46}O_{17}N_8Zr$ for coordination and terpolymer, respectively. Deviations are due to solvents in the sample, e.g., NMP (Figure A-8, Appendix)[23] which appears in the ^{1}H-NMP spectrum.

Table II. ^{1}H-NMR spectral assignment

	coord. polymer, δ ppm	terpolymer, δ ppm
H-O (carboxylic acid)	(off range) (2)	(off range) (2)
amideH-N-(C=O)-	8.2s (2)	8.2-8.4 (4)
imineH-C=N	8.7d(4)	8.7d(4)
PMDA H's	7.9s (2)	7.9s (2)
1,2-phenylenediamine H's	7.5-7.3m (6)	7.5-7.3m (6)
salicylidene H's (ortho) (para) (meta)	7.0br (4) 6.5br (4) 5.9d (8)	7.0br (4) 6.5br(4) 5.9d (8)
ODA H's (ortho) (meta)	/ /	7.8d (4) 7.05d (4)
Total H's	**32**	**42**

s-singlet; d-doublet; m-multiplet; br-broad.

Table III. Elemental analysis for polymers

	C%		H%		N%	
	Cal.	Found	Cal.	Found	Cal.	Found
coord.	62.05	59.54	3.31	4.52	8.69	9.56
terp.	62.38	59.51	3.32	4.04	8.08	8.44

Inherent viscosity, $[h]_{inh}$, was 0.12 dL/g and 0.45 dL/g for coordination polymer and terpolymer, respectively. The inherent viscosity of the precursor $Zr(adsp)_2$ was 0.015 dL/g. The viscosity of $Zr(adsp)_2$ and the coordination polymer are a little different from that previously published,[17] the reason being that the reaction conditions were different for the two cases.

Thermal gravimetric analysis (TGA) (Figure A-9 and A-10, Appendix) showed that the decomposition temperature of coordination polymer and terpolymer is about 387°C and 447°C, receptively. The mole percentage of Zr in the two polymers can be calculated from TGA. The calculation was based on the second weight loss, since there were some NMP solvent in the sample that appears in NMR spectrum. At the point of the second weight loss, the NMP solvent (b.p. 202°C)[11] has already evaporated and the polymers has imidized.[16] After imidization, the coordination polymer and terpolymer lost 2 and 4 H_2O, respectively.

For coordination polymer,

$$\text{Zr\% mole} \approx \frac{\text{weight of } ZrO_2 \text{ / MW of } ZrO_2}{\dfrac{\text{weight of polymer after imidization}}{\text{MW of repeat unit of polymer - } 2H_2O}}$$

$$= \frac{0.5857 / 123.2}{4.8037 / (968 - 36)} = 92\%$$

For terpolymer,

$$\text{Zr\% mole} \approx \frac{\text{weight of } ZrO_2 \text{ / MW of } ZrO_2}{\dfrac{\text{weight of polymer after imidization}}{\text{MW of repeat unit of polymer - } 4H_2O}}$$

$$= \frac{0.6737 / 123.2}{6.7504 / (1386 - 72)} = 106\%$$

They are close to the expected value (100%).

Film formation

The first layers of film for each blend containing 10% (mol/mol) zirconium were homogeneous. The thickness of the first layer in each case was about 8.0 mm on average. No visible phase separation was observed. No cracks were apparent in either film after imidization. However, cracking occurred upon imidization after applying the second layer to the film in most cases.

SEM pictures of 10% Zr(mol/mol) terpolymer/PI film and coordination/PI film are shown in Figure 9 and 10. Before etching, the surface of the two films appears smooth, without any phase separation. There exist some bubbles probably formed in the imidization process. After two hours etching, the surface of coordination polymer roughened. There were more irregular pits on the surface of terpolymer.

In addition to blend compatibility, the rate of atomic oxygen diffusion into the surface is thought to be a factor in how pits form in the surface. X-ray diffraction experiments should indicate whether the different oxygen etching behavior, observed by SEM, is due to inhomogeneity of the polymer blend films.

Conclusion

The complex $Zr(pdsp)_2$ was successfully prepared. Organically wrapped Zr complexes, $Zr(bdsp)_2$, $Zr(dsp)_2$, $Zr(dsdp)_2$, were mixed respectively with commercial PA cast into films and imidized to make Zr complex/polyimide composites. A 4% (mole) concentration limit for the three composite was observed for crack initialization on the film upon imidization. Preparation of multilayer film samples was possible but only up to a small number of layers.

In order to increase the Zr complex concentration in PA, $[Zr(adsp)_2\text{-}PMDA]_n$ coordination polymer and $[Zr(adsp)_2\text{-}PMDA\text{-}ODA\text{-}PMDA]_n$ terpolymer were successfully synthesized and blended with commercial PA, respectively. The inorganic concentration for the two polymers was 10% by mole Zr. However, cracking occurred upon imidization after applying the second layer to the film in most cases.

References (for Appendix A)

[1] Banks, B.A. "SiOx Coatings for Atomic Oxygen Protection of Polyimide Kapton in Low Earth Orbit", April 16-17, 1992, Dallas, TX.

[2] Rutledge, S.K.; Paulsen, P.E.; Brady, J.A.; "Oxidation and Protection of Fiberglass-Epoxy Composite Masts for Photovoltaic Arrays in the Low Earth Orbital Environment", MRS Spring Meeting , Reno, NV, April 5-9,1988.

[3] Leger, L.J.; Vissentine, J.T. "A Consideration of Atomic Oxygen Interaction with the Space Station", *J. of Spacecr. and Rockets*, **1986**, 23(5), 505-511.

[4] Banks, B.A. "SiOx Coatings for Atomic Oxygen Protection of Polyimide Kapton in Low Earth Orbit", April 16-17, 1992, Dallas, TX.

[5] Banks, B.A.; "Ion Beam Sputter-Deposited Thin Film Coating for the Protection of Spacecraft Polymers in Low Earth Orbit', Aerospace Science Meeting, Reno, NV, January 14-17, 1985.

[6] Rutledge, S.K. and Olle, R.M. "Durability Evaluation of Photovoltaic Blanket Materials Exposed on LDEF Tray S1003", The First LDEF Post-Retrieval Symposium, Kissmmee, Florida, June 2-8, 1991.

[7] Banks, B.A.; Auer, B.M.; Rutledge, S.K. "Monte Carlo Modeling of Atomic Oxygen Interaction with Protected Polymers for Projection of Material Durability in Low Earth Orbit", MRS Spring Meeting 92, San Francisco, CA.

[8] Rutledge, S.K; Cooper, J.M.; Olle, R.M. "The Effect of Atomic Oxygen on Polysiloxane-Polyimide for Spacecraft Application in Low Earth Orbit', Space Operations, Applications and Research Symposium, Albuquerque, NM, June 26-28, 1990.

[9] Banks, B.A.; Rutledge, S.K. "The Implications of the LDEF Results on Space Station Freedom Power System Materials", 5th International Symposium on Materials in a Space Environment, Cannes-Mandelieu, France, September 16-20, 1991

[10] Illingsworth, M.L.; Banks, B.A.; Smith, J.W.; Jayne, D.; Garlick, R.G.; Rutledge, S.K.; de Groh, K.K., "Plasma and Beam Facility Atomic Oxygen Erosion of a Transition Metal Complex", *Plasma Chem. and Plasma Proc.*, **1996**, 16(2), 209-205.

[11] Handbook of Chemistry and Physics, CRC, 74th edition, 1993-1994.

[12] Courtney, R.E.; Illingsworth, M.L; "Synthesis and Characterization of Bis(4-benzoyl-N,N'-disalicylidene-1,2-phenylenediamino)zirconium(IV)", ACS, 37th Undergraduate Reseach Symposium, Rochester, NY, April 25, 1992.

[13] Archer, R.D.; Day, R.O.; Illingsworth, M.L. *Inorg. Chem*., **1979**, 18, 2908.

[14] Browning, Todd; Illingsworth, M.L., private communication.

[15] Illingsworth, M.L.; Wagner, S.R.; He,L.; Betancourt, J.A.; Chen, Y. "Polymeric Materials with Improved Atomic Oxygen Resistance (I)", the 6th NASA JOVE Retreat, July, 1995, CA.

[16] Polyimides: Synthesis, Characterization and Applications. Vol. 1: K.L. Mittal, Ed.; Plenum, New York, 1984.

[17] Illingsworth M.L.; Rheingold, A.L. *Inorg. Chem*. **1987**, 26, 4312

[18] Hughes, K. A.; Illingsworth, M. L.; Chen, Y.; Jensen, A. J., "Synthesis and Characterization of Zr(pdsp)(ndsp)", 25th ACS NERM, Rochester, NY, October 22-25, 1995.

[19] Imai Y.; Maldar, N.N.; Kakimoto, M.J. *Polym. Sci., Polym. Chem. Ed*. **1985**, 23, 2077.

[20] Burks, H.D.; St. Clair, T.L. *J. Appl. Polym. Sci.* **1985**, 30, 2401.

[21] Chen, Y. 'Summary for Winter-Quarter Research", RIT, Rochester, NY, Jan. 1996.

[22] Pouchert, C.J.; "The Aldrich of FT-IR Spectra" Ed 1, Aldrich Chemical Company, Inc. 1985, p. 1210.

[23] Pouchert, C.J.; Behnke, J. "The Aldrich of ^{13}C and ^{1}H FTNMR Spectra" Ed 1, Aldrich Chemical Company, Inc. 1993, Vol. 2, p. 485.

Appendix B.

X-ray Diffraction Data for the 24-layer 10% (mol) $Zr(acac)_4$/PI Sample After Complete AO Ashing

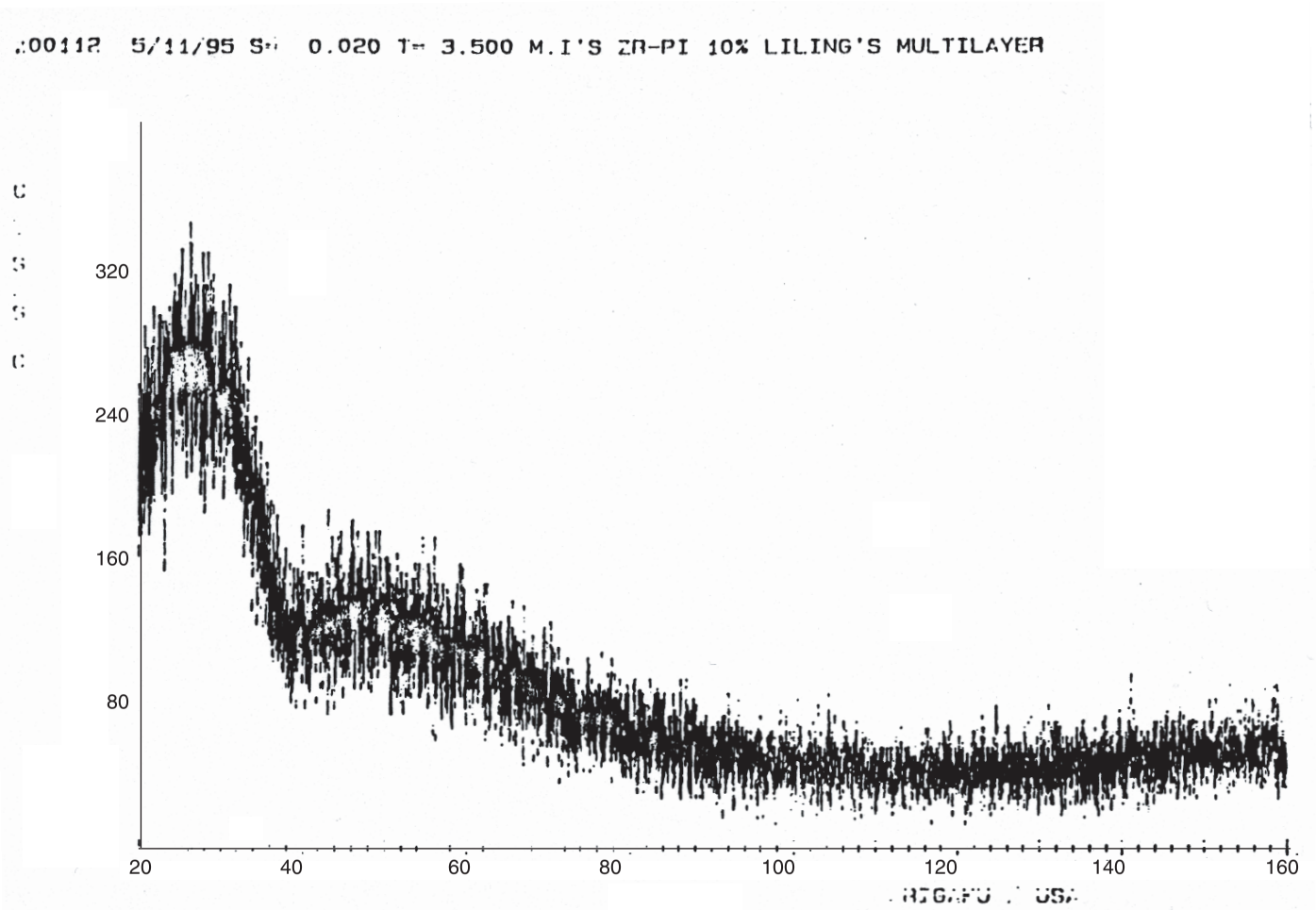

X-ray diffraction spectrum of the surface of the 24-layer 10% $Zr(acac)_4$/PI (mol/mol) composite sample after complete ashing

Appendix C.

Juan A. Betancourt, MS Thesis, "Characterization of Kapton Polymer Containing an Inorganic Additive"

Chapter 1. Introduction

New types of materials are being developed for the construction of space satellites, communication devices in space and even for the future International Space Station (ISS). These kinds of devices need a good protective material, so they can withstand the environmental conditions of Low Earth Orbit (LEO). These altitudes are about 60 to 180 km from the earth surface. See Figure 2.

These regions are known as the ionosphere because ions are prevalent. Because of the rarefied atmosphere and the effects of ionizing radiation, oxygen in the upper atmosphere exists in forms that are different than those at lower levels. In addition to molecular oxygen, O_2, the upper atmosphere contains high concentrations of oxygen atoms, O, excited oxygen atoms, and ozone, O_3. The atomic oxygen (AO), the major component of this very thin atmosphere, is very reactive and is generated by the photodissociation of oxygen by solar photons having shorter wavelengths than 2430 angstrom (A°). See Figure 1.

$$O_2 + h\nu \rightarrow O + O$$

Figure 1. Photodissociation of oxygen.

Only 16 % of the solar energy has the energy required to photodissociate the oxygen, but because there is low concentration of oxygen molecules, a large percent of them are converted to atomic oxygen. i.e. rates of dissociation are higher than rates of re-association in this case.[2]

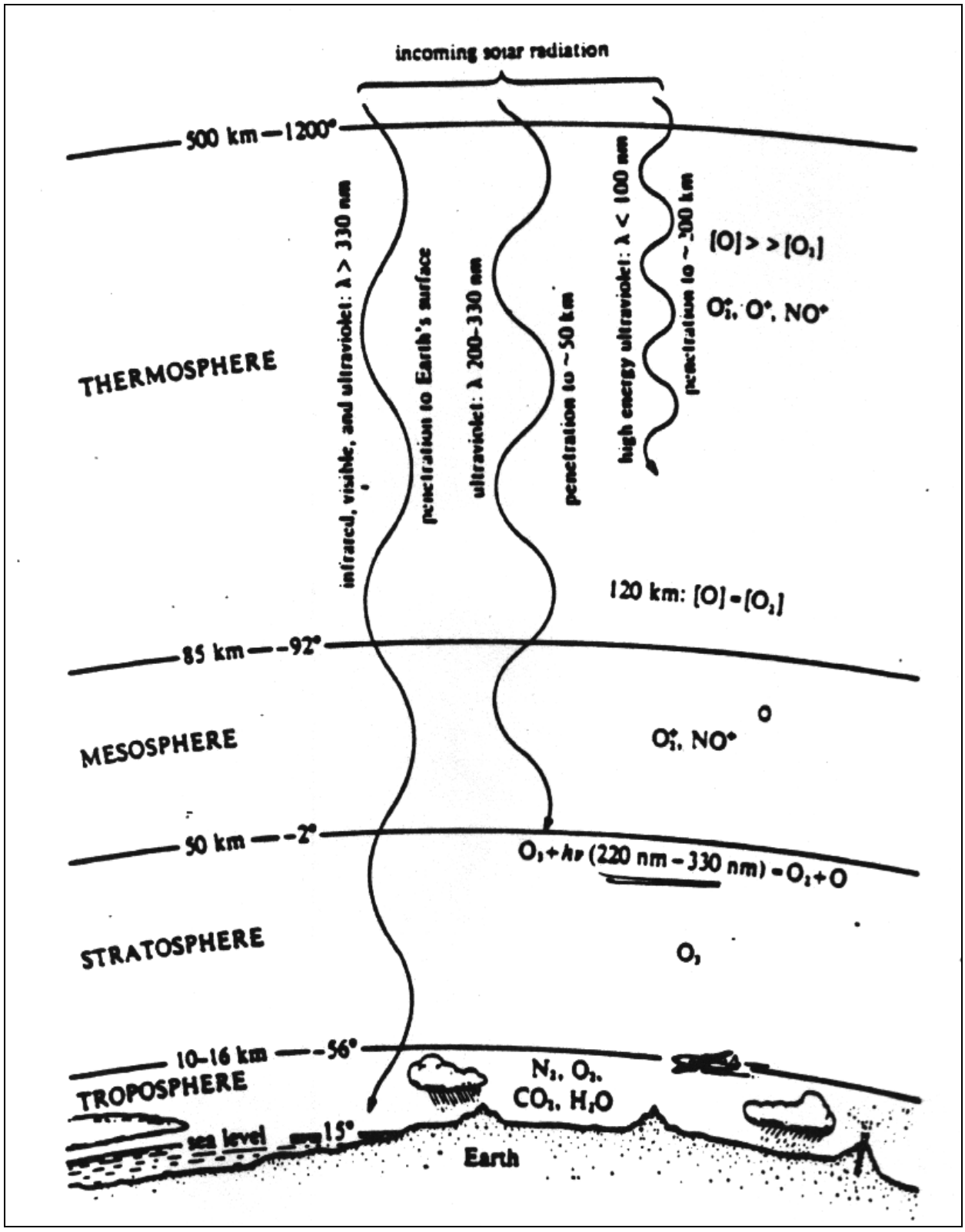

Figure 2. Major regions of the atmosphere (not to scale).[1]

Materials used for the construction of these space devices are based on polyimides because of their high electrical resistivity, strength and insulating properties. The only problem is that they can not stand the atomic oxygen impact/exposure which causes erosion of the material. This erosion causes a decrease in the thickness of the polyimides and with time its complete consumption.

Collisional energies of the oxygen with the surface of the polymer are enough to break chemical bonds and to oxidize organic and some metallic materials. Byproducts of this atomic oxygen include the liberation of CO_2, H_2O and nitrogen oxides. See Figure 3.

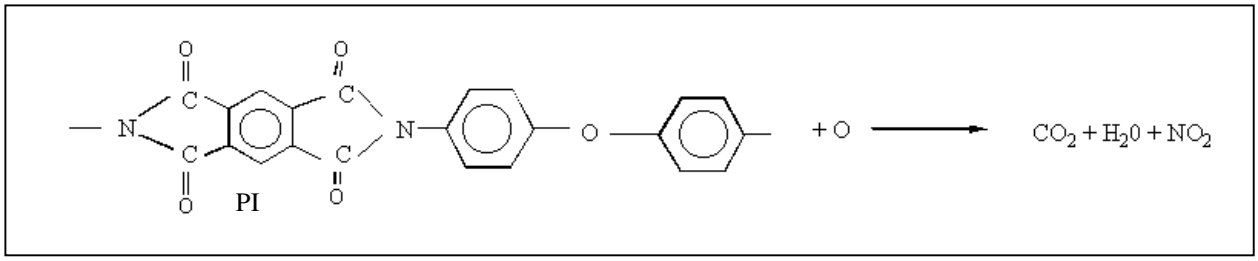

Figure 3. Reaction of polyimide with monoatomic oxygen. Reaction is not balanced as it only shows the products it generates.

Taking into consideration the requirements for the durability of these vehicles in space, use of the polymer alone is not good enough. Considering the anticipated fifteen years minimum life of the ISS, polyimides which are eroded away in a matter of months are inadequate.

Cost is crucial but the tradeoffs must be considered to prolong the life of these space devices. It is preferred that somewhat expensive materials with long life be used rather than inexpensive ones with frequent replacement. The latter will tend to be more expensive in the long run.

The actual polymer used for construction of the space devices is the polyimide known as Kapton ™, which is manufactured by Dupont. Kapton ™ is produced by the imidization of a polyamic acid (PA). The polyamic acid is made from the reaction of pyromellitic anhydride (PMDA) and oxy,bis(4-aminophenyl) (ODA). See Figure 4.

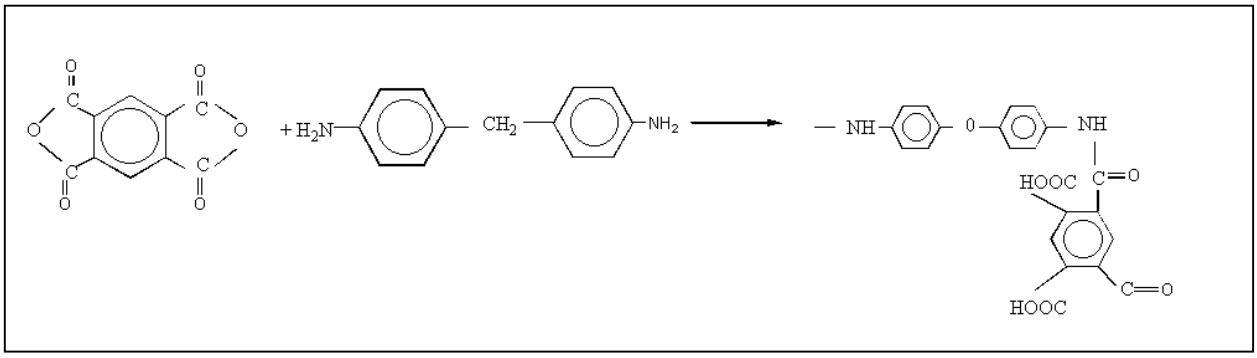

Figure 4. Reaction to obtain polyamic acid.[3]

After the polyamic acid is obtained, it is converted to the polyimide by the imidization process. This process consists of three heating steps each at a different temperature. The first one at 100° C causes evaporation of most of the solvent from the sample, the second one at 200° C finishes the evaporation of solvent and starts the conversion of the polyamic acid to a polyimide, and the last one at 300°C finishes the conversion[3]. The latter two heating steps cause water to be liberated. See Figure 5.

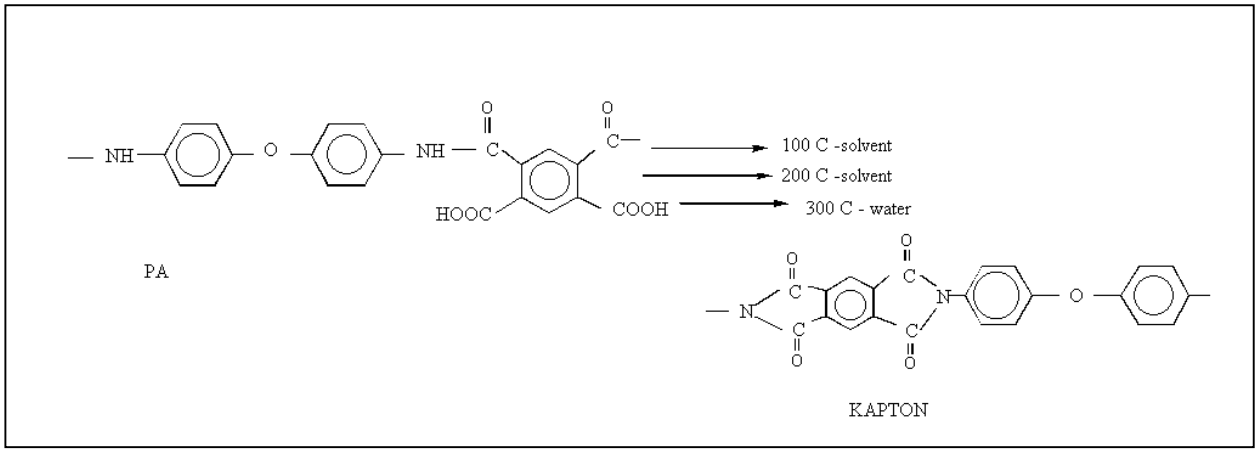

Figure 5. The imidization process. [3]

Kapton ™ was selected as a thermal control because it has low density (compared to metals), good UV stability, good flexibility and high strength. Continuing use of Kapton™ then requires new approaches for AO protection. The most viable alternative, when compared to use of paint coating or fibers, is the use of inorganic additives.

Fiber Additives

The use of epoxy-fibers in Kapton™ is one method providing temporary AO protection. Even though the mass loss of the protective surface is not significant, the removal of the epoxy to expose the fibers is a concern. Any handling, debris collision or stress will cause the fibers to break and get loose from the surface leaving the polymer without protection.[4]

Protective Coatings

Another type of protection is the use of paint coatings. These paints are coated on the surface of the polymer and they seem to help reduce the AO erosion of the material. After some exposure to the atomic oxygen, though, the coating starts to crack and some atomic oxygen starts to penetrate the coating causing erosion of the polymer underneath it. Another problem with paints is that any bubbles or pinhole defects allow erosion of the polymer underneath, and, in the event of debris collision or paint removal, no further protection is available.[5]

Silicone Additives

Silicon oxides of the type SiO_x and more commonly SiO_2 result in excellent protection for polyimide materials. These oxides arises from AO erosion of silicones which are applied to the surface of the polymeric material as layers or are just sprayed onto it. It has been observed that, when treated in plasma ashers (which simulate the vacuum of space as well as the atomic oxygen erosion), the treated polymer erodes at rates that are slower than the plain unprotected material. This is a result of the glassy SiO_2 surface produced in the areas where the atomic oxygen has made contact.[6]

Silicon in the form of silicone (polysiloxane) is used because the R groups attached to the chains are organic and help the Si to disperse well in the Kapton™ polymer. Remember that organic and inorganic don't mix well, like oil and water. If the silicon oxides are not well dispersed, organic areas will erode much faster than the areas containing the silicon oxide.

The liberation of dark fumes that get darker with time of exposure to atomic oxygen, is another shortcoming of silicone-Kapton blends. These can contaminate some of the adjacent components on these space devices, an example being the solar arrays.[6,7] See Figure 6.

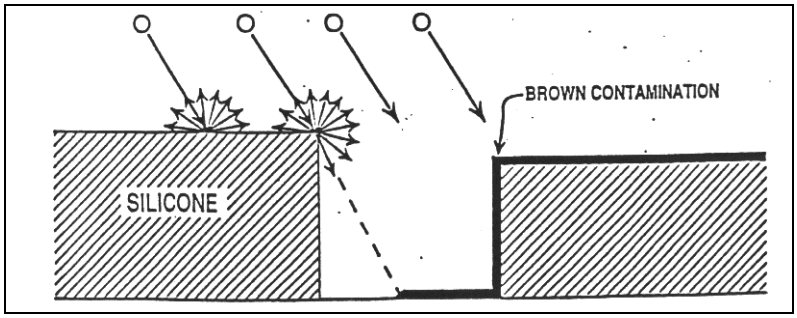

Figure 6. Contamination of adjacent areas of solar arrays after reaction of oxygen with silicone oxides. [6]

Concerns with this alternative are not based on the material's durability, but more with the number of pin holes and non-uniformities produced during manufacturing.

New Inorganic Additives

Because no viable alternative has been found that could protect Kapton™ from the atomic oxygen attack without contamination, other inorganic additives need to be considered. Using the silicon additives results as a starting point, we see that forming metal oxide layers seems to work if no contamination is produced from the reaction with the atomic oxygen. Looking into the properties of Si (group IVB), we observed that

group IVA of the periodic table has similar properties as group IVB. They both have some free d orbitals and four valence electrons. See Figure 7.

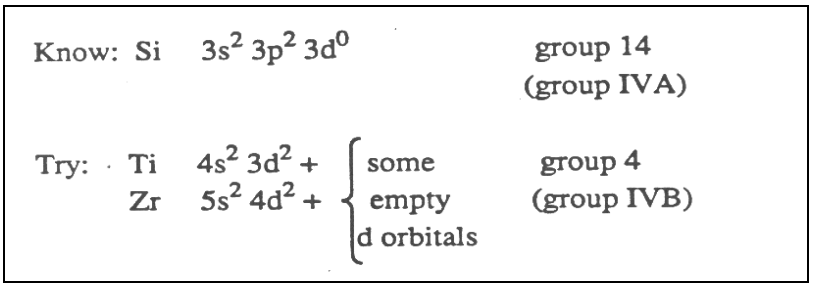

Figure 7. Valency and free orbitals for groups IVA and IV B.

We can choose the heavier element from group IVB and expect that, because it is heavier than silicon, no fumes or volatile contaminants will be produced from the reaction with atomic oxygen. Thus, zirconium (Zr) is chosen to do the same job as Si. When zirconium complexes were studied it was found that they are stable, cheap and don't produce harmful fumes as does silicon.[8] From the variety of Zr complexes available, $Zr(acac)_4$ was observed to give homogeneous films having the highest Zr concentration[9]. See Figure 8.

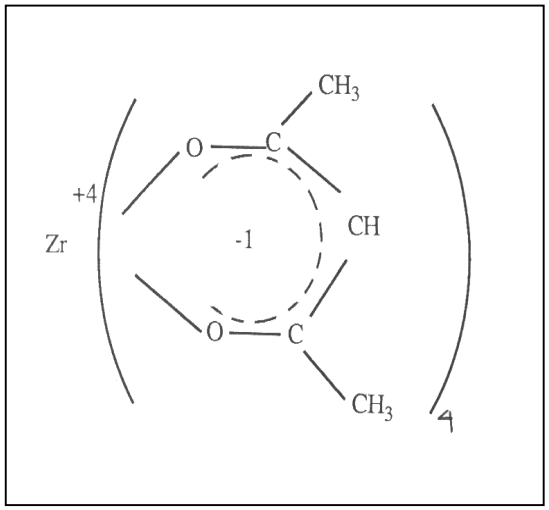

Figure 8. Zirconium acac complex.

This complex consists of a Zr surrounded by organic material. This organic material will help the complex to be well dispersed in the polymer. The distribution and homogeneity of the metal in polyimides have been studied by M. Nandi, et. al. with metals such as Cr, Ti, Si, and Fe.[10] Since Zr is in the same family as Ti, its oxidation is expected to be similar .

If the metal complex is well dispersed in the polymer, it could create a Zr oxide barrier to the penetration of the atomic oxygen into the polymer surface. The collision of oxygen with the metal will produce zirconium oxide (ZrO_2) which is very stable. Some polymer surface will be eroded away by the atomic oxygen but eventually a metal oxide layer should be formed all over the polymer that will protect it from further oxygen attack. In the event that debris or meteoroids collide with the protective surface and take away a piece, or create pin holes, the exposed Zr complex will react with any atomic oxygen that enters the pin hole, become oxidized, and block the propagation of any cracks or defects under the oxide layer.See Figure 9.

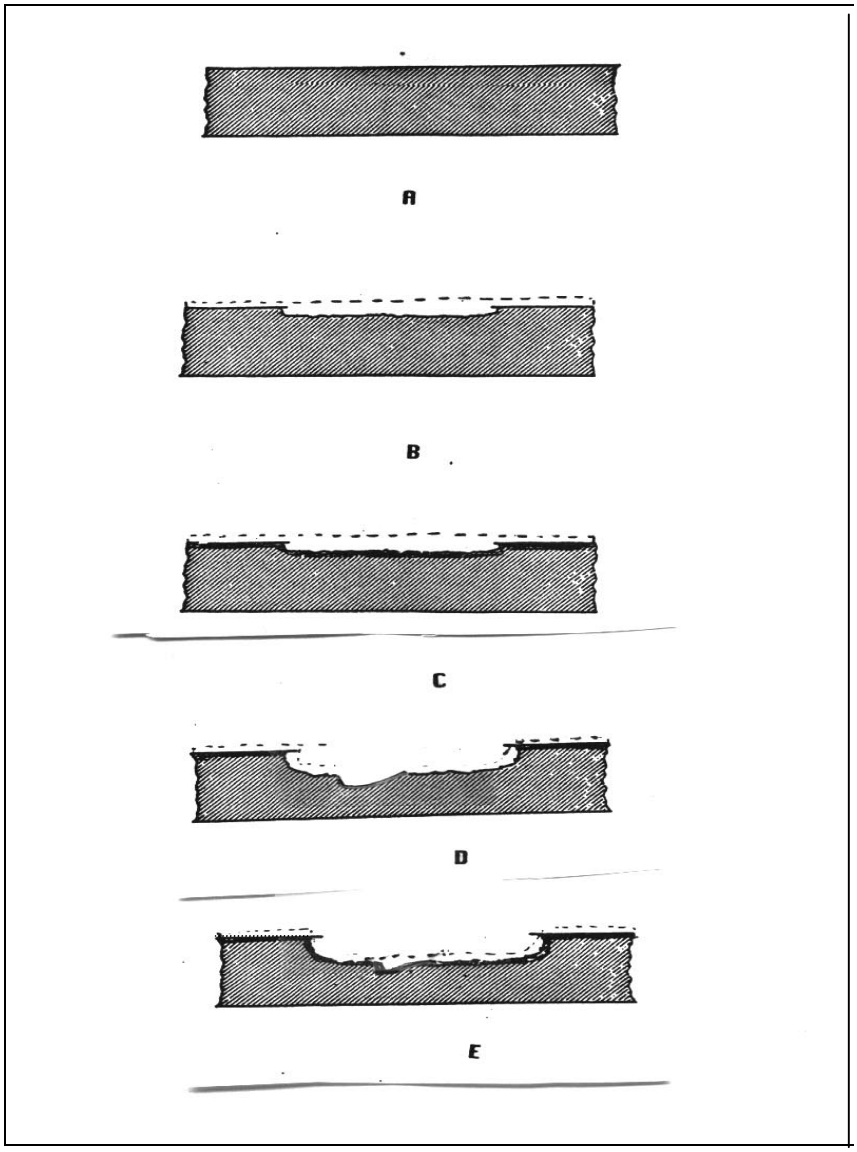

Figure 9. (a) Kapton™ surface without atomic oxygen erosion, (b) Kapton™ surface with erosion started, (c) Kapton™ surface with oxide layer formation, (d) Debris hits Kapton™ surface, (e) Formation of oxide layer in area of debris contact.

No harmful fumes or abrupt reactions are associated with the oxidation of Zr, unlike the lighter elements tested.[11] The reaction of the zirconium complex with atomic oxygen generates the zirconium oxide, water and carbon dioxide. See Figure 10.

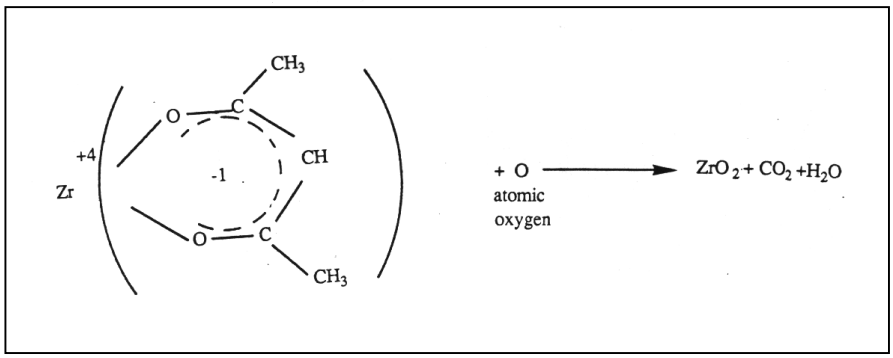

Figure 10. Reaction of atomic oxygen with the zirconium complex.

Studies must now be done on this Zr complex composite in order to test its viability. The experimentation must show how the properties of the material change with the addition of this additive and demostrate that in fact it reduces the erosion of the polymer by atomic oxygen attack. Some aspects of the study include analysis of samples containing different amounts of the complex to see how their AO erosion rates differ and how the strength of the samples is affected. Using surface analysis techniques such as Scanning Electron Microscopy (SEM), and Atomic Force Microscopy (AFM), any changes to the surface of the samples due to AO erosion can be detected.

Once the films are obtained, their thickness is measured using a Sloan Dektak profilometer. See Figure 11. This is an instrument for measurement of surface profiles and surface elevations from a minimum of 25 A° up to a maximum of 1,000,000 A°. In this method films on the substrate are placed over a movable platform, where a needle lays on top of the film. When the platform moves it will cause the needle to move over the film surface until it reaches its edge and falls onto the substrate surface.

The rise and fall over the surface of the sample is recorded on a chart and the reading is then converted to the thickness of the film using the appropriate conversion factors. See Figure 12.

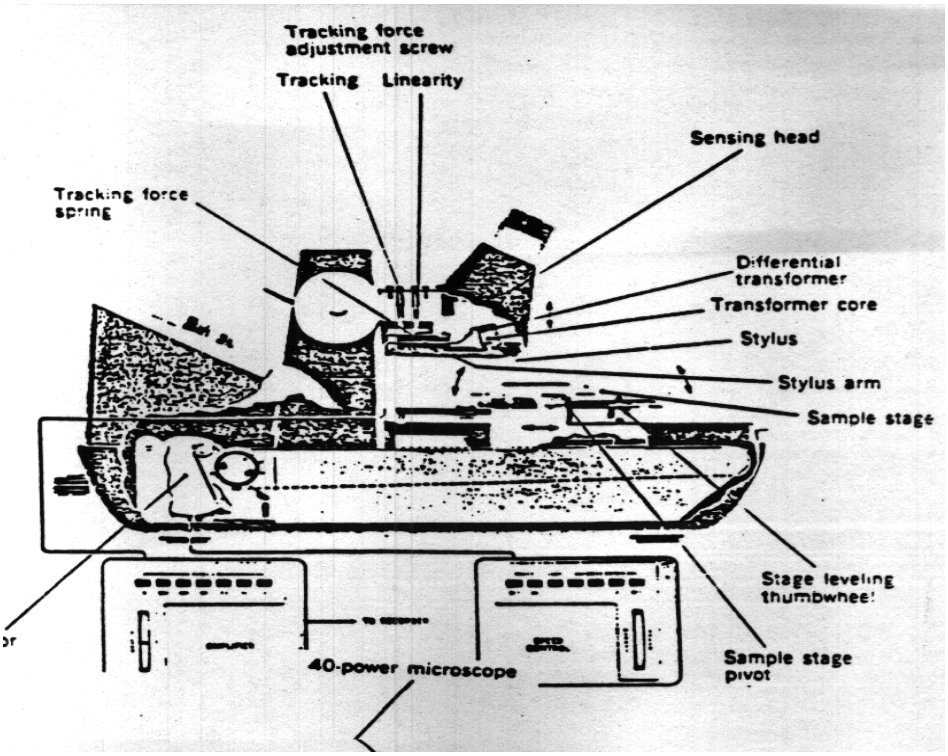

Figure 11. Profilometer instrument. [11]

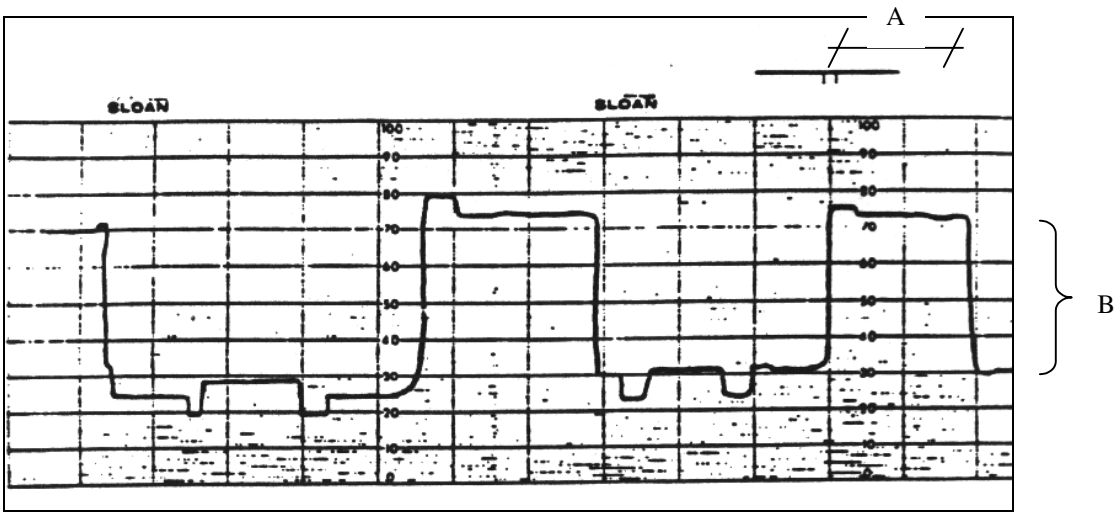

Figure 12. Profilometer output. [11] Point A represents the needle moving over the surface of the film and point B the rise and fall over the sample edge.

Mechanical Testing

One way to observe the physical properties of the film, such as strength and deformation, is to perform mechanical tests on it. One of the typical ones is tensile testing.

Tensile testing will be used to evaluate the strength of the films prepared and the maximum deformation they can handle. In this method the sample being tested is pulled to failure over a short period at a constant rate. An Instron instrument is used and ASTM standard #886 is followed. See Figure 13.

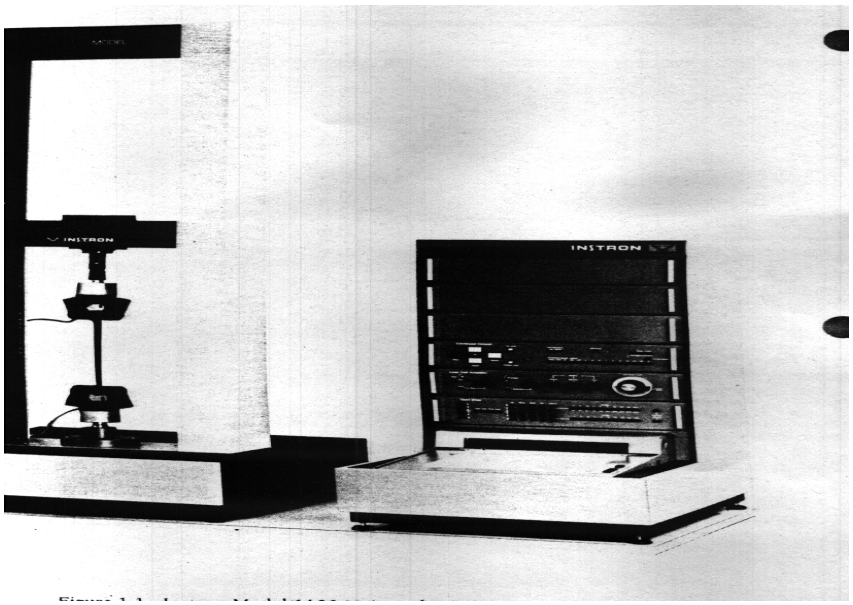

Figure 13. Instron instrument.[12]

A load is applied to the film sample and plotted on a moving chart paper. At the same time the elongation will be plotted as well. The values of load and elongation are then converted to stress (load/cross sectional area of film) and strain (elongation/original gage length). With these values on hand a plot of stress vs. strain is prepared and from the curve the ultimate tensile strength is obtained as the maximum point on the curve and reported in psi or Pa.

Because of the sample's thermoset behavior, the maximum elongation can be evaluated from the ultimate tensile strength which corresponds to the point of failure or when the fims breaks. The expected behavior of a film of Kapton should resemble the behavior shown in Figure 14.

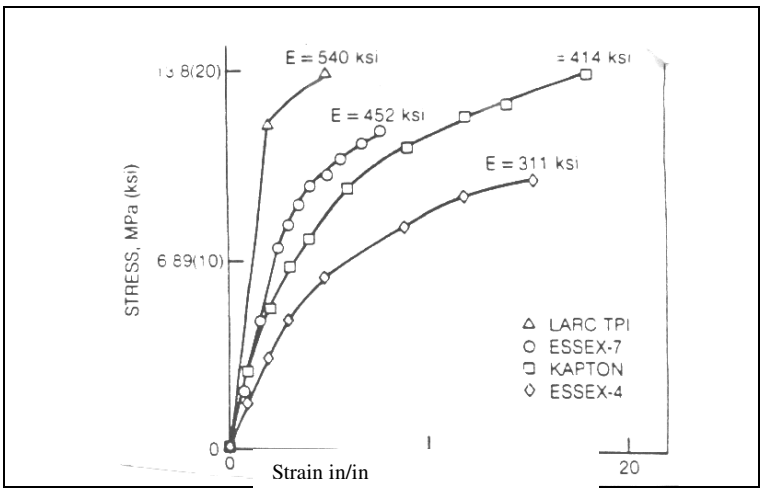

Figure 6. Behavior expected for tensile test on Kapton™.[13]The chart is intended to show shape of the mechanical behavior of Kapton™.

Pneumatic grips are used. This type of grip offers better grasp of samples and allows the sample to break in the middle and not near the grips. More than 3 samples are run for each data point and the results are averaged. The variation between samples is less than five percent.

Atomic Force

Scanning probe microscopes (SPMs) are a family of instruments used for studying the surface properties of materials at the atomic to micron level. All SPMs contain the components illustrated in Figure 15.

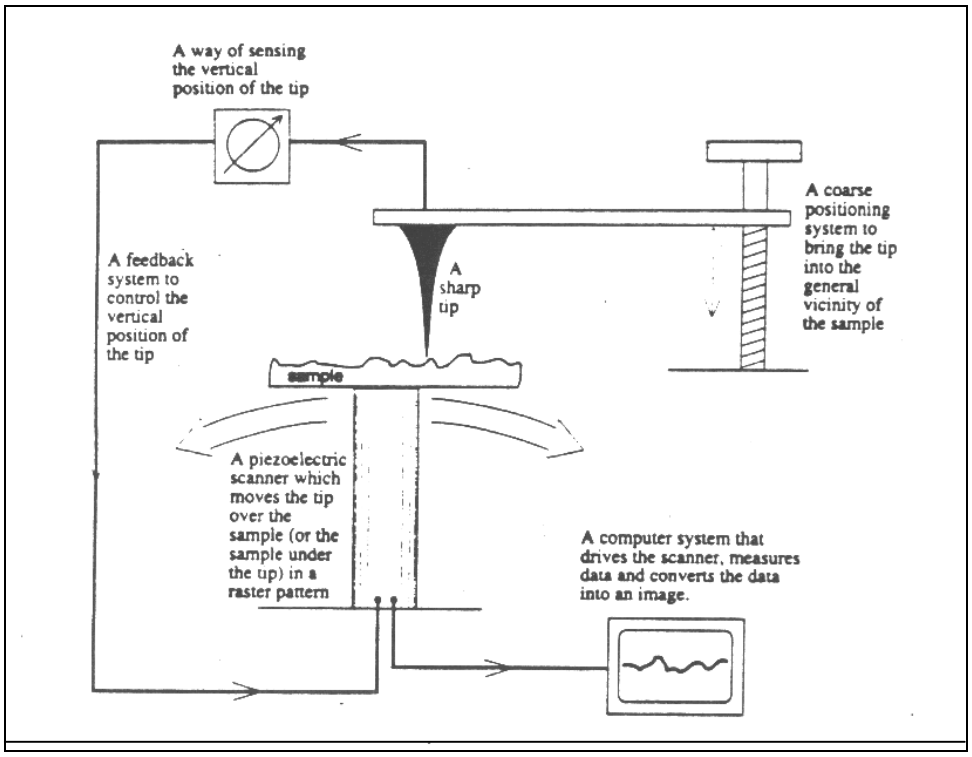

Figure 15. Schematic of a generalized scanning probe microscope [14]

Atomic force microscopes probe the surface of a sample with a sharp tip, approximately 2 microns long and often less than 100 angstroms in diameter. The tip is located at the end of a cantilever 100-200 μm long. Forces between the sample and the tip cause the cantilever to bend or deflect. A detector measures the cantilever deflections as the tip is scanned over the sample, or the sample is scanned over the tip. This information allows a computer to generate a map of the surface topography.

When using polymer samples a variation of the AFM experiment is used. This variation is known as the tapping mode. Here the cantilever oscillates at its resonance frequency with a high amplitude on the order of 1000 A°. The tip touches the sample during each oscillation. This technique is less likely to damage the sample than contact techniques, because it eliminates lateral forces such as friction. The tapping forces are higher than capillary forces (10^{-6} N) and allow the tip to penetrate a drop of water. See Figure 16.

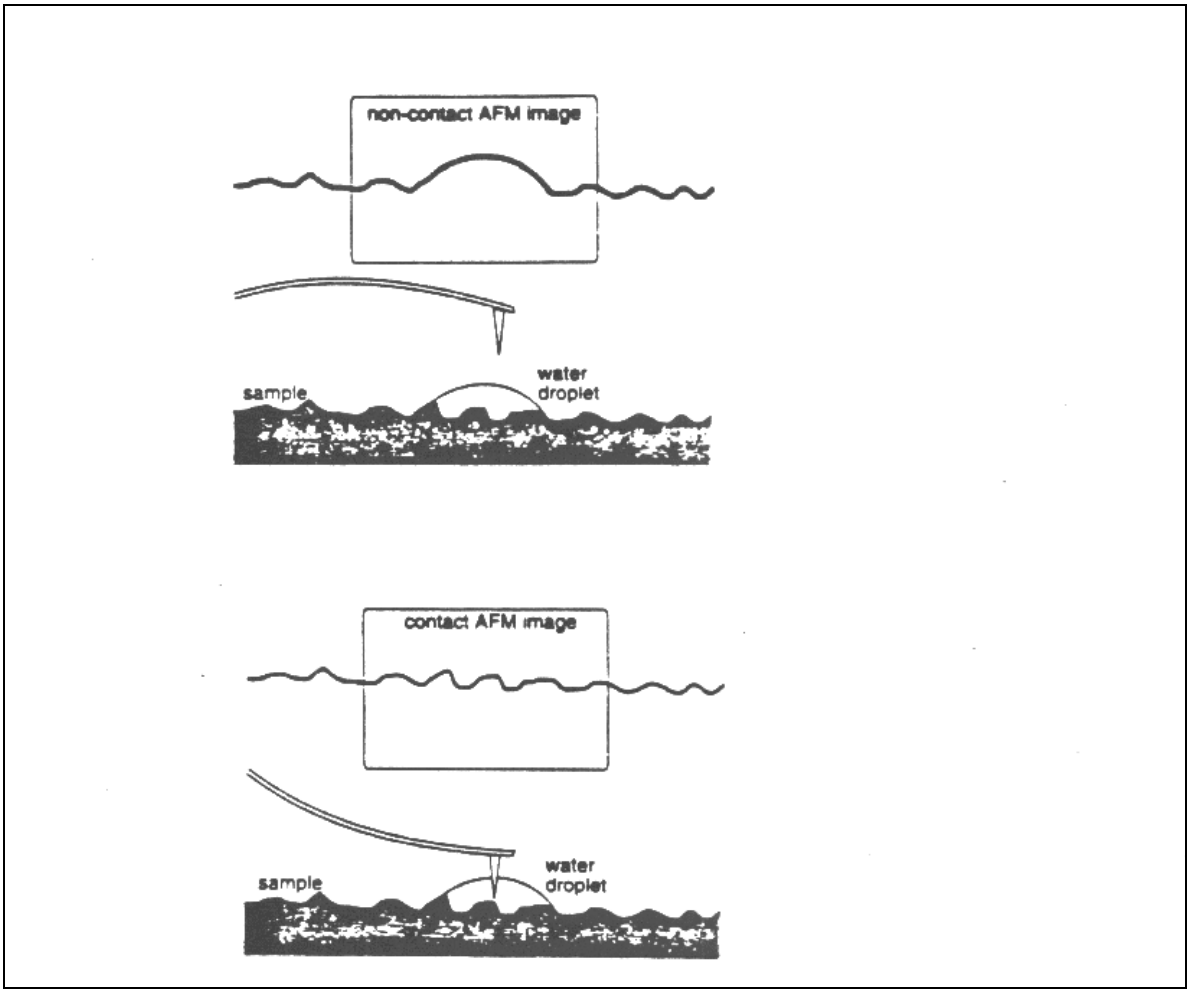

Figure 16. Comparative schematic depicts contact and no contact AFM images of a surface with a tiny droplet of water.[15]

The instrument available does not allow for atomic resolution but the resolution possible is good enough to obtain a surface topography of the film samples to 100 X100 μm.

Plasma Resistance

An oxygen plasma reactor will let us understand the behavior of the films under simulated space conditions, particularly AO attack. See Figure 17. This instrument consists of a solid state driver and two vacuum tube power amplifiers operated in parallel to conservatively provide a continuous wave power of 100 watts. Power transfer to the reactor chamber is accomplished by the electric field between the semitubular electrodes.

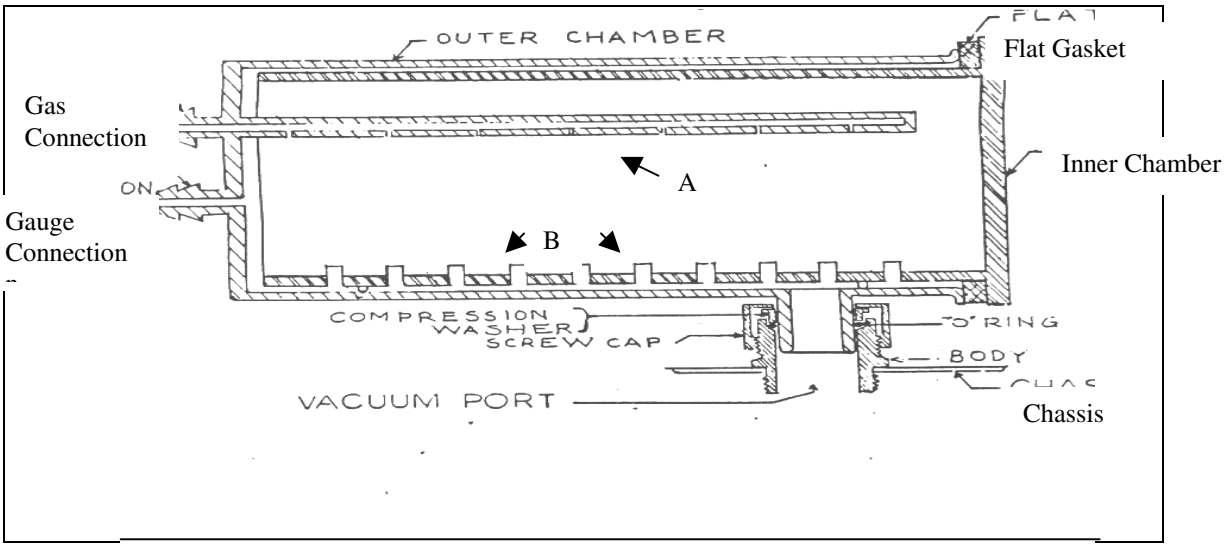

Figure 17. SPI-Plasma Prep II instrument.[15] The sample is placed in point B and the monoatomic oxygen bombards the sample (coming out from rod shown in point A).

The plasma process in the chamber is obtained through the use of a low pressure RF induced gas discharge of typical pressures of 50-120 μm^4. The material specimen is loaded into the reaction chamber. The chamber is evacuated to vacuum. Gas is then passed through the chamber, in our case O_2, and a radio frequency power of around 13.56 MHz is applied. This is enough to cleave the O_2 molecules into excited atomic oxygen that will hit the sample. Electrons produced in the ionization of the gas

gain energy in the electric field. This causes a chain reaction of the molecules, producing more ionic atomic oxygen.

The AO erosion process is one of oxidation. The reactions occur nearly at room temperature and any gases produced in the chamber are taken out in the gas outlet stream.

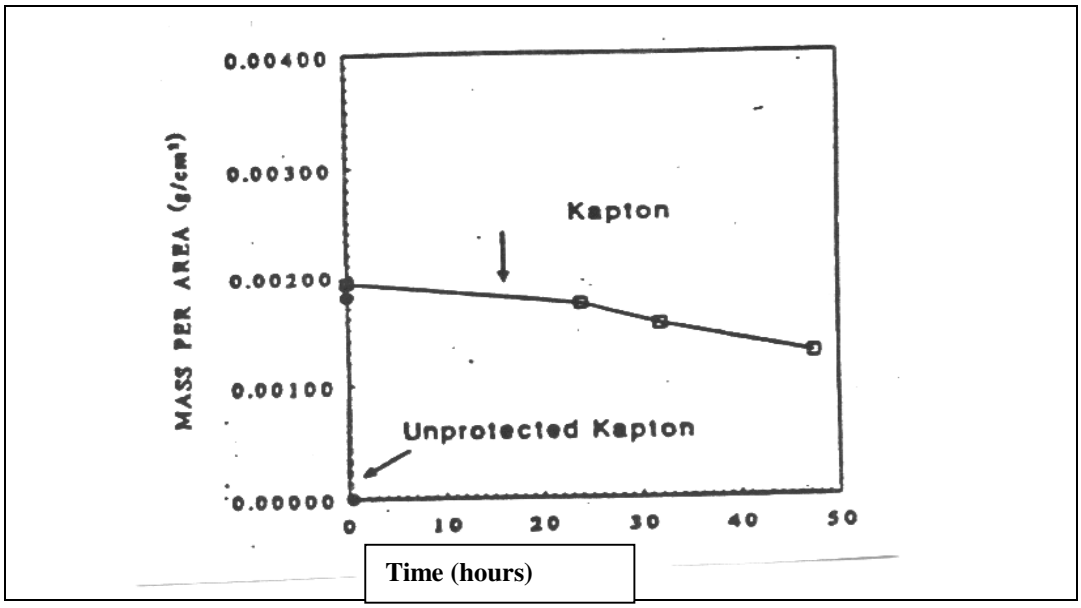

Figure 18. Expected behavior for protected Kapton (with inorganic additive) and unprotected Kapton.[13] Chart is intended to represent that unprotected Kapton erodes faster than protected Kapton.

Scanning Electron Microscopy

Another technique that looks on the surface of the samples is known as scanning electron microscopy (SEM). See Figure 19. Here a sample is bombarded with a beam of electrons generated from an electron gun. The gun is basically a tungsten filament that is exposed to a current to obtain the electrons. The electrons emitted are accelerated down a column by using a high voltage anode. The trajectory of the electrons in the column is not linear and that is why a set of lenses are needed. These lenses are a set of magnetic coils that take the diverging beam and convert it into a converging beam at a focal point. The last step is to have the beam hit the sample. This is achieved by using an objective lens. The objective lens takes the beam and focuses it onto the sample surface. The amount of beam the samples sees is determined by the aperture of the objective lens. See Figure 20.

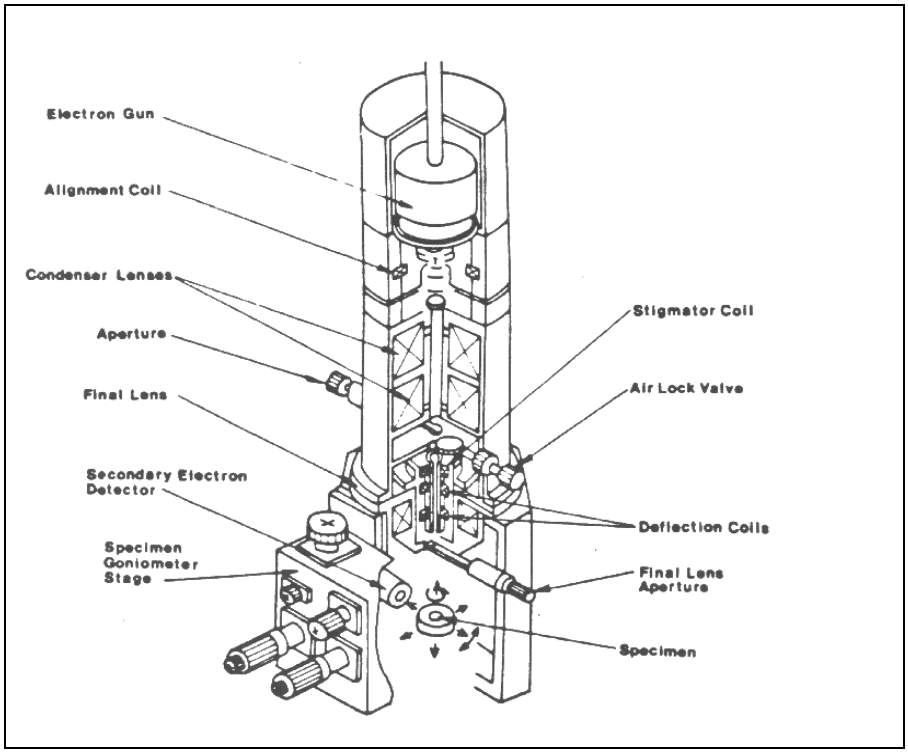

Figure 19. SEM Instrument.[16]

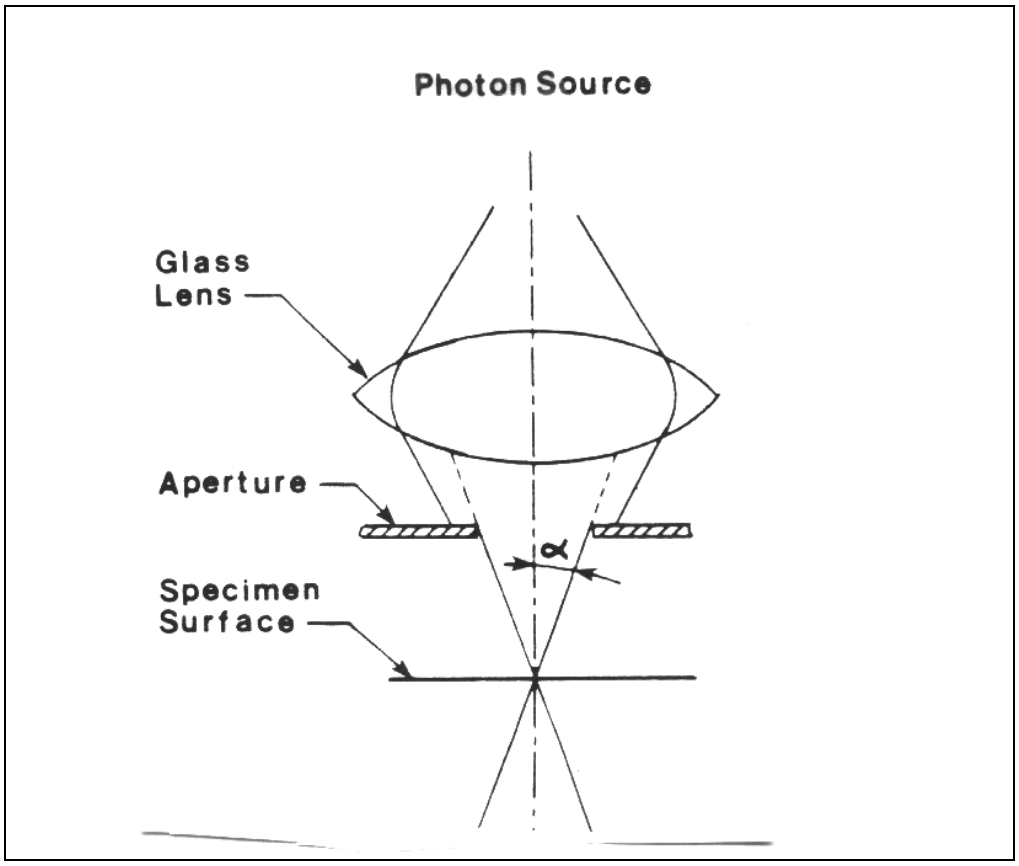

Figure 20. Objective lens and electron beam hitting a sample.[16]

After the sample is hit with the beam, a set of signals is generated. See Figure 21. From all these signals only secondary electron emissions are collected. These signals are converted into topographic information of the sample. Secondary emissions give good information about sample surfaces and are not hard to obtain.

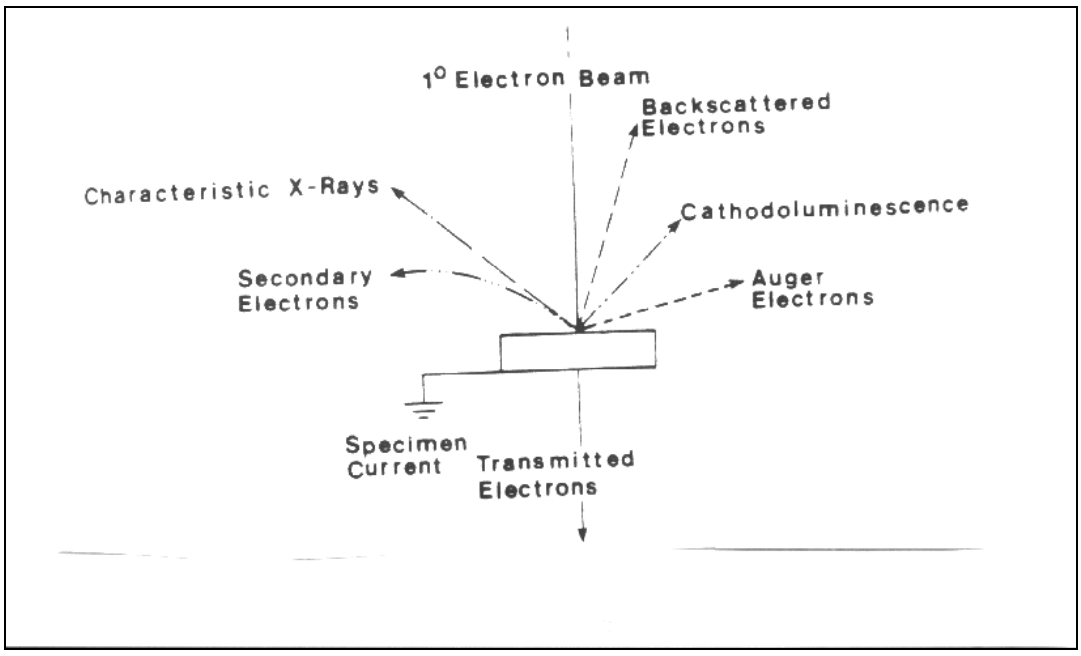

Figure 21. Signals generated after e-beam hitting surface of sample on SEM.[16]

If we collect the X-rays generated from the film after the beam hits the surface, a qualitative and quantitative analysis of the elements present in the film can be made. This technique is known as Energy Dispersive X-ray analysis. The principal way this is done is by analyzing the X-rays generated when the electron beam interacts with the sample. X-rays are generated when the primary beam ejects an inner shell electron thus exciting the atom. As an electron from an outer shell drops to fill the vacancy and deexcite the atom, an X-ray is emitted. The energy of this X-ray is specific to each individual element in the periodic table and is also specific to what particular electron is ejected and what particular electron dropped to fill the vacancy.

The analysis can be done two ways, by Energy Dispersive (EDS) or Wavelength Dispersive approaches. In our case, we will use the EDS approach. As the name implies, this method sorts the X-rays according to their difference in energies. In an EDS detector, an X-ray photon is converted into a charge pulse within the EDS semiconductor detector. This charge pulse is then converted into a voltage with an

amplitude equal to the energy of the incoming X-ray. The voltage is then supplied to a multi channel analyzer which sorts the pulses and displays them as a continuous spectrum of all elements present. See Figure s 22 and 23.

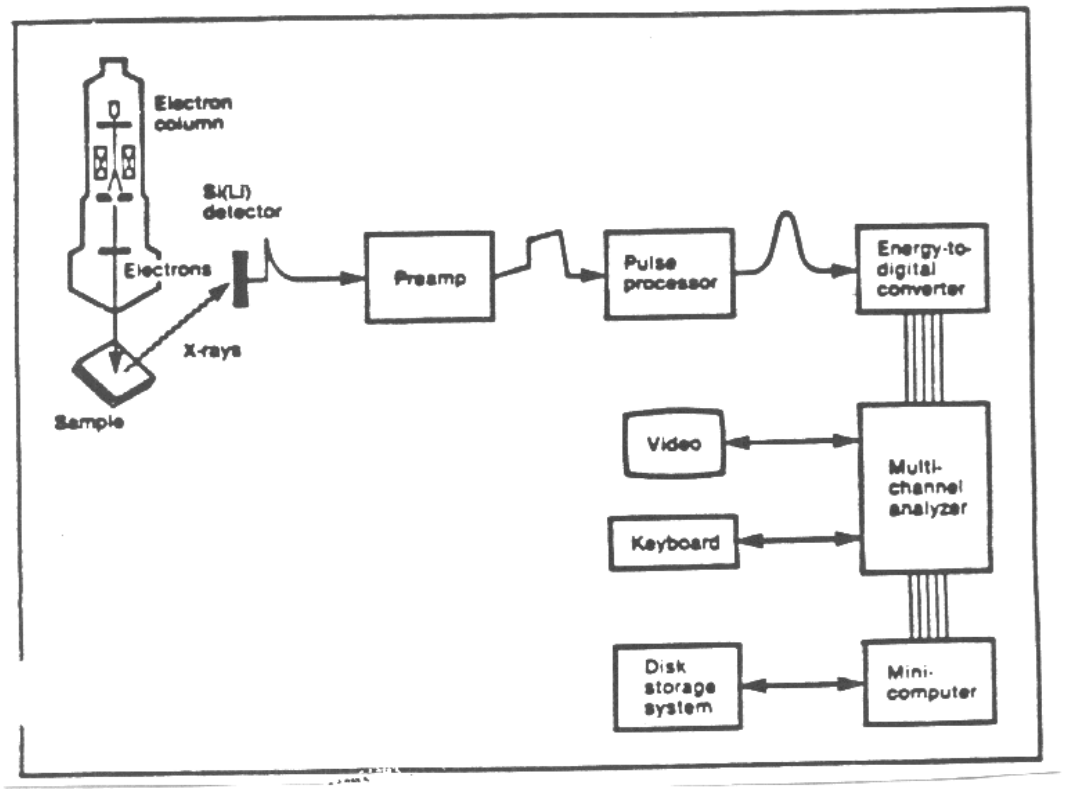

Figure 22. Schematic of a typical EDS system. [15]

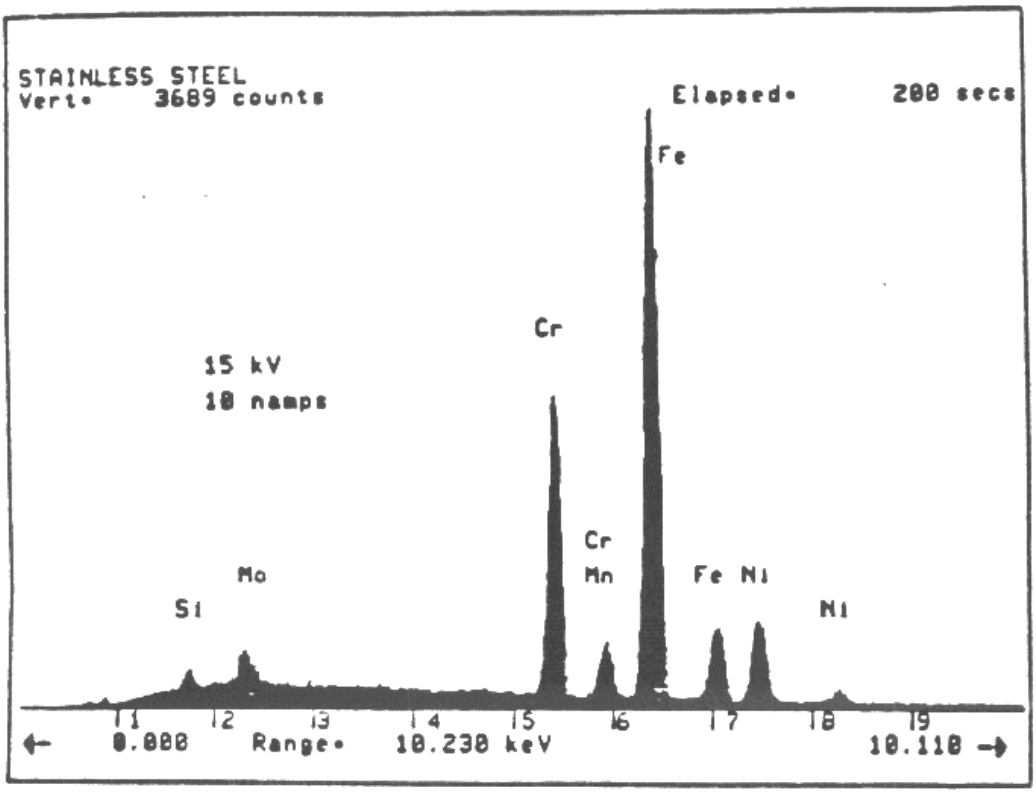

Figure 23. A Typical EDS spectrum.[15]

Optical Microscopy

We can use optical microscopy if we only want to take pictures of the film surface at low magnifications. Two techniques were used for this research, Brightfield and Darkfield microscopy.

In Brightfield microscopy photons are emitted from the illumination source and pass through the aperture and field diaphragms and strike the beam splitter. These photon rays are directed towards the object plane. Light rays striking the object plane are reflected back through the objective. See Figure 24.

This technique will give us a highly magnified and distinct image with true specimen color. The complementary approach is using Darkfield Microscopy. Here a darkfield annulus is inserted into the ray path prior to the beam splitter. This annulus prevents rays from passing through the central portion of the objective as in Brightfield. Instead, the rays proceed around the darkfield stop and are deflected to and strike the sample at an oblique angle, not perpendicular as in Brightfield. Thus, any featureless specimen will appear black. Any specimen with features which refracts or causes scattering of light will stand out clearly. See Figure 25.

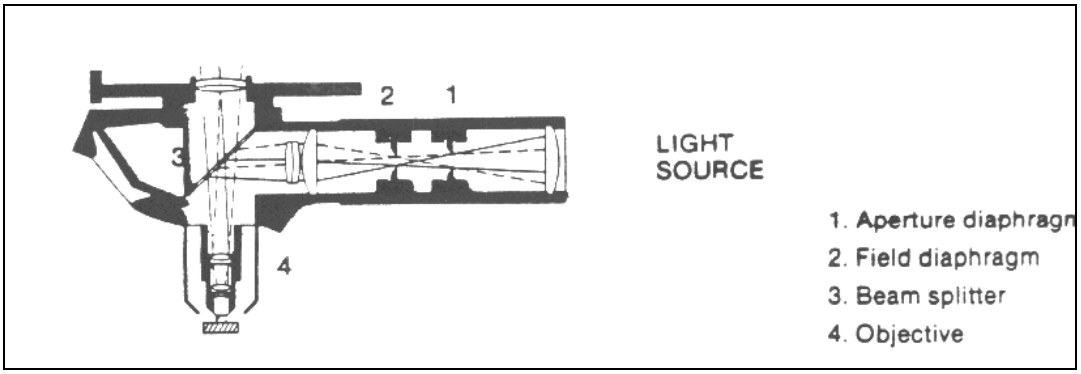

Figure 24. Brightfield Microscopy [16]

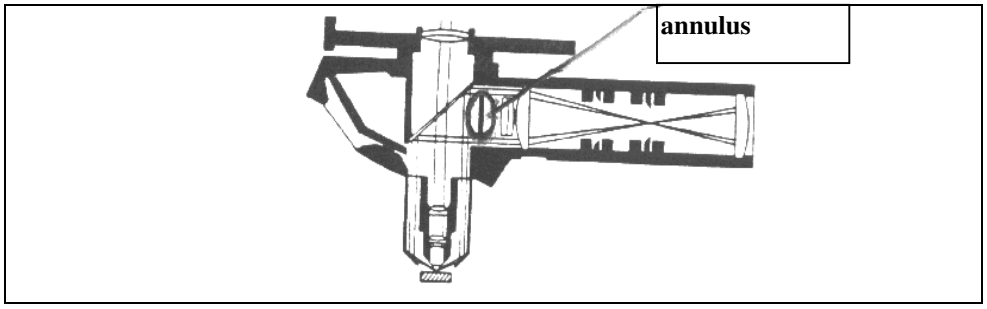

Figure 25. Darkfield Microscopy. [16]

REFERENCES (for Appendix C)

1. Manahan, Stanley, "Environmental Chemistry " William Grant Press, Boston, 1984.
2. "Performance & Properties of Atomic Oxygen Protective Coatings" SAMPE 1992.
3. McCaffens, "Lab Preparation for Macromolecular Chemistry" Mc Graw Hill, 1970.
4. "Oxydation & Protection of Fiberglass-epoxy composite materials" , B.A. Banks, NASA Lewis, Cleveland, Ohio,1991.
5. "SiOx coatings for Atomic Oxygen protection of PI Kapton™ in LOE", B.A. Banks, NASA Lewis, Cleveland, Ohio 1991.
6. "Atomic Oxygen Iterations with Silicones on LDEF" B.A. Banks, Gebauer, Linda, Hill, Carol, Florida 1991.
7. "Implications of LDEF Results on SSF Powwer sysstems Materials", B.A. Banks, Cleveland, Ohio , NASA Lewis,1991.
8. "Plasma and beam facility atomic oxygen erosion of a transition metal complex" M.L. Illingsworth, B. A. Banks , J. W. Smith, et. al. Plasma Chemistry and Plasma Processing. Vol 16, No 1, 1996. 209-225.
9. He, L. MS Thesis RIT 1996.
10. "Molecular level ceramic/polymeric composites synthesis of Polymer trapped silica oxides nanoclusters" N. M. Nandi et.al. Chem Mater, 1990, vol 2, 772-76.
11. Profilometry handbook. Sloan Instruments Corp., Ca , June 1980,M-648(a)-680
12. Instron Company, Instrument manual.1985,Instron Company, Ma.
13. “Polyimides”. Wilson D., Chapman & Hall, NY, 1990.
14. How to Buy a Scanning Probe Microscope. Park Scientific Instruments, Ca, 8/1997.
15. SPI-Plasma Prep II catalog, SPI supplies, PA, 1996.
16. Scanning Electron Microscopy, A Student Handbook. M.T. Postek Ladd Research Industries, Ca, 1990

REPORT DOCUMENTATION PAGE

Form Approved
OMB No. 0704-0188

1. AGENCY USE ONLY (*Leave blank*)	2. REPORT DATE	3. REPORT TYPE AND DATES COVERED
	August 2001	Technical Memorandum

4. TITLE AND SUBTITLE

Zr-Containing 4,4'-ODA/PMDA Polyimide Composites
Parts I and II

5. FUNDING NUMBERS

WU–251–30–1E–00

6. AUTHOR(S)

M.L. Illingsworth, J.A. Betancourt, L. He, Y. Chen,
J.A. Terschak, B.A. Banks, S.K. Rutledge, and M. Cales

7. PERFORMING ORGANIZATION NAME(S) AND ADDRESS(ES)

National Aeronautics and Space Administration
John H. Glenn Research Center at Lewis Field
Cleveland, Ohio 44135–3191

8. PERFORMING ORGANIZATION REPORT NUMBER

E–12944

9. SPONSORING/MONITORING AGENCY NAME(S) AND ADDRESS(ES)

National Aeronautics and Space Administration
Washington, DC 20546–0001

10. SPONSORING/MONITORING AGENCY REPORT NUMBER

NASA TM—2001-211099

11. SUPPLEMENTARY NOTES

M.L. Illingsworth, J.A. Betancourt, L. He, Y. Chen, and J.A. Terschak, Department of Chemistry, Rochester Institute of Technology, Rochester, New York 14623; B.A. Banks and S.K. Rutledge, NASA Glenn Research Center; and M. Cales, Cleveland State University, 1983 E. 24th Street, Cleveland, Ohio 44115–2403. Work funded under NASA Grant NAG–1008 and the NASA/University Joint Venture (JOVE) program. Responsible person, Bruce A. Banks, organization code 5480, 216–433–2308.

12a. DISTRIBUTION/AVAILABILITY STATEMENT

Unclassified - Unlimited
Subject Category: 27 Distribution: Nonstandard

Available electronically at http://gltrs.grc.nasa.gov/GLTRS

This publication is available from the NASA Center for AeroSpace Information, 301–621–0390.

12b. DISTRIBUTION CODE

13. ABSTRACT ***(Maximum 200 words)***

The objective of this research is to improve the atomic oxygen resistance of Kapton^{TM}, a polyimide (PI) made from pyromellitic acid dianhydride (PMDA) and 4,4'-oxydianiline (ODA), while retaining or enhancing the desirable properties of the pure polymer. Toward this end, zirconium-containing complexes and polymers were used to make composites and blends. Tetra(acetylacetonato)zirconium(IV), $Zr(acac)_4$, which is commercially available, was identified as the best zirconium-containing complex for enhancing the atomic oxygen resistance of polyimide composites of the 10 complexes screened. Films prepared from the commercially-available polyamic acid (PAA) of PMDA-ODA (DuPont) have good uniformity, flexibility, and tensile strength. A 24-layer 10% (mol) $Zr(acac)_4$/PI composite film showed significant improvement (ca. 20 fold) of atomic oxygen resistance over the pure polyimide. However, 10% (mol) $Zr(acac)_4$ represents an upper concentration limit, above which films undergo cracking upon thermal imidization. In order to increase the Zr complex concentration in PMDA-ODA PI films, while retaining good film properties, $[Zr(adsp)_2\text{-PMDA}]_n$ coordination polymer [bis(4-amino-N,N'-disalicylidene-1,2-phenylenediamino)zirconium(IV)-pyromellitic dianhydride] and $[Zr(adsp)_2\text{-PMDA-ODA-PMDA}]_n$ terpolymer were synthesized and blended with commercial PAA, respectively. Several techniques were used to characterize the films made from the polymer containing $Zr(acac)_4$. Plasma studies of films having 2% (mol) incremental concentrations of Zr in the Kapton up to 10% (mol) show that the overall rate of erosion is reduced about 75 percent.

14. SUBJECT TERMS

Zr containing polyimides; Atomic oxygen

15. NUMBER OF PAGES

138

16. PRICE CODE

17. SECURITY CLASSIFICATION OF REPORT	18. SECURITY CLASSIFICATION OF THIS PAGE	19. SECURITY CLASSIFICATION OF ABSTRACT	20. LIMITATION OF ABSTRACT
Unclassified	Unclassified	Unclassified	